Study of Stability and Bifurcation Analysis of Plant-Growth Dynamics using Delay Differential Equations

A Thesis

Submitted for the Award of the Degree of

DOCTOR OF PHILOSOPHY

in

MATHEMATICS

By

Davneet Kaur

Registration Number: 42000131

Supervised By

Dr. Pankaj Kumar

Professor

Department of

Mathematics

LOVELY PROFESSIONAL UNIVERSITY, PUNJAB

2025-2026

Declaration

I hereby declare that the presented work in the thesis entitled **"Study of Stability and Bifurcation Analysis of Plant-Growth Dynamics using Delay Differential Equations."** in fulfilment of the degree of **Doctor of Philosophy (Ph. D.)** is the outcome of research work carried out by me under the supervision of **Dr. Pankaj Kumar**, working as Professor, in the School of Mechanical Engineering of Lovely Professional University, Punjab, India. In keeping with the general practice of reporting scientific observations, due acknowledgement has been made whenever the work described here has been based on the findings of other investigators. This work has not been submitted in part or full to any other university or institute for the award of any degree.

(Signature of Scholar) 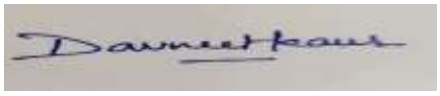

Name of the scholar: **Davneet Kaur**

Registration No.: **42000131**

Department/school: **Department of Mathematics**

Lovely Professional University,

Punjab, India

Certificate

This is to certify that the work reported in the Ph. D. thesis entitled **"Study of Stability and Bifurcation Analysis of Plant-Growth Dynamics using Delay Differential Equations."** submitted in fulfillment of the requirement for the reward of the degree of **Doctor of Philosophy (Ph.D.)** in the School of Mechanical Engineering is a research work carried out by **Davneet Kaur**, is bona fide record of his/her original work carried out under my supervision, and that no part of the thesis has been submitted for any other degree, diploma, or equivalent course.

(Signature of Supervisor) Pankaj Kumar | 11893

Name of supervisor: **Dr. Pankaj Kumar**

Designation: Professor

Department/school: School of Mechanical Engineering

University: Lovely Professional University

Dedicated to my almighty God and Parents

ACKNOWLEDGEMENT

I express my heartfelt gratitude to my thesis supervisor, Dr. Pankaj Kumar, Assistant Professor, School of Chemical Engineering and Physical Sciences, Lovely Professional University, Phagwara, Punjab for his interest, excellent rapport, untiring cooperation, invaluable advice and encouragement throughout of my Ph.D. program. Without his unfailing support and belief in me, this thesis would not have been possible. I am indeed feeling short of words to express my sense of gratitude towards him. Besides being a scholar par eminence, He is a person par excellence - a perfect embodiment of dedication, intelligence and humility.

Above all, I feel very much obliged to my father Mr. Gurvinder Singh, mother Mrs. Surinder Kaur, my father-in-law Mr. Kulwant Singh, my mother-in-law Mrs. Parminder Kaur for what I have received from them in the form of inspiration, love, encouragement and moral support. I also feel blessed to my sons, Nirvair Singh and Nirbhau Singh for coming in this span of time and making my degree more memorable. Last but not the least, I am highly grateful to my husband, Mr. Rajan Chawla, without whose help it would have really been impossible to carry out this task. He has supported me unconditionally and relentlessly over all these years. Dear Rajan, this degree is yours, not mine.

Jan 2026 Davneet Kaur

Abstract

The research work investigates how delays in nutrient uptake, utilization, and efficiency caused by soil or plant toxicants impact plant growth dynamics (PGD). Plants rely heavily on readily available nutrients, and toxicants disrupt the supply and utilization of these essential resources. This disruption, modelled as a time delay, is a central focus of the study. We propose and analyze mathematical models for single plant, tree, and plant population growth (PPG), incorporating these delays caused by toxicants. The models are then validated numerically and compared with existing data on plant growth under various toxicant exposures.

Mathematically, we employ the comparison theorem to guarantee the positivity and boundedness of all analytical solutions. We then identify and analyze all possible interior and exterior equilibria. Local stability of the interior equilibria is established. When incorporating the delay parameter, the stability analysis reveals a Hopf bifurcation, indicating complex dynamical behaviour. Rouche's theorem is applied for a detailed investigation of the roots' nature. Finally examining, how state variables change in response to variations in model parameters is conducted using the 'Direct Method' for most models. Numerical simulations in MATLAB, with assigned parameter values, reveal the critical delay parameter (DP). Below this value, the system remains stable but above it, the system transitions from a stable state to an unstable one, exhibiting a Hopf bifurcation.

In chapter-1, General introduction: The chapter introduced about PGD under the effect of toxicants. The remarkable work done is by the researchers is cited and the gaps have been identified through extensive literature review. All the important concepts of plant physiology and the necessary mathematical concepts required for their study have also been described. It also includes the proposed objectives of the study.

In chapter-2, Delay-induced bifurcation in plant growth plant growth dynamics: In the chapter, the study proposes a mathematical model for PGD, incorporating the effects of delayed nutrient uptake using delay differential equations. Plant biomass and nutrient concentration are the model's state variables. The delayed nutrient concentration is hypothesized to negatively impact plant growth. The analysis establishes the positivity of solutions, calculates a feasible internal equilibrium point, and investigates the system's

stability around this point. Interestingly, Hopf bifurcation is observed around a critical value of the delay parameter. MATLAB simulations support the analytical findings.

In chapter-3, A mathematical analysis of delay differential equations to understand the stability and bifurcation behaviour of plant growth systems: A two-compartment model, In the following chapter a novel mathematical model for PGD, considering separate root and shoot compartments. The model tracks two key variables: concentration of the nutrient and the structural dry weight of each compartment. Building on logistic growth principles, it explores how the root system supplies essential nutrients to the shoot. However, external and internal factors can impede this nutrient transfer, introducing a delay in nutrient consumption by the shoot. This delay, captured by a newly incorporated parameter, can damage the shoot's structural dry weight. The analysis investigates the system's stability around an internal equilibrium point. Interestingly, Hopf bifurcation emerges beyond a critical delay parameter value. Finally, the model's sensitivity to parameter variations is examined, with MATLAB simulations supporting the analytical results.

In chapter-4, A delay differential equation approach to investigate the impact of toxicity on plant growth patterns, In the given chapter, study leverages a mathematical model to investigate how delayed effects of toxicity impact plant growth under stress. The model demonstrates that toxic substances alter soil structure and microbial activity, leading to a decline in available nutrients. Since nutrient availability is crucial for biomass accumulation, plant growth suffers a double blow: both nutrient deficiency and direct toxicity. Notably, the detrimental effects of toxicity manifest after an incubation period, necessitating the inclusion of a delay parameter in the model's state variables. Interestingly, the model predicts a Hopf bifurcation at a critical delay value, suggesting the emergence of periodic oscillations in plant growth. Utilizing established techniques, the analysis explores the direction and stability of these newly formed periodic solutions. Furthermore, sensitivity analysis assesses the model's response to changes in parameter values.

In chapter-5, Analyzing the competitive dynamics of two plant populations under the influence of toxic decay. The chapter discussed a mathematical model to analyze the growth of competing plants under toxic stress. The model reveals that the presence of toxic compounds disrupts soil structure and activity, hindering the growth of these competitive plants. Both plant populations are assumed to follow logistic growth dynamics. Interestingly, the impact of toxicity is not immediate; it exhibits an incubation period captured by a delay

parameter (τ). The analysis establishes the positivity and existence of a non-zero equilibrium point. Furthermore, stability analysis around this equilibrium reveals a complex phenomenon – Hopf bifurcation – at a critical delay value (τc). By employing established methods, the study explores the direction and stability of the newly formed periodic solutions arising from this bifurcation. Sensitivity analysis is then conducted to assess the model's response to parameter variations. Finally, MATLAB simulations are utilized to validate the analytical findings.

List Of Abbreviations

Plant Growth Dynamics	PGD
Delay Differential Equations	DDEs
Mathematical Models	MM
Variational Iteration Method	VIM
Pollution Accumulation Model	PAM
Relative Growth Rate	RgR
Specific Growth Rate	SgR
Initial Value Problems	IVPs
Delay Parameter	DP
Hopf- bifurcation	HB
Interior equilibrium	IE
Critical Value	CV
Initial Value	IC

List of Published and Communicated Papers

- Pankaj Kumar and Davneet Kaur (2021). Bifurcation induced by delay parameter in plant growth dynamics. (Paper published in Journal of Physics: conference series 2021).
- Pankaj Kumar and Davneet Kaur (2022). Stability and Bifurcation Analysis of Plant Growth Dynamics using Delay Differential Equation: A Two Compartment Model. (Paper Accepted in IEEE conference MESIICON 2022), (Paper Published in Palestine Journal of Mathematics 2025)
- Pankaj Kumar and Davneet Kaur (2022). Analysis of plant growth dynamics under the effect of toxicity: A delay differential equation. (Paper Published in Malaysian journal of Science 2022).
- Pankaj Kumar and Davneet Kaur (2023). Studying the role of delay caused by toxicity in two mutual competiting plant population. (Paper Submitted in International journal of applied and computing mathematics 2025).

List of Conferences Attended

- Presented a paper as Poster Presentation entitled “Bifurcation induced by Delay Parameter in Plant Growth Dynamics” in 3rd International Conference on Recent Advances in Fundamental and Applied Sciences” (RAFAS 2021) held on 25th - 26th June 2021 at Lovely Professional University, Phagwara, Punjab, India.
- Presented a paper as Paper Presentation entitled “Stability and Bifurcation Analysis of Plant Growth Dynamics using Delay Differential Equation: A Two Compartment Model” in International Interdisciplinary Conference on Mathematics, Engineering and Science” (MESIICON 2022) held on 11th - 12th November 2022 Dr. B. C. Roy Engineering College, Durgapur.

Contents

List Of Figures

Chapter 1

General Introduction

1.1 Introduction:

Plant ecology delves into the intricate relationships between plants, other organisms, and their environment. It examines how plants disperse, thrive, and interact with the world around them. Plant ecology investigates how individual plants and populations respond to different environmental factors, including genetics, living organisms (biotic), and non-living elements (abiotic). This knowledge helps us cultivate high-quality food, animal feed, and plant life. As the ecosystem's primary producers, plants thrive based on the surrounding physical environment. The environment includes factors like sunlight, water availability, temperature, and the nutrients present in the soil and the availability of these essential elements [light, water, temperature, nutrients] is further influenced by a complex interplay of factors. The interplay includes the size and efficiency of plant leaves (leaf-area ratio and net assimilation rate), the movement of water through the soil (leaching and runoff), the breakdown and storage of organic matter, and the activity of soil microbes (mineralization and immobilization of nutrients). Soil, a vital medium for plant growth, is a complex mixture of organic and mineral components. Organic matter, like decomposed plants and microorganisms, enriches the soil. Minerals, on the other hand, originate from the breakdown of rocks through weathering. Plants anchor themselves within the soil, which acts as a nurturing reservoir. It provides them with the essential moisture and nutrients they need to flourish and produce beautiful flowers and fruits. The exchange of nutrients between soil and plants isn't just a one-on-one interaction. The effects of are evident at all levels of plant organization, from individual plants to entire ecosystems. Nutrients directly impact the growth of individual plants, which in turn influences the dynamics of plant populations. This ultimately affects the overall success of crop production. As the global population grows, so does the demand for food, leading to intensified agriculture and industry, which puts a strain on soil, a crucial filter for pollutants. Unfortunately, this has resulted in the decline of soil quality and quantity, a phenomenon known as soil degradation. A variety of factors contribute to soil degradation, including erosion, salinization, contamination, and

changes in soil properties. The causes of soil degradation are often multifaceted, involving a combination of factors. Toxic chemicals in the soil wreak havoc on forests, agricultural crops, and all types of vegetation. These contaminants destroy the plants' natural characteristics and hinder their ability to produce. Heavy metal ions can directly interfere with tree metabolism, particularly impacting root physiology. This disrupts nutrient uptake, potentially reducing the tree's health and growth. Zinc (Zn) and Copper (Cu) are essential micronutrients, not macronutrients, required by plants in small but crucial amounts for optimal growth. While they play a vital role, they are naturally found at very low concentrations in soil. In contrast, some metals like cadmium (Cd), nickel (Ni), chromium (Cr), arsenic (As), mercury (Hg), lead (Pb), and selenium (Se) are harmful to plants, even at low levels. Soil acidification arises from a multitude of factors, including the improper disposal of municipal and industrial waste, the overuse of chemical fertilizers, pesticides, insecticides, and herbicides, atmospheric pollutants settling on the land, and the discharge of untreated wastewater. It causes soil acidification and increases heavy metal concentrations. This accumulation of heavy metals is a major contributor to the decline in plant growth. Among the most prevalent heavy metals in soil is cadmium (Cd). Plants readily absorb cadmium, hindering the growth and nutrient uptake of agricultural crops like barley. Acid rain disrupts soil properties, impacting root growth and function. Soil acidification elevates inorganic aluminium levels in the root zone. At sublethal concentrations, this aluminium disrupts the rate at which roots take up essential nutrients. At lethal concentrations, it significantly increases root death. Soil acidification, caused by an increased level of acidity entering the system, can trigger leaching of nutrients. This leaching process can damage plant roots, hindering their ability to absorb essential elements. Studies have shown that xenobiotics, particularly agricultural pesticides, can accumulate in soil. The contaminants are toxic to soil organisms, hindering seed germination and suppressing plant growth. Acid rain, a major cause of soil acidification, disrupts the balance of ions in the soil, which can lead to an increased exchange of hydrogen ions with nutrient cations, causing them to be leached out of the soil more rapidly. As soil pH declines due to acid rain, the concentration of heavy metals taken up by plants generally increases, because lower pH creates conditions that favour the release of metals from the soil and their subsequent absorption by plant roots. In simpler terms, the more acidic the soil (lower pH), the more metals plants tend to accumulate. India, a nation where agriculture is

the backbone of the economy with roughly 70% of its population relying on farming, faces a critical challenge. To ensure food security for such a large population, farmers often resort to intensive use of pesticides, insecticides, herbicides, and chemical fertilizers, aiming to boost crop yields. India's reliance on intensive chemical use in agriculture, including pesticides, insecticides, herbicides, and fertilizers, presents a complex challenge. While this approach aims to increase crop yields and feed a large population, it can have unintended consequences. Excessive use can lead to soil degradation, reducing fertility and ultimately crop yields. Additionally, these chemicals can accumulate in crops, potentially introducing harmful heavy metals and toxins into the food chain, posing a risk to human health. It's become clear that both individual plants and entire populations face a multitude of stressors includes limited nutrient availability, soil acidification (leading to lower pH), fluctuating temperatures, drought conditions, and the presence of harmful elements in the soil like salts, aluminium, heavy metals, and other toxic chemicals. These environmental stressors take a toll on plants in various ways, hindering their growth and yield. Some of the adverse physiological effects include stunted leaf area development, restricted root growth, and premature canopy senescence. In research, modeling plays a vital role. It allows scientists to Integrate existing knowledge from various sources and test hypotheses in a quantitative way (using numbers and data). To effectively build a model, researchers first need to clearly define the system they are studying. In horticulture and agriculture, modeling often focuses on individual plants or, more commonly, groups of interacting plants, such as rows or entire crop canopies. Many researchers incorporate time delays into biological models to reflect real-world scenarios. Unlike a model with instant response, real plants and populations don't react immediately to changes within their own group. Instead, there's a time lag before the effects become evident. Several factors can introduce time delays in plant growth, such as the presence of toxic metals in the soil, the rate at which plants utilize nutrients (utilization coefficient), and the overall efficiency with which they use nutrients (nutrient use efficiency). Mathematical models that account for these time delays, called DDEs, are significantly more complex than those of ordinary differential equations. The presence of a time delay can destabilize a previously stable equilibrium in plant growth, causing fluctuations. Investigating the effects of time delays on plant growth in the presence of toxic metals is an emerging and promising area of research.

Mathematical models in ecology don't simply copy reality; rather, they cleverly combine environmental and ecological data to represent real-world processes. When building mathematical models of natural phenomena, scientists must focus on the most relevant variables and factors. The sheer number of variables in the real world makes it impossible to include everything. By carefully selecting these key elements, researchers can gain a logical understanding of how the system behaves. The research investigates how time delays in plant growth dynamics, caused by factors like toxic soil contaminants, affect plant health and yield using mathematical models. These models will quantify the damage mechanisms and yield reductions caused by these toxins.

1.2 Review of Literature

The quest to understand how plants grow stretches far back in history. Even nomadic societies in ancient times noticed that crops planted during specific seasons yielded more food compared to others. While the link between seasons and plant growth was recognized much earlier, Leonardo da Vinci, during the Middle Ages, took a pioneering step. He was the first to systematically observe seasonal growth patterns and certain characteristics of plant form. Building on this foundation, the 17th century saw the emergence of theories about how leaves arrange themselves on stems and axes. Laying the groundwork for rhizosphere models, in the model the study of plant-soil interaction began with Hiltner's (1904) pioneering single-root model, which focused on nutrient uptake by roots [1]. Pioneering work by Dalton and Gardner (1975) in the 1960s and 1970s laid the foundation for modeling water uptake by single roots [2]. Temperature, respiration, humidity, radiation, photosynthesis, transpiration and carbon dioxide are all key environmental factors that influence a plant's growth. In 1976, Thornley broke new ground by developing the first mathematical models that incorporated the individual and combined effects of these environmental factors on plant growth. Watkinson (1980) [3]- [4] introduced a ground breaking theoretical model that captured the dynamics of plant growth. The model considered three key factors such as Growth rate slows down as a plant approaches its maximum size. Plants within a population naturally exhibit differences in size and growth potential. As plant density increases, competition for resources intensifies, particularly affecting smaller plants, potentially reducing their growth and leading to mortality. Gifford and Evans (1981) [5] emphasized the critical role of soil properties

and water availability in maximizing plant and crop yield through breeding programs. Miller (1984) [6] proposed a key principle: if the concentration of nutrients in long-lasting plant tissues remains stable (indicating efficient nutrient use), then the amount of nutrients a plant contributes to the overall ecosystem is directly proportional to the accumulation of biomass in those long-lived tissues. Reynolds and Acock (1985) [7] raised concerns about the long-term consequences of rising global carbon dioxide concentrations. Their analysis suggests that these increases could have detrimental effects on both agricultural productivity and the health of natural ecosystems. Valentine (1985) [8] proposed a novel approach to understanding tree growth. The model simplifies a tree into a network of pipes, each experiencing constant growth. Makela (1986) criticized that the partitioning coefficients defined by Reynolds and Thornley, are only applicable to models that assume equal turnover rates of root and shoot. Expanding on Partitioning Coefficients: Makela (1986) provided a more general approach to these coefficients, encompassing the models by Reynolds and Thornley as a specific case. Building on this, Pugliese (1988) [9]-[10] delved into age-dependent plant growth, proposing a continuous model that incorporates both growth and reproduction. Kickert and Krupa (1991) [11] broke new ground by proposing and analyzing models applicable to a wider range of vegetables, moving beyond individual plant species. Czaran and Bartha (1992) [12] pioneered the study of spatiotemporal dynamic models for plant populations and communities. Thornley (1995) [13] delved into root-shoot allocation in plants using mathematical modeling. He compared two approaches: the transport-resistance method and the teleonomic method. The analysis considered both steady-state growth (constant plant size) and exponential growth (continuously increasing plant size) to evaluate the effectiveness of each approach under different growth scenarios. Thornley (1997) [14] introduced a powerful two-compartment MM for plant growth. The model incorporates two key processes: transport and chemical conversion. Its strength lies in its ability to align well with both theoretical observations and practical applications. In 1998, Thornley [15] proposed a novel mathematical model based on transport resistance. The model tackles the allocation of nitrogen and carbon within the plant, specifically focusing on the root and shoot compartments. Thornley (1999) [16] took plant modeling a step further by proposing a mathematical model that specifically examines how stem height and diameter growth are interrelated in plants. Deleuze and Houllier (1997) [17] proposed a comprehensive model that tackles two key challenges in

understanding wood growth. First, it incorporates the Münch theory, which explains how carbon translocation affects total wood production. Second, the model addresses the factors influencing stem form and wood quality. Diekmann et al. (1998) [18] made significant strides in the field of population modeling by formulating and analyzing general deterministic structured population models. Somma et al. (1998) [19] broke new ground by developing a comprehensive three-dimensional model that integrates several crucial processes: simultaneous growth of roots, water and nutrient uptake by plants, along with water and solute transport within the soil. The past 30 years have witnessed a dramatic rise in global food production, fuelled in large part by technological innovation. Khush (1999) [20] highlights the development of high-yielding wheat and rice varieties as a prime example of this progress. Lacointe (2000) [21] pointed out limitations in applying Thornley's models universally. The analysis suggests that these models might be too specific and may not be adaptable to a wide variety of plant types or growth conditions. Tinker and Nye (2000) ushered in a new era of plant-soil modeling by incorporating root hairs into their models. Luis Garcia-Barrios et al. (2001) [22]-[23] showed how mathematical models of growth of mixed crop in combination with empirical data can reduce the time and investment required for the task. The study shows how plant arrangement and varied sowing times in intercropping significantly influence the ecological relationships between the crops which in turn, affects the overall health and productivity of the intercropping system. To understand plant community dynamics, Bolker et al. (2003) investigated a model that incorporates spatial factors [24]. Hedden's research in 2003 identified the genes responsible for the dwarfing trait in crops, a key factor in the significant rise of wheat and rice yields [25]. Ioslovich and Gutman (2005) proposed a plant growth model that accounts for the gradual shift from vegetative to reproductive stages. Their model considers the varying efficiency of photosynthesis depending on whether energy is directed towards growth or reproduction [26]. Valentine and Mäkelä (2005) developed a unique tree growth model that bridges the gap between process-based and empirical approaches. This model can function in both detailed (process-based) and data-driven (empirical) modes [27]. Verkroost and Wassan (2005) created a straightforward plant growth model that confirmed the well-established linear relationship between a plant's relative growth rate and its nitrogen content [28]. Vance and Nevai (2007) developed a mathematical model to simulate plant population growth while considering competition for light within a plant canopy [29]. Their model acknowledges the

crucial role of gibberellin (GA), a plant hormone essential for the growth and development of flowering plants. Overman (2008) developed two mathematical models using analytical functions to link plant biomass accumulation with the uptake of mineral nutrients (nitrogen, phosphorus, and potassium) [30]. Harberd et al. (2009) investigated how plants utilize the hormone gibberellin (GA) to overcome growth arrest and enhance their adaptability in challenging environments. Fowler et al. (2009) developed a mathematical model that predicts tree growth patterns by simulating how trees allocate and store carbon [31]-[32]. Liu et al. (2010) introduced a spatial plant growth model that analyzes and predicts how plant populations arrange themselves spatially [33]. They combined mathematical techniques with computer simulations to achieve this. In their research on modern rice breeding, Asano et al. (2011) highlighted the semi-dwarf phenotype as a crucial agronomic trait for Oryza sativa L. (cultivated rice) [34]. Pingali (2012) examined the Green Revolution's impact on productivity, environmental factors, and economic aspects, highlighting its successes and failures [35]. Importantly, nitrogen availability is critical for both photosynthetic canopy growth and crop yield. Quilliam et al. (2012) demonstrated that amending soil with biochar can yield a triple benefit: improved soil quality, reduced nutrient leaching, and increased crop yields [36]. Clough et al. (2013) conducted a critical review of biochar-nitrogen research, highlighting both emerging trends and existing knowledge gaps [37]. The research plays a critical role in sustainable agriculture and climate change mitigation. Clark et al. (2014) addressed a challenge in predicting the impact of global warming on plant growth. By combining discrete observations of growing seasons with continuous data on temperature variations, they developed a method to forecast how rising temperatures will accelerate the start of plant growth [38]. Hawkesford (2014) highlighted that maximizing crop production goes beyond simply supplying nitrogen. The study emphasizes that strategically capturing and efficiently utilizing nitrogen is key to optimizing the consumption of this crucial macronutrient [39]. Vanderwel and Purves (2014) employed a straightforward data model to forecast significant changes in forest ecosystems across the United States over the next 500 years [40]. Unlike many researchers who focus on soil phosphorus loss, King et al. (2015) emphasized the importance of the quantity and quality of phosphorus leaching below the surface soil layer, their work highlights the negative impact of this sub-surface phosphorus loss on plant growth [41]. Serrano-Mislata et al. (2017) revealed that DELLA proteins regulate both stem growth and the size of the

inflorescence meristem, the region where flowers develop [42]. A study by Paxson and Simon (2017) demonstrated that computers can be used to directly control and monitor plant growth [43]. Sanderman et al (2017) analyzed archived soil samples from crop rotations. The findings indicated a direct link between increased biological activity, faster carbon cycling, and higher rates of carbon stabilization in the soil [44]. In a 2018 review, Dahiru examined the influence of key growth regulators – abscisic acid, auxin, cytokinin, ethylene, and gibberellins – on plant growth [45]. Additionally, Ciereszko's 2018 research highlighted the crucial role of sugar in plant defence mechanisms [46]. Prior to the 1970s, MM weren't widely used to assess the impact of toxins on populations. Pioneering research by Bazzaz et al. (1974) investigated the effects of cadmium on photosynthesis and transpiration in excised corn and sunflower leaves, exemplifying this new approach. Bazzaz et al. (1975) investigated how lead exposure inhibits photosynthesis in corn and sunflower plants. Hewitt (1979) dedicated the final two chapters of his book to exploring the role of various elements in plant health [47]-[49] included one essential element (chlorine), three elements with beneficial but non-essential roles (silicon, cobalt, and vanadium), and a group of elements with potential toxicity (iodine, bromine, fluorine, aluminium, nickel, chromium, selenium, lead, and cadmium) along with other heavy metals. Rodecap and Tigey (1981) investigated how cadmium disrupts various plant processes, leading to reduced growth [50]. Hallam et al. (1983) proposed a two-part modeling framework to understand the impact of toxicants on plant populations at the system level. Their first model [51] depicted the effects of chronic or acute toxicant doses, while their second model [52] focused on the interaction between toxicants and plant populations, highlighting the detrimental effects of pollutants. Building on their previous work on exposure pathways, Hallam and de Luna (1984) explored how toxicants affect populations exposed through both environmental and food chain contamination [53]. Subsequently, de Luna and Hallam (1987) developed a set of three general models for toxicant-population interactions, each incorporating three key variables: population size, internal toxicant concentration within organisms, and external environmental toxicant concentration [54]. Gatto and Rinaldi (1987) employed MMs to demonstrate that even small variations in human exploitation of a natural forest can trigger dramatic changes in its overall biomass [55]. Shukla et al. (1989) developed a model demonstrating that rising industrial pollution threatens forest biomass with extinction, highlighting reforestation as a critical solution [56].

While Wolf et al. (1989) investigated long-term crop responses to fertilizer and nitrogen using modeling techniques, Freedman and Shukla (1991) focused on the impact of toxicants on ecological systems. Their study employed models to explore how single influxes, constant doses, and periodic doses of toxins affect both single-species growth and predator-prey dynamics [57]- [58]. De Leo et al. (1993) developed a MM that combined soil chemistry with tree biomass to analyze the impact of proton concentration on equilibrium states. In contrast, Brune and Deitz (1995) employed a more direct approach. Their experiment exposed barley seedlings in a controlled hydroponic environment to toxic levels of various heavy metals, revealing distinct effects on the elemental composition of leaves and roots [59]-[60]. Shukla et al. (1996) employed a MM to investigate how rising industrial pollution translates to a decline in resource biomass density [61]. The model suggests that this decrease in biomass can ultimately lead to the extinction of species reliant on those resources. While Curtis and Wang (1998) used meta-analysis to examine the effects of elevated CO2 on various aspects of woody plants, including biomass, gas exchange, and leaf composition [62], Bonnet et al. (2000) investigated the impact of a different element, zinc, on the growth and chlorophyll content of ryegrass [63]. Highlighting a major challenge for plant growth in acidic soils, Mossor-Pietraszewska (2001) identified aluminium toxicity as a key culprit [64]. In a separate study, Pishchik et al (2002) explored potential solutions for cadmium contamination and the experiment investigated the use of plant growth promoting rhizobacteria to achieve ecologically safe barley production in cadmium-polluted soils [65]. Dubey et al. (2003) focused on a specific mathematical model to analyze how industrialization and pollution impact the resource biomass of plants and trees [66]. In contrast, Van Ittersum et al. (2003) presented a broader perspective, providing an overview of various crop and crop-soil modeling approaches used at Wageningen University [67]. Researchers have explored various factors influencing plant growth using diverse methods. Shenker et al. (2004) investigated the impact of manganese nutrition on tomato growth and chlorophyll concentration [68]. Dercole et al. (2005) took a more theoretical approach, formulating a mathematical model that incorporates the effect of leaf shading using partial differential-integral equations [69]. Meanwhile, Sheldon and Menzies (2005) employed a controlled environment experiment to study the effects of copper toxicity on the growth and root structure of Rhodes grass [70]. Mathematical modeling offered distinct approaches to understanding plant interactions with pollutants. Thomas et al.

(2005) proposed a model simulating how plants absorb metals from soil for phytoremediation purposes [71]. In contrast, Naresh et al. (2006) developed a model to analyze the impact of intermediate toxic byproducts on plant biomass growth [72]. Several studies in 2007 explored various aspects of plant growth under challenging conditions. Lauchli and Grattan (2007) provided a comprehensive review of how salinity affects the growth and development of crop plants [73]. Verma et al. (2007) focused on a specific contaminant, developing a model to predict cadmium accumulation in spinach, radish, carrot, and cabbage [74]. Wu et al. (2007) took a modeling approach to understand water and heat transport within a soil-mulch-plant-atmosphere system, applying it to winter wheat cultivation [75]. Researchers have investigated various ecological interactions in polluted environments using mathematical models. Liu and Zhang (2008) analyzed the persistence and stability of an N-species food chain model incorporating a feedback control system, applicable to polluted environments [76]. Shukla et al. (2009) developed a nonlinear model that considers the simultaneous impact of a toxicant on both populations and resources within an ecosystem [77]. In a separate study, Hayat et al. (2010) focused on plant physiology, using modeling to explore how salicylic acid influences various plant growth and development processes [78]. Heavy metal contamination in plants has been a concern due to its impact on ecosystems. Nagajyoti et al. (2010) conducted a study on the occurrence and harmful effects of heavy metals in plant life, emphasizing their environmental significance [79]. Singh and Agrawal (2010) investigated a potential source of such contamination, studying the suitability of using sewage sludge as fertilizer for mung bean plants [80]. The research evaluated how different application rates of sewage sludge affected plant growth, yield, and the accumulation of heavy metals [80]. While Sinha et al. (2010) developed a mathematical model to explore how competition between two plant species is affected by both a toxicant and an infectious disease [81], Tsonev and Lidon (2012) employed a more direct approach, measuring the degree of plant injury caused by elevated zinc concentrations. Similarly, Mishra and Kalra (2012) focused on modeling the impact of toxic metals on individual plant growth using a two-compartment MM [82]-[83]. Highlighting the challenges of industrial activity on plant health, Ahmad et al. (2013) identified the uptake of non-essential elements like chromium alongside essential nutrients as a key factor in reduced crop growth and biomass [84] and concern was further emphasized by Guo et al. (2013), who investigated the presence of heavy

metals in both soil and agricultural products near an industrial district [85]. Researchers have employed various methods to investigate the impact of heavy metals on plants. Pavel et al. (2013) conducted a controlled experiment to evaluate the phytotoxicity of chromium and cadmium in Lepidium Sativum [86]. Misra and Kalra (2013) used a mathematical modeling approach with two compartments to analyze the influence of toxic metals on a plant's structural dry weight [87]. In contrast, Shukla et al. (2013) adopted a broader perspective, developing a nonlinear model to study how acid rain forms in the atmosphere and affects plant species [88]. Phosphorus management is crucial for sustainable agriculture. Gupta et al. (2014) emphasized the importance of proper phosphorus fertilizer practices to optimize plant uptake and minimize environmental losses [89]. In a related study, Bedbabis et al. (2015) conducted a ten-year field experiment in Tunisia to compare the effects of well water and treated wastewater irrigation on an olive orchard [90].

While a field experiment (mentioned previously) showed no significant impact of water quality on standard quality indices and oil content, other studies explored different environmental stress factors on plants. Boros and Micle (2015) investigated sunflower (Helianthus annuus) tolerance to copper, examining its effects on seed germination and plant growth [91]. In a separate theoretical approach, Sundar and Naresh (2015) developed a nonlinear dynamical model to analyze how biological populations survive under environmental pollution [92]. Several studies have examined how plants respond to heavy metals in the environment. Cu (2015) conducted a field experiment in Vietnam to directly assess the impact of heavy metals on soil, water, and plant biomass [93]. Chi Peng et al. (2016) adopted a modeling approach, developing a pollution accumulation model (PAM) to simulate long-term changes in soil heavy metal concentrations [94]. In contrast, Mustafa and Komatsu (2016) focused on plant tolerance mechanisms, highlighting the various strategies plants have evolved to cope with the accumulation of heavy metals alongside essential nutrients from the soil [95]. Mathematical modeling has been applied to understand the impact of pollution on various ecological components. Kumar et al. (2016) proposed a model to analyze how a toxicant affects biological populations, considering scenarios where some species are already under stress from the toxicant [96]. In a separate study, Sundar et al. (2017) developed a model to explore how industrialization that depends on population and population density affects forestry

resources [97]. Yan et al. (2018) investigated the potential ecological risks associated with heavy metal accumulation during the anaerobic co-digestion of plant matter [98] and the study investigated how varying initial substrate concentrations, digestion temperatures, and plant material ratios influenced.

While DDEs have a rich history dating back over 200 years, their initial applications emerged in geometry and number theory. However, it wasn't until after 1940 that they gained significant traction due to their powerful applications in engineering systems and control theory. Building upon the foundational concepts presented in Chapter II of the book "Delay-Differential Equations" (1966) [99], which established a general theory for this mathematical field, Mackey and Glass (1977) applied these equations to a specific biological domain. Their work explored the use of first-order, nonlinear DDEs to model the dynamics of respiratory systems [100]. Research in DDEs has explored diverse applications. The equations themselves can exhibit complex behaviours, including limit cycle oscillations and chaotic solutions, as demonstrated in earlier work [equations displayed]. Mackey and Glass (1979) further explored this field by developing a mathematical model that explores how a biological oscillator can synchronize with an external sinusoidal stimulus [101]. In a separate vein, Cooke and Grossman (1982) highlighted the importance of considering time delays inherent in various systems, including biological, physical, and social phenomena [102]. The field of delay-differential equations has applications in ecology. Donald et al. (1992) explored the theoretical and practical aspects of using these equations to understand populations and ecological systems, considering the characteristics of individual organisms [103]. In a complementary resource, Gopalsamy's (1992) book provided a survey of recent progress in understanding the stability and oscillatory behavior of autonomous DDEs, which are relevant to ecological modeling [104]. DDEs offer a powerful tool to analyze population dynamics. Kuang's (1993) book provided a comprehensive exploration of this field, encompassing both autonomous and non-autonomous systems with time delays [105]. The book delved into critical topics such as stability, population coexistence, and oscillatory behavior in these systems. Belair et al. (1995) applied these concepts by developing an age-structured model for erythropoiesis (red blood cell production) that could be reduced to a system of DDEs with two delays [106]. Roussel (1996) [107] used DDEs in Chemical Kinetics. He (1997) [108] concluded that for analytical approximate solutions of DDEs, the VIM

can be very useful. Li et al (1999) [109] studied the stability and bifurcation of DDEs involving two delays. DDEs pose analytical challenges, but researchers have developed methods to address them. Engelborghs et al. (2000) established numerical methods and software tools specifically for analyzing bifurcations in these equations [110]. This aligns with the approach taken by Bocharov and Rihan (2000), who emphasized the importance of DDEs for modeling biological phenomena and advocated for numerical approaches to solve them [111]. While Ruan and Wei (2001) delved into the mathematical analysis of third-degree transcendental polynomials [112], other researchers focused on computational tools for DDEs. Shampine and Thompson (2001) developed a MATLAB code, DDE23, specifically designed to solve equations with constant delays [113]. Engelborghs et al. (2002) built upon this concept by creating DDE-BIFTOOL, A MATLAB-based software package designed to analyze bifurcations in systems of delay differential equations with fixed, discrete time lags [114]. Researchers have explored various applications of DDEs, particularly in population dynamics and nonlinear systems. Kubiaczyk and Saker (2002) investigated oscillation and stability within these equations in the context of population models [115]. Kuznetsov (2004) adopted a broader approach, studying how nonlinear dynamical systems and their bifurcations can be analyzed using DDEs by varying parameter values [116]. Lenbury and Giang (2004) specifically focused on applying DDEs to model population growth dynamics [117]. While these studies concentrated on applications, Li and Wei (2005) took a more theoretical approach, analyzing the distribution and properties of roots in fourth-degree exponential polynomials [118]. Time delays are an important concept in biological modeling. Ruan (2006) explored how time delays of various forms can be incorporated into models that analyze the dynamics of single-species populations [119]. This area of research aligns with the book by Erneux, which provides a comprehensive resource for researchers in biology, engineering, and other fields who leverage mathematical and statistical modeling in their work [120]. DDEs present unique analytical challenges. Roose and Szalai (2007) addressed this by focusing on continuation and bifurcation analysis, which are methods for exploring how solutions change under varying conditions [121]. In contrast, Balachandran et al. (2009) took a more computational approach, developing a new code specifically designed to solve DDEs numerically [122]. While these studies aimed to solve and analyze delay-differential equations, Zhang et al. (2009) explored a distinct mathematical area, analyzing the

distribution and properties of roots in fifth-degree transcendental polynomials [123]. The field of DDEs offers a rich history and diverse applications. Smith's (2011) book provides a foundation for understanding this field, equipping readers with the essential tools to delve into its historical development and explore its use in various models [124]. In a more specific vein, Mallet-Paret and Nussbaum (2011) analyzed a particular class of autonomous DDEs with state-dependent delays, focusing on solutions exhibiting linear asymptotic stability [125]. While stability analysis is crucial in DDEs, the presence of time delays can pose challenges. Sieber and Szalai (2011) addressed this by proposing a method to modify the characteristic matrix, a mathematical tool used for stability analysis, to improve its accuracy [126]. Their approach involved strategically positioning the poles (important factors in the analysis) within a small region near the origin of the complex plane. In a complementary study, Wolfrum et al. (2011) investigated the dynamical properties, such as stability of stationary points (equilibrium states), in DDEs where the time delays are very large [127]. DDEs are powerful tools for modeling various phenomena, but their analysis can involve numerical and theoretical challenges. Kuang (2012) provided a practical guide on using the popular MATLAB solver dde23 (developed by Shampine and Thompson) to numerically solve these equations and perform stability analysis [128]. This approach complements the work of Huang et al. (2016) who focused on the global stability analysis of specific nonlinear DDEs by analysing global stability used in population dynamics [129]. Meanwhile, Berezansky and Braverman (2016) investigated a different analytical property, studying boundedness and persistence in delay-differential equations with mixed nonlinearities [130]. A landmark paper by Hopf (1942) introduced the concept of Hopf bifurcation. It describes a scenario where a system transitions from an equilibrium state to a periodic oscillation (like a self-excited oscillation) as a parameter undergoes a critical change [131]. This bifurcation occurs mathematically when a pair of complex eigenvalues become purely imaginary, limiting Hb to systems with at least two dimensions.

Hopf bifurcation is a critical concept in dynamical systems. Marsden et al. (1978) provide a comprehensive analysis of Hb, exploring its mathematical details, applications, and stability calculations [132]. Highlighting its practical applications, Hsu and Hwang (1999) employed Hopf bifurcation to study a well-established

ecological model, the Holling-Tanner predator-prey system [133]. Their work demonstrates how Hb can be used to analyze transitions in ecological dynamics. Hb, a critical transition in dynamical systems, can be influenced by time delays. Reddy et al. (1999) conducted a detailed study on how time delays affect the collective dynamics of coupled oscillators undergoing Hb [134]. In a complementary theoretical approach, Manfredi and Fanti (2004) examined the relationships between stability theorems and the classifications of Hb (simple and general), providing clarity on the mathematical underpinnings of this phenomenon [135]. Hb is a valuable tool for analyzing transitions in population dynamics. Wei and Li (2005) investigated the occurrence of Hb in Nicholson's blow-flies equation, demonstrating how increasing time delays beyond a critical point can trigger periodic oscillations in the blowfly population [136]. Similarly, Gupta and Chandra (2013) applied Hb analysis to a modified Leslie-Gower predator-prey model, incorporating the influence of non-linear prey harvesting on the system's stability [137]. These studies highlight the versatility of Hb in understanding population dynamics with time delays and external pressures. Researchers investigated the phenomenon of Hb in various systems likely Xiao et al (2013) [138] analyzed how varying the interaction parameter in a neural network model triggers Hb. Zhang and Guo (2013) [139] applied the centre manifold theorem to study the direction and stability of Hb in the classic Van der Pol equation. Wang et al (2014) [140] employed normal-form theory and the centre manifold theorem to explore the direction and stability of Hb within a phytoplankton-zooplankton model.

Dickinson and Galinas (1976) [141] introduced the "Direct Method" to analyze how sensitive solutions of ODEs are to imprecise parameters and method relies on calculating partial derivatives with respect to those parameters. Building on this concept, Baker and Rihan (1999) [142] developed a new method specifically for DDEs. The method estimates the sensitivity of variables to both model parameters and non-linearity effects. Frey and Patil (2002) [143] compared and categorized existing sensitivity analysis methods used across various scientific fields. Their work provided a valuable guide for selecting the most appropriate method for a specific application. Rihan (2003) [144] focused on models with time delays. He developed a general theory for sensitivity analysis using both adjoint equations and direct methods, assuming constant model parameters. Caswell (2007) [145] introduced a powerful approach using matrix calculus to analyze how sensitive transient population

dynamics are to changes in various factors. Kepler (2010) [146] employed both the adjoint method and the direct method for sensitivity analysis of mathematical models, allowing for a comprehensive exploration of model behavior. Perumal and Gunawan (2011) [147] caution that uncritical application of parametric sensitivity analysis can be misleading. It may not reveal the true dynamics of the system and could even lead to erroneous results. Rihan (2013) [148] delves into the application of DDEs in dynamical systems. Their exploration encompasses computational tools, parameter estimation techniques, and sensitivity analysis methods relevant to these systems. Wu (2014) proposed a novel methodology for sensitivity analysis within functional-structural plant models (FSPMs) in his thesis [149]. The approach aimed to gain deeper insights into the biological processes governing plant growth. Ingalls et al. (2017) [150] introduced a novel method for sensitivity analysis of DDEs. The method focuses on parameter sensitivity and its role in understanding the direction of long-term evolutionary change within systems governed by DDEs. While DDEs offer a powerful tool for modeling time-delayed effects, their application in plant physiology to understand the impact of toxicants on growth dynamics remains relatively limited. Only a few studies have leveraged this approach. Dubey and Hussain (2004) addressed the detrimental effects of environmental pollution on forestry biomass through a mathematical model [151]. The work incorporates time delays within a diffusive system to analyze the dynamics of this adverse impact. Pastor and Walker (2006) proposed a mathematical model to explore the link between delayed nutrient cycling and population fluctuations. The model suggests that time lags associated with nitrogen release from decaying litter can trigger population oscillations [152]. Naresh et al. (2014) employed DDEs to construct a mathematical model. This model investigates the delayed effects of toxicants on plant biomass, allowing for a deeper understanding of this critical relationship [153].

1.3 Proposed objectives of the study

On the basis of literature review and research gaps, the following objectives have been proposed in this present study:

1. To perform stability and bifurcation analysis of model for plant growth dynamics using delay differential equations.
2. To perform stability and bifurcation analysis of plant growth dynamics with root shoot compartments model using delay differential equations.

3. To perform stability analysis, sensitivity analysis and directional analysis of plant growth dynamics under the effect of toxicity using delay differential equation

1.4 Foundational Plant Physiology Concepts for Research work

1.4.1 Structure and Storage

Plant models inherently involve significant simplifications of real systems. One such simplification, grounded in physiological relevance, partitions plant material into two primary categories: structural and storage compartments [3].

We denote the total dry weight of the plant by W. Let Ws and Wr represent the dry weights of the structural and storage compartments, respectively. Mathematically, this relationship is expressed as:

$$W = Ws + Wr. \tag{1.1}$$

If we define "growth" solely in terms of dry matter accumulation, then differentiating Eq. (1.1) with respect to time, t, yields the following equation Eq. (1.2) and also reveals that the total growth rate, represented by $W'(t)$, is comprised of two contributing factors

$$W'(t) = W_s'(t) + W_r'(t). \tag{1.2}$$

- The rate of change in structural dry weight, $W_s'(t)$;
- The rate of change in storage dry weight, $W_r'(t)$.

The total growth rate of a plant, W'(t), is determined by the combined effects of the structural growth rate $W_s'(t)$, and the storage growth rate $W_r'(t)$, as shown in Eq. (1.2). Interestingly, this equation allows for the possibility of a negative total growth rate even when the structural growth rate is positive. It can occur if the rate of depletion from storage $W_r'(t)$ (negative) outweighs the contribution of structural growth. The concept can be illustrated by overnight plant growth. During this period, many plants tap heavily into storage materials for immediate needs, leading to a significant decline in storage dry weight $W_r'(t)$ (negative). However, structural growth $W_s'(t)$ (positive) can still occur. Despite this, overall dry weight might decrease due to respiration. Physiologists traditionally use the symbol RgR (Relative Growth Rate) or SgR (Specific Growth Rate) to quantify this phenomenon. Mathematically, RgR is defined by Eq. (1.3):

$$R_G = \frac{1}{W} W'(t). \tag{1.3}$$

Eq. (1.3) shows that RgR is calculated by dividing the total growth rate W'(t) by the total dry weight (W) of the plant at a specific time. This dimensionless quantity provides a standardized measure of growth rate relative to the plant's size. While Specific Growth Rate (SgR), defined

by Eq. (1.3), considers the total dry weight (W) of the plant, it may be more informative to track structural growth specifically. To address this, we can define the

$$\mu_G = \frac{1}{W_G} W_G'(t). \tag{1.4}$$

Specific Structural Growth Rate (SSgR), denoted by SSgR, as shown in Eq. (1.4).

1.4.2 Source and Sink strength

The source strength of a region reflects the net flow of a quantity (material, energy, etc.) exiting that region. It can be entirely determined by analyzing the transport processes occurring at the region's boundaries. Mathematically, source strength is defined as

F_X =Net rate at which X is transported out of that region of the plant;

Sink strength is the negative of source strength, so that if F_X is negative, then a sink of size $-F_X$ is operating.

1.4.3 Utilization of Substrate

The section explores a frequently employed concept in plant models: the phenomenological substrate utilization equation. The equation captures the dependence of plant organ growth and development on the sufficient availability of essential substrates.

Rectangular Hyperbola (Single Substrate)

For plant modelers, the Michaelis-Menten relation stands as one of the most valuable single equations. This equation, familiar to biologists, finds wide applicability when a process hinges on the concentration of a single substrate. The Michaelis-Menten relation expresses the rate of substrate utilization as:

$$U = \frac{kX}{K+X}. \tag{1.5}$$

Where k and K are constants and the symbol X denotes the density of the substrate X.

1.4.4 Translocation

Essential for growth, plant transport systems facilitate the movement of materials to specific utilization sites. While many transport mechanisms themselves are fundamentally non-polar, the overall process exhibits polarity due to the spatial arrangement of sources (where materials are produced) and sinks (where they are utilized). Interestingly, this polarity determines the direction of transport, and it can be reversed by altering the relative strengths of these sources and sinks.

1.4.5 Light Interception by Plants and Crops

A critical aspect of many plant and crop growth models involves simulating the interaction with the light environment. This interaction determines the light flux density (amount of light energy per unit area per unit time) received by various plant or crop surfaces. Light availability significantly influences growth patterns and extent through its role in photosynthesis.

Let I_0 represent the uniform light flux density incident on a field of area A_f. If J_0max denotes the maximum light available for absorption by the plant canopy, then...

Here's what's changed:

- Replaced "concerned with" with "involves simulating" for a more active tone.

$$J_0 = A_f I_0. \tag{1.6}$$

- Defined light flux density for clarity.
- Explained the role of light availability in photosynthesis and growth.
- Introduced notation for clarity (I_0 for incident light flux density, A for field area, and J_0max for maximum light absorption).

- Let J_c be the actual light flux absorbed by a crop covering a field. The overall efficiency of light absorption by the crop, f_c , is given by

Let the crop consists of n_c plants and let $n_c J_P$ be the light flux absorbed by the crop, so that J_P is the light flux absorbed by an average plant. If f_P is the efficiency of light absorption of the plants in the crop, f_P is given by:

$$f_c = \frac{J_c}{J_0} \tag{1.7}$$

1.4.6 Photosynthesis

The rectangular hyperbola equation is a widely employed tool for describing the steady-state

$$f_P = \frac{J_c}{n_c J_P}; \tag{1.8}$$

$$P_s = \frac{\alpha I \beta C}{\alpha I + \beta C}. \tag{1.9}$$

relationship between photosynthetic response and light and carbon dioxide levels.

Where P_s is the steady-state photosynthetic rate (no distinction is made here between net and gross photosynthesis), I is the light flux density, C is the carbon dioxide density, α and β are constants. This equation is popular because it often gives an acceptable description of actual response and is manageable.

1.4.7 Transport of Substrate

The flux of substrate, B (referred to as the mass transfer rate) from compartment i to compartment $(i-1)$ is given by

$$B = \frac{s_i - s_{i-1}}{r_i}. \tag{1.10}$$

Where r_i is the transport resistance between $i^{th}$and $(i-1)^{th}$compartment and s_i is the substrate concentration in the i^{th} compartment.

1.4.8 Plant Growth Curve

In the beginning (lag phase) the plants are characterized by a decelerated rate of growth. and sluggish. Then, there comes a swift and expeditious increase (exponential phase) in the plant growth. Henceforth, the growth rate steadily decreases (stationary phase) due to impediment of nutrients. The typical sigmoid or S- shaped curve obtained by plotting growth and time is known as plant growth curve which is represented in the Figure (1.1)

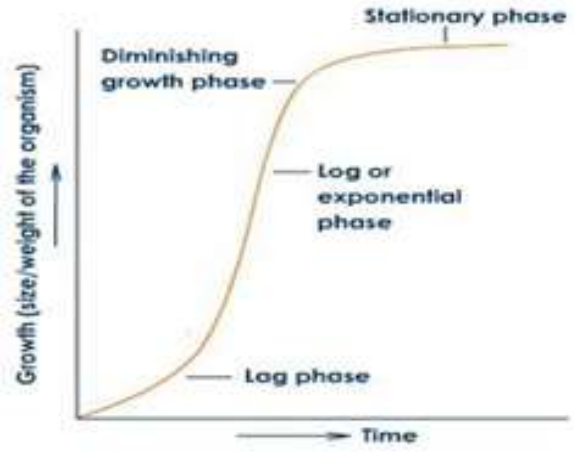

Figure 1.1: A curve in the shape of sigmoid represents plant growth

1.4.9 Plant Growth Rate

The interaction between plants and resources is characterized by the constraint imposed by a limiting factor, which influences plant performance at the individual, population, and ecosystem levels. The growth rate of an individual plant is positively

$$r(R) = \eta \mu_m W_r \frac{R}{k_R + R}. \tag{1.11}$$

correlated with the availability of nutrients in its environment [154].

where, R is the availability of nutrient. η is the nutrient use efficiency. W_r is the proportion of total biomass allocated to root mass, μ_m is the resource-saturated rate of resource uptake per unit of root mass and k_R is a half-saturation constant for nutrient uptake.

1.5 Mathematical Preliminaries

1.5.1 Existence of Unique, Bounded as well as Positive Solution of Delay differential equation

In a DDE, the derivative at a given time depends on the solution and its derivatives at previous times, indicating a memory effect in the system. Here an initial history function, rather than an initial condition, needs to be defined. The concept of a delayed state variable allows for the representation of the dependence of a system's current state on its previous states in the context of DDEs. The state variable derivative is not a required component in this particular scenario. The corresponding DDEs with a single delay $\Im > 0$ is given by [155]

$$\dot{x}(t) = f\big(x, x(t), x(t-\Im)\big); \tag{1.12}$$

Assume that $f(t,x,y)$ and $f_x(t,x,y)$ are continuous on R^3. Let $s \in R$ and $\emptyset: [s-\Im, s] \to R$ be continuous. We seek a solution $x(t)$ of equation (1.12) satisfying

$$x(t) = \varphi(t), t \in [s-\Im, s], x(0) = x_0 \tag{1.13}$$

And satisfying equation (1.12) on $t \in [s,\ s+\sigma]$ for some $\sigma > 0$.

Theorem 1.5.1 (Existence of U.S). Let $f(t,x,y)$ and $f_x(t,x,y)$ are continuous on R^3. Let $s \in R$ and $\varphi: [s-\Im, s] \to R$ be continuous. Then there exists $\sigma > s$ and U.S of the IVP (1.12)- (1.13) on $[s-\Im, \sigma]$.

Theorem 1.5.2 (Boundedness of solution). Let f satisfy the hypothesis of theorem1.5.1 and let $x: [s-\Im, \sigma) \to R$ be the noncontinuable solution of the IVP (1.12)- (1.13). If $\sigma < \infty$ then $\lim_{t\to\sigma-}|x(t)| = \infty$

Remark 1.5.3 Theorems 1.5.1 and 1.5.2 extend immediately to the case that $x \in R^n$ and $f: R \times R^n \times R^n \to R^n$, it also extends to multiple discrete delays $\Im_0 < \Im_1 < \cdots < \Im_m$ where $f = f(t, y(t), y(t-\Im_0), y(t-\Im_1), \dots, y(t-\Im_m))$.

Theorem 1.5.4 (Positivity of solution). Suppose that $f: R \times R_+^n \times R_+^n \to R^n$satisfies the hypothesis of theorem 1.5.1 and remark 1.5.3 and for all i, t and for all $x, y \in R_+^n$:

$$x_i = 0 \Rightarrow f_i(t,x,y) \geq 0$$

If the initial data φ in equation (1.13) satisfy $\varphi \geq 0$, then the corresponding solution $x(t)$ of equation (1.12) satisfy $x(t) \geq 0$ for all $t \geq s$ where it is defined.

1.5.2 Stability by Variational matrix method

$$\frac{dy}{dt} = f(y) \tag{1.14}$$

Let an autonomous system of equations be

Where y is an n-tuple vector i.e. $y = (y_1, y_2, - - -y_n)$. Let $\phi(t)$ be the solution of system (1.14). The linear part of the expansion of the system (1.14) about $\varphi(t)$ is given by the variational equation of the system (1.14) with respect to $\varphi(t)$, written as

$$\frac{dx}{dt} = f_y(\varphi(t))x \tag{1.15}$$

Where $f_y(\varphi(t)) = \frac{df_i}{(dy_j)_{n\times n}}$ at $\varphi(t)$. Since the stability of the variational system depicts the stability of any solution of a non- linear system governed by it, so stability of $x = 0$ of the equation (1.15) determines the stability of $y = \varphi(t)$ of the equation (1.14). Particularly, when $\varphi(t) = \varphi_0$, a constant, the system (1.14) becomes

$$\frac{dx}{dt} = Ax \tag{1.16}$$

Where $A = f_y(\varphi_0)$. Since a small perturbation of the system (1.14) is represented by system (1.15), so the stability of $y = \varphi_0$ of (1.16) actually gives the stability of the solution of $x = 0$ of (1.15) .The description of stability of every solution of $x' = Ax$ is given by following theorems [156]

Theorem 1.5.5 If all the characteristic roots of A have negative real parts, then every solution of the system $x' = Ax$,where $A = (a_{ij})$ is a constant matrix, is asymptotically stable.

Theorem 1.5.6 If all the characteristic roots of A with multiplicity grater than one has negative real parts and all its roots with multiplicity one has non-positive real parts, then all the solutions of the system $x' = Ax$ are bounded and hence stable. Following theorem [156] is to determine the sign of real parts of the roots of characteristic equation.

Theorem 1.5.7 Hurwitz's Theorem. A necessary and sufficient condition for the negativity of the real parts of all the roots of the polynomial

$L(\lambda) = \lambda^n + a_1\lambda^{n-1} + a_2\lambda^{n-2} + - - - - + a_n$ with real coefficients is the positivity of all the principal diagonals of the minors of the Hurwitz matrix

$$H_n = \begin{bmatrix} a_1 & 1 & 0 & 0 & 0 & 0 & \cdots & 0 \\ a_3 & a_2 & a_1 & 1 & 0 & 0 & \cdots & 0 \\ a_5 & a_4 & a_3 & a_2 & a_1 & 1 & \cdots & 0 \\ \vdots & \vdots & \vdots & \vdots & \vdots & \vdots & & 0 \\ 0 & 0 & 0 & 0 & 0 & 0 & \cdots & 0 \end{bmatrix}$$

Theorem 1.5.8. Let $\varsigma_{1,}\varsigma_2 \ldots . \varsigma_m$ are all non-negative and $\zeta_i^{\,j}(j = 0,1,2, \ldots m: i = 1,2, \ldots n)$ are constants. As $(\varsigma_1, \varsigma_2, \ldots, \varsigma_m)$ vary, the sum of the orders of the zeros of exponential polynomial $P(\chi, e^{-\chi\varsigma_1}, \ldots . , e^{-\chi\varsigma_m})$ on the open right half plane can change only if a zero appears on or crosses the imaginary axis, where:

$$P(\chi, e^{-\chi\varsigma_1}, \ldots . , e^{-\chi\varsigma_m}) = \chi^n + {\zeta_1}^0\chi^{n-1} + \cdots + {\zeta_{n-1}}^0\chi^n + {\zeta_n}^0 + \left[{\zeta_1}^1\chi^{n-1} + \cdots + {\zeta_{n-1}}^1\chi^n + {\zeta_n}^1\right]e^{-\chi\varsigma_1} + \cdots + \left[{\zeta_1}^m\chi^{n-1} + \cdots + {\zeta_{n-1}}^m\chi^n + {\zeta_n}^m\right]e^{-\chi\varsigma_m}$$

Ruan and Wei (2001, 2003) [112], [157] proved this theorem using Rouches theorem (1960) [158].

1.5.3 Hopf-Bifurcation

Hopf's crucial contribution was the extension from two dimensions to higher dimensions. Sometimes HB is also called as "Poincaré-Andronov-Hopf bifurcation" [132]. Hb theorem describes the way that a topological feature of a flow vary as one or more parameters are varied. The fundamental observation of flows is that if the stationary point is hyperbolic, i.e. eigenvalues of the linearized flow at the stationary point all have non-zero real pairs, then the local behaviour of the flow is completely determined by the linearized flow. Hence, bifurcations of stationary points can only occur at parameter values for which a stationary point is non-hyperbolic. More, precisely, a bifurcation value of a parameter is a value at which the qualitative nature of the flow changes.

The HB is several orders of magnitude harder to analyse since it involves a non-hyperbolic stationary point with linearized eigenvalues $\mp i\omega$, and thus a two-

dimensional centre manifold, and bifurcating solutions are periodic rather than stationary.

Theorem 1.5.9. Hopf-Bifurcation Theorem.

Let us consider one parameter family of delay equations

$$x'(t) = F(x_t, \mu) \tag{1.17}$$

Where $F: C \times R \to R^n$ is a twice continuously differentiable in its arguments and $x = 0$ is a steady state for all values of μ: $F(0, \mu) \equiv 0$.

We may linearize F about $\varphi = 0$ as follows

$$F(\varphi, \mu) = L(\mu)\varphi + f(\varphi, \mu)$$

Where $L(\mu): C \to R^n$ is a bounded linear operator and f is higher order:

$$\lim_{\emptyset \to 0} \frac{|f(\varphi, \mu)|}{\|\varphi\|} = 0$$

Following is the characteristic equation about L:

$$|\lambda I - A(\mu, \lambda)| = 0, A_{ij}(\mu) = L(\mu)_i(e_\lambda e_j)$$

The roots of this equation constitute the main assumption. The characteristic equation will be having a pair of simple roots $\mp i\omega$ with $\omega_0 \neq 0$ and no other root that is an integer multiple of $i\omega_0$ for $\mu = 0$. Here a root of order one means [159]a simple root. If the characteristic equation is written as $h(\mu, \lambda) = 0$, then (H) implies $h_\lambda(0, i\omega_0) \neq 0$. So, by the implicit function theorem, there exists a continuously differentiable family of roots $\lambda = \lambda(\mu) = \alpha(\mu) + i\omega(\mu)$ for small μ satisfying $\lambda(0) = i\omega_0$. In particular, $\alpha(0) = 0$ and $\omega(0) = \omega_0$. Next assumption is that as μ increases through zero, the line of imaginary axis is crossed transversally by these roots. Actually, the assumption is:

In case $\alpha'(0) < 0$, we always ensure that equation (1.18) holds by changing the sign of the parameter i.e. we take parameter $v = -\mu$. Thus, the positive sign is basically a normalization which ensures that if $\mu < 0$, then the pair of roots has a negative real part and if $\mu > 0$, then it has positive real part.

$$\alpha'(0) > 0 \tag{1.18}$$

Theorem 1.5.10. Let (H) and equation (1.18) hold. Then there exist $\varepsilon_0 > 0$, real valued even function $\mu(\varepsilon)$ and $T(\varepsilon) > 0$ satisfying $\mu(0) = 0$ and $T(\varepsilon) = {}^{2\pi}/_{\omega_0}$, and a non-constant $T(\varepsilon)$- periodic function $p(t, \varepsilon)$ with all functions being continuously differentiable in ε for $|\varepsilon| < \varepsilon_0$, such that $p(t, \varepsilon)$ is a solution of equation (1.17) and $p(t, \varepsilon) = \varepsilon\, q(t, \varepsilon)$ where $q(t, 0)$ is a ${}^{2\pi}/_{\omega_0}$-periodic solution of $q' = L(0)q$.

Moreover, there exist $\mu_0, \beta_0, \delta > 0$ such that if equation (1.17) has a non-constant periodic solution $x(t)$ of period P for some μ satisfying $|\mu| < \mu_0$ with $max_t|x_t| < \beta_0$ and $\left|P - {}^{2\pi}/_{\omega_0}\right| < \delta$, then $\mu = \mu(\varepsilon)$ and $x(t) = p(t + \theta, \varepsilon)$ for some $|\varepsilon| < \varepsilon_0$ and some θ.

$$\mu(\varepsilon) = \mu_1\varepsilon^2 + O(\varepsilon^4); \tag{1.19}$$

$$T(\varepsilon) = \frac{2\pi}{\omega_0}[1 + \Im_1\varepsilon^2 + O(\varepsilon^4)] \tag{1.20}$$

If F is five times continuously differentiable then:

If all other characteristic roots for $\mu = 0$ have strictly negative real parts except for $\mp i\omega$ then $p(t, \varepsilon)$ is asymptotically stable if $\mu_1 > 0$ and unstable if $\mu_1 < 0$.

1.5.4 Sensitivity Analysis of State Variables with respect to Model Parameters

Systematic evaluation of the effects of model parameters on system solutions is called sensitivity analysis. There are number of methods to do sensitivity analysis of systems without delay, but there are only a few methods for sensitivity analysis of systems involving delays. The knowledge of how a small change in model parameter can bring change in the state variable, can be a great help in modelling process. It helps in elimination of ineffective and irrelevant parameters. It gives a complete insight into the overall behaviour of the proposed model.

If all the parameters in the given system (1.12)- (1.13) are considered to be constants, then sensitivity analysis includes just the calculation of partial derivatives of solution

$$S(t) \equiv S(t, \alpha) = \left[\frac{\partial}{\partial\alpha}\right]^T x(t, \alpha) \tag{1.21}$$

with respect to each parameter [144]. The matrix of sensitivity functions is of the form:

Its jth column is: $$S_j(t,\alpha) = \left[\frac{\partial x_j(t,\alpha)}{\partial \alpha_1}, \frac{\partial x_j(t,\alpha)}{\partial \alpha_2}, \dots, \frac{\partial x_j(t,\alpha)}{\partial \alpha_n}\right]^T;$$

This column vector gives sensitivity of the solution $x_j(t,\alpha)$ for small change in parameter $\alpha_i, i = 1,2,3,\dots,n.$

$$S'(t) = J(t)S(t) + J_{\Im}(t)S(t-\Im) + B(t), t \geq 0; \quad (1.22)$$

Theorem 1.5.11. $S(t)$ satisfies the DDEs:

Where $J(t) = \frac{\partial}{\partial x} f(t,x,x_\tau)$, $J_{\Im}(t) = \frac{\partial}{\partial x_\tau} f(t,x,x_{\Im})$, $B(t) = \frac{\partial}{\partial \alpha} f(t,x,x_{\Im})$

1.6 Outline of the thesis work

The thesis work consists of six chapters whose detail is as follows:

In chapter-1, General introduction: The chapter introduced about PGDs under the effect of toxicants. The remarkable work done is by the researchers is cited and the gaps have been identified through extensive literature review. All the important concepts of plant physiology and the necessary mathematical concepts required for their study have also been described. It also includes the proposed objectives of the study.

In chapter-2, Delay-induced bifurcation in plant growth plant growth dynamics: In the chapter, the study proposes a MM for PGDs, incorporating the effects of delayed nutrient uptake using DDEs. Plant biomass and nutrient concentration are the model's state variables. The delayed nutrient concentration is hypothesized to negatively impact plant growth. The analysis establishes the positivity of solutions, calculates a feasible internal equilibrium point, and investigates the system's stability around this point. Interestingly, HB is observed around a critical value of the delay parameter. MATLAB simulations support the analytical findings.

In chapter-3, A mathematical analysis of delay differential equations to understand the stability and bifurcation behavior of plant growth systems: A two-compartment model, In the following chapter a novel MM for plant growth dynamics, considering separate root and shoot compartments. The model tracks two

key variables: nutrient concentration and the structural dry weight of each compartment. Building on logistic growth principles, it explores how the root system supplies essential nutrients to the shoot. However, external and internal factors can impede this nutrient transfer, introducing a delay in nutrient consumption by the shoot. This delay, captured by a newly incorporated parameter, can damage the shoot's structural dry weight. The analysis investigates the system's stability around an internal equilibrium point. Interestingly, Hb emerges beyond a critical delay parameter value. Finally, the model's sensitivity to parameter variations is examined, with MATLAB simulations supporting the analytical results.

In chapter-4, A delay differential equation approach to investigate the impact of toxicity on plant growth patterns, In the given chapter, study leverages a MM to investigate how delayed effects of toxicity impact plant growth under stress. The model demonstrates that toxic substances alter soil structure and microbial activity, leading to a decline in available nutrients. Since nutrient availability is crucial for biomass accumulation, plant growth suffers a double blow: both nutrient deficiency and direct toxicity. Notably, the detrimental effects of toxicity manifest after an incubation period, necessitating the inclusion of a delay parameter in the model's state variables. Interestingly, the model predicts a HB at a critical delay value, suggesting the emergence of periodic oscillations in plant growth. Utilizing established techniques, the analysis explores the direction and stability of these newly formed periodic solutions. Furthermore, sensitivity analysis assesses the model's response to changes in parameter values.

In chapter-5, Analyzing the competitive dynamics of two plant populations under the influence of toxic decay, the chapter discussed a MM to analyze the growth of competing plants under toxic stress. The model reveals that the presence of toxic compounds disrupts soil structure and activity, hindering the growth of these competitive plants. Both plant populations are assumed to follow logistic growth dynamics. Interestingly, the impact of toxicity is not immediate; it exhibits an incubation period captured by a delay parameter (τ). The analysis establishes the positivity and existence of a non-zero equilibrium point. Furthermore, stability analysis around this equilibrium reveals a complex phenomenon – Hopf bifurcation – at a critical delay value ($\Im_c$). By employing established methods, the study explores the direction and stability of the newly formed periodic solutions arising from this

bifurcation. Sensitivity analysis is then conducted to assess the model's response to parameter variations. Finally, MATLAB simulations are utilized to validate the analytical findings.

Chapter 2

Delay-induced bifurcation in plant growth dynamics

2.1 Introduction

Mathematical modeling is natural phenomenon and substitute method for examine plant growth under effect of respective variables such as nutrients concentration, toxicity, contaminants etc. [1,59,163]. Thornley [3] and Lacointe [21] designed numerous mathematical modeling in plant physiology under certain condition and for a specific plant species. Mishra [83] showed that Plant growth shows unfavorable effect of toxicity, general lack in uptake concentration of nutrients and plant biomass in root shoot compartment. The study of depletion of plant biomass undergoing effect of toxicants with time lag was studied by Naresh, et.al. [72]. DDEs have been explored in distinct surroundings in distinct models of biological and physical methodology by Kuang [128]. The impact of delay parameter in plant growth carry out by toxicants was studied by Kalra and Kumar [160,161]. Rouches theorem analysis the distribution of roots of exponential polynomial by Dieudonne [158]. The study of nature of zeros polynomial in exponential characteristic equation examined by Ruan and Wei [112]. The overall stability of structure of nonlinear DDEs was studied by Huang et.al [129]. There was attained explicit formulae used to regulate values of HB at critical point using theory of Manifolds and reductions by Hassard [162]. Hb brought out by delay parameter in depletion of forest biomass examined by Kumar [164]. The delay models about its positive equilibrium point been asymptotically stable under some necessary and sufficient conditions for all positive solutions obtained by Gopalsamy [165] and Ladas [166]. The effect of time lag in plant growth is studied using a two-compartment mathematical model by Kalra and Kumar [167].

2.2 Mathematical Model

The proposed mathematical model is governed by the following system of DDEs:

$$\frac{\mathrm{d}P}{\mathrm{d}t} = \alpha N\,(t-\Im)P - \beta P; \tag{2.1}$$

$$\frac{\mathrm{d}N}{\mathrm{d}t} = I - \gamma N(t-\Im)\,P - \delta N; \tag{2.2}$$

Variables/Parameters	Description
$\boldsymbol{P}$	Plant biomass
$\boldsymbol{N}$	Nutrient concentration
$\boldsymbol{I}$	Constant inflow of nutrients
$\boldsymbol{\alpha}$	Rate of utilization of nutrients
$\boldsymbol{\beta}$	Natural decay rate of plant biomass
$\boldsymbol{\gamma}$	Rate of consumption of nutrients
$\boldsymbol{\delta}$	Natural decay rate of nutrients
$\boldsymbol{\Im}$	Delay parameter

Figure 2.1 Description of variables and parameters of the system.

2.3 Analysis of the Model

2.3.1 Positivity of Solutions:

From equation (2.1):

$\frac{\mathrm{d}P}{\mathrm{d}t} \geq -\beta P$;

$\Rightarrow \frac{\mathrm{d}P}{P} \geq -\beta dt$;

$\Rightarrow P \geq \mathrm{e}^{-\beta\Im}$;

$\Rightarrow P \geq 0$;

From equation (2): $\frac{\mathrm{d}N}{\mathrm{d}t} \geq -\delta N$;

$\Rightarrow N \geq \mathrm{e}^{-\delta t}$;

$\Rightarrow N \geq 0$;

So, $P \geq 0, N \geq 0$ for all $t > 0$.

Hence solution set of the given system remains positive for all time t. It ensures the system persists.

2.3.2 Equilibrium point $\boldsymbol{E^*(P^*, N^*)}$:

At the point of non-zero equilibrium $E^*(P^* \neq 0, N^* \neq 0)$, $N^*(t-\tau) \approx N^*(t)$

$\frac{\mathrm{d}P^*}{\mathrm{d}t} = 0 \Rightarrow N^* = \frac{\beta}{\alpha}$;

$\frac{\mathrm{d}N^*}{\mathrm{d}t} = 0 \Rightarrow P^* = \frac{I\alpha - \delta\beta}{\gamma\beta}$;

Thus, the non-zero equilibrium is $E^*(\frac{I\alpha-\delta\beta}{\gamma\beta}, \frac{\beta}{\alpha})$.

2.3.3 Stability of Equilibrium E^* and Hopf-Bifurcation:

The system of equations governing the nutrient-plant dynamics about the equilibrium E^* is given by:

$$\frac{\mathrm{d}P^*}{\mathrm{d}t} = \alpha N^*(t-\Im)P^* - \beta P^*; \tag{2.3}$$

$$\frac{\mathrm{d}N*}{\mathrm{d}T} = I - \gamma N^*(t-\Im)P^* - \delta N^*. \tag{2.4}$$

The characteristic equation of system of equations (2.3) - (2.4) is given by:

$$(\lambda^2 + a\lambda + b) + \mathrm{e}^{-\lambda\Im}(\mathrm{c}\lambda + d) = 0; \tag{2.5}$$

Where $a = \beta + \delta$, $b = \beta\delta$, $c = \gamma P^*$, $d = \beta r p^*$

By Hurwitz criteria

When $\Im = 0$, the equation (5) becomes

$$\boldsymbol{\lambda^2 + (a+c)\,\lambda + (b+d) = 0.} \tag{2.6}$$

By Routh Hurwitz criteria, roots of the equation (2.6) will have negative real part i.e. the system is stable if:

$(\boldsymbol{T_1})$: $\boldsymbol{(a+c) > 0;}$

$(\boldsymbol{T_2})$: $\boldsymbol{(b+d) > 0}$

Now, we would like to check the shifting of negative real part of the roots to positive real parts with variations in the values of$\Im$.

Let put $\lambda = \mathrm{i}\omega$ be a root of equation (2.5), then equation (2.5) becomes:

$$(\mathrm{i}\omega)^2 + a(\mathrm{i}\omega) + b + (c(\mathrm{i}\omega) + d)\mathrm{e}^{-(\mathrm{i}\omega)\tau} = 0;$$

$$-\omega^2 + a(\mathrm{i}\omega) + b + (c(\mathrm{i}\omega) + d)(\cos\omega\Im - \mathrm{i}\sin\omega\Im) = 0.$$

Separating real and imaginary parts:

$$-\omega^2 + b = -d\cos\omega\Im - c\omega sin\,\omega\Im; \tag{2.7}$$

$$a\omega = -c\cos\omega\Im + d\sin\omega\Im. \tag{2.8}$$

Squaring and Adding

It follows that ω satisfies:

$$\omega^4 + (a^2 - c^2 - 2b)\omega^2 + (b^2 - d^2) = 0$$

$$\omega^4 - (-a^2 + c^2 + 2b)\omega^2 + (b^2 - d^2) = 0. \tag{2.9}$$

The two roots of equation (2.9) are:

$$\left(\omega_{1,2}\right)^2 = \frac{(2\mathrm{b} + c^2 - a^2) \pm \sqrt{(2\mathrm{b} + c^2 - a^2)^2 - 4(b^2 - d^2)}}{2}. \tag{2.10}$$

$(\boldsymbol{T_3})$: $(c^2 - a^2 + 2b) < 0\ and\ (b^2 - d^2) > 0\ or\ (c^2 - a^2 + 2b)^2 < 4(b^2 - d^2)$

Thus, implies equation (10) doesn't have positive roots if condition (T_3) holds.

2.3.4 Conjecture 1.

If $(\boldsymbol{T_1}) - (\boldsymbol{T_2})$ hold, then entire roots of equation (2.5) have negative real parts for all $\Im \geq 0$.

On the other side, if:

$(\boldsymbol{T_4})$: $(b^2 - d^2) < 0\ or\ (c^2 - a^2 + 2b) > 0\ and\ (c^2 - a^2 + 2b)^2 = 4(b^2 - d^2)$

Then, +ve root of equation (2.7) is ω_1^2.

On the same base, if:

$(\boldsymbol{T_5})$: $(b^2 - d^2) > 0\ or\ (c^2 - a^2 + 2b) > 0\ and\ (c^2 - a^2 + 2b)^2 > 4(b^2 - d^2)$

Then, two +ve roots of equation (2.7) are $\omega_{1,2}^2$.

In both- $(T_4)$and (T_5), the equation (2.5) gives purely imaginary roots when $\Im$ takes definite values. The critical values $\Im_j^{\pm}$ of $\Im$ can be planned from the system of equations (2.5) - (2.6), given by:

$$\Im_j^{\pm} = \frac{1}{\omega_{1,2}} \cos^{-1}\left[\frac{s\left(\omega_{1,2}^2 - q\right) - pr\omega_{1,2}^2}{r^2\omega_{1,2}^2 + s^2}\right] + \frac{2j\pi}{\omega_{1,2}}, j = 0,1,2, \ldots \tag{2.11}$$

The above analysis can be condensed in follow conjectures.

2.3.5 Conjecture 2.

(I) If $(T_1) - (T_2)\ and\ (T_4)$ hold and $\Im = \Im_j^+$, then equation (2.5) has a pair of purely imaginary roots $\pm \mathrm{i}\omega_1$.

(II) If $(T_1) - (T_2)\ and\ (T)$ hold and $\Im = \Im_j^+ \left(\Im = \Im_j^-\ respectively\right)$, then equation (2.5) has a pair of purely imaginary roots $\pm \mathrm{i}\omega_1 (\pm \mathrm{i}\omega_2\ respectively)$.

Our expectation is the shifting of negative real part of some roots of equation (2.5) to positive real part when $\Im > \Im_j^+$ and $\Im < \Im_j^-$. To look into this possibility, let us denote:

$\Im_j^{\pm} = \mu_j^{\pm}(\Im) + \mathrm{i}\omega_j^{\pm}(\Im); j = 0,1,2,3, \ldots$

The roots of equation (2.5) satisfy: $\mu_j^{\pm}\left(\Im_j^{\pm}\right) = 0, \omega_j^{\pm}\left(\Im_j^{\pm}\right) = \omega_{1,2}$

We can prove that the following transversality condition holds:

$\frac{\mathrm{d}}{\mathrm{d}\tau}\left(Re\ \lambda_j^+\left(\Im_j^+\right)\right) > 0\ and\ \frac{\mathrm{d}}{d\tau}\left(Re\ \lambda_j^-\left(\Im_j^-\right)\right) < 0$

It concludes that $\Im_j^{\pm}$ are bifurcating values. The succeeding postulate gives the scattering of the zeros of the equation (2.5)

2.4 Numerical Simulation

The following set of parametric values is taken to represent graphically the dynamics depicted by the system of equations (2.1) - (2.2)

$\alpha = 0.5, \beta = 0.6, \gamma = 0.9, \delta = 0.7, I = 2$ with $P(0) = 1, N(0) = 1$

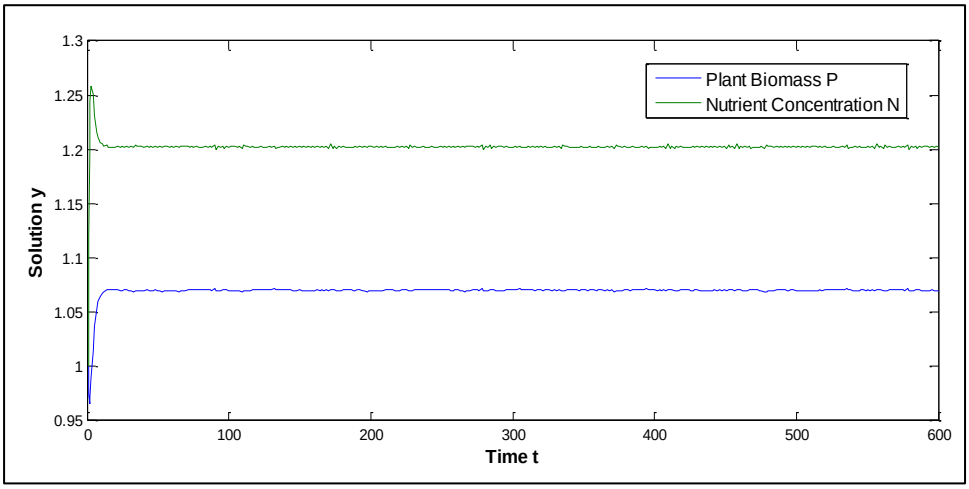

Figure 2.2 Absolute stable equilibrium $\boldsymbol{E^*}$ in the absence of delay i.e., $\mathfrak{J} = \mathbf{0}$.

The change of behaviour of the system of equations (2.1)- (2.2) from being stable to complex dynamics about the equilibrium $E^*(1.0702, 1.2025)$ for different values of delay parameter $\mathfrak{J}$ is shown below.

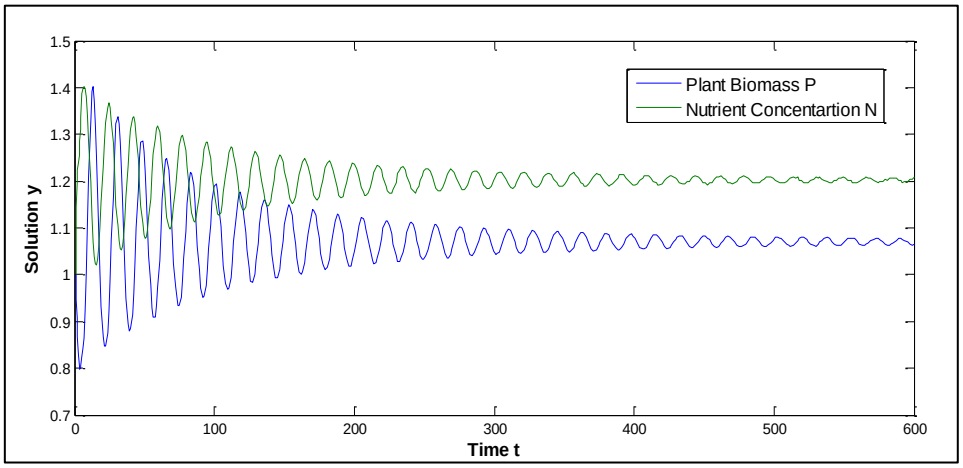

Figure 2.3 Asymptotically stable equilibrium $\boldsymbol{E^*}$ when delay parameter is below the critical value i.e., $\mathfrak{J} < \mathbf{2.1}$.

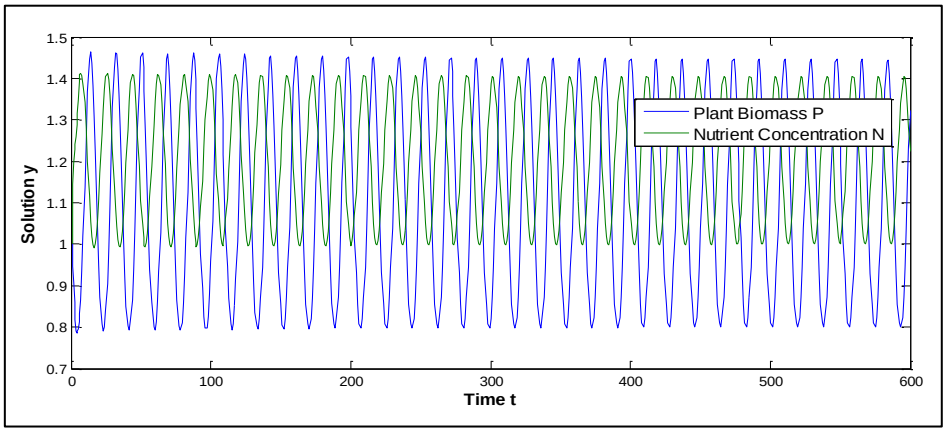

Figure 2.4 Equilibrium $\boldsymbol{E^*}$ looses stability and Hopf- bifurcation is observed when delay parameter crosses the critical value i.e.,$\boldsymbol{\Im \geq 2.1}$.

2.5 Conclusion

The role of delay parameter on nutrient- plant biomass is studied with the help of proposed model. The state variables considered are: plant biomass P and nutrient concentration N. It is assumed that the delayed nutrient concentration adversely affects the plant growth. The positivity of solutions is established and the feasible interior equilibrium point $E^*$is calculated. The stability of the system around the interior equilibrium is checked. It is shown that the equilibrium point E^* is absolutely stable in the absence of delay that is when $\Im = 0$ as shown in figure (2.1). The equilibrium point E^* is asymptotically stable when the delay parameter is below a critical value that is when $\Im < 2.1$ as shown in figure (2.2). The equilibrium point E^* loses stability and Hb is observed when the DP crosses the critical value that is when $\Im \geq 2.1$ as shown in the figure (2.3).

Chapter 3

A mathematical analysis of delay differential equations to understand the stability and bifurcation behavior of plant growth systems

3.1 Introduction

In plant ecology, nutrients availability and solubility play significant role in growing plants. There are some other essential elements which help in the plant growth: oxygen, carbon and hydrogen comes from air and also water and nutrients taken up from soil. The interaction between plant-soil describes the process in which roots help to transport the nutrients from soil which give rise to the growth of plant. Hiltner was the first who to initiate the modelling between plant- soil interaction [1]. In some situations, due to lack of mobility in nutrients plants do not get sufficient amount of nutrients for their normal growth which cause decreases in plant productivity. Hence the soil properties and availability of water are the main factors responsible for plant growth [2],[180]. Thornley was the first to propose mathematical models including these factors individually and in combination to the several issues in plant physiology to estimate the outcome of variables: humidity, temperature, transportation, respiration, guard cells, rate of photosynthesis etc. [3] [4]. The models have been categorized and explained the growth of specific plants in crop [168]. For modeling purposes, the plant is split up into root compartment and shoot compartments in which, concentration of nutrients and dry weight are considered as the conditional variables [169],[7]. It's assumed that due to the existence of toxic metal in root compartment, resistance increases in transport nutrients from root to shoot compartment [170], [167]. Copper and zinc are the important macronutrients which are necessitated for the normal growth of the plants. Normally, these are found in very low concentration in soil. Whereas, metals like chromium, cadmium, lead, mercury, nickel etc. are toxic to plants [83], [171]. Such heavy metals get in the way to the up taking and absorbing of vital nutrients minerals from the soil and results unbalancing nutrients levels in plant [172], [167]. Nutrients influence stressed on discrete plant growth, that ensuing effect on non-linear population growth dynamics which arise the

impact on production of standing crop yield. The theoretical model discussed in which the assumptions were that there was a dynamic growth process whose rate was dependent on the size of the plant, reduced the growth rates, possibly resulting in mortality [4]. There are 30 percent difference shown between the uptaking of nutrients theoretically and computed uptakes [115]. Models of biological phenomena whose dynamics is explained better by DDEs and numerical approaches are the tools considered for their solutions [111]. Rouches theorem plays an essential role during the analysis of exponential polynomials and their roots distribution [174],[175]. The stability and oscillations studied in the set of non-linear differential equations with delay [176]. Also, the Boundedness and Persistence is calculated of mixed nonlinearity DDEs [177]. Under certain necessary and sufficient criteria, the system of DDE models over its positive equilibrium point, has been asymptotically stable for all positive solutions [178]. The phenomenon of HB shown up at the equilibrium point when the delay increased from critical point [179,180]. The sensitivity analysis for nonlinear DE systems with time delays utilising direct when the constituting model parameters were altered with respect to time, not remain constant only [181]. Theoretical findings for sensitivity are presented with relation to the delays. The study of the parametric sensitivity is used to examine the periodic responses to DDEs [182].

3.2 Mathematical Model

For the analysis of the plant growth, the plant has been divided into the shoot compartment and root compartment. Structural dry weight and nutrients concentration are corresponding state variables. Let the nutrients concentration in shoot and root as N_2 and N_1, respectively. Let structural dry weights in root and shoot as W_1 and W_2, respectively. It is supposed that the structural dry weight is damaged due to hinderance in up taking of nutrients caused by some exogenic activities. This hypothesis is in corporated in the model by delay parameter in nutrients utilization. The above notations generate following mathematical:

$$\frac{dN_1}{dt} = rN_1\left(1 - \frac{N_1}{K}\right) - \mu\, W_1 N_1\,(t - \Im) - d_1 N_1. \tag{3.1}$$

$$\frac{dN_2}{dt} = rN_2\left(1 - \frac{N_2}{K}\right) - \mu\, W_2 N_2 - d_2 N_2. \tag{3.2}$$

$$\frac{dW_2}{dt} = (\alpha N_2 - \gamma_2)\, W_2 - \Delta_2\, W_2^2\,. \tag{3.3}$$

$$\frac{dW_1}{dt} = (\alpha N_1 - \gamma_1)\, W_1 - \Delta_1\, W_1^2. \tag{3.4}$$

The definition of system parameters are as follows:

$r(1-\frac{N_1}{K})$, $r(1-\frac{N_2}{K})$,

are considered as logistic growth where *K* be the carrying capacity. r is natural rate of growth of nutrients, μ is utilization coefficient or consumption coefficient, α is considered as nutrient-use efficiency. Natural decay of W_1 and W_2 are represented as γ_1 and γ_2, respectively. Natural decay of N_1 and N_2 are represented as d_1 and d_2, respectively. Δ_2 is rate of self-limiting growth of W_2 and Δ_1 is rate of self -limiting growth of W_1.

With initial conditions: $N_1(0) > 0$, $N_2(0) > 0$, $W_1(0) > 0$ and $W_2(0) > 0$, for all $t > 0$ and $N_1(t-\Im) = \text{Constant}$, for all $t \in [0, \Im]$

3.2.1 Boundedness

The lemma provides the boundedness of solutions of the model as (3.1) -(3.4):

Lemma 1. All solution of the model lying between the region $D_1 = \left[(N_1, N_2, W_1, W_2) \in {Q_+}^4 : 0 \le N_1 + N_2 + \frac{\mu}{\alpha}W_1 + \frac{\mu}{\alpha}W_2 \le \frac{r}{\varphi}\right], as\ t \to \infty$, for all positively initial values $\{N_1(0), N_2(0), W_1(0), W_2(0),\ N_1(t-\tau) = \text{Constant}$, for all $t \in [0, \Im]\} \in D_1 \subset {Q_+}^4$ where $\varphi = min(d_1, d_2, \gamma_1, \gamma_2)$.

Proof: Assume the function $F(t)$, such that:

$$F(t) = N_1(t) + N_2(t) + \frac{\mu}{\alpha}W_1(t) + \frac{\mu}{\alpha}W_2(t);$$

$$\frac{dF(t)}{dt} = \frac{d}{dt}\left[N_1(t) + N_2(t) + \frac{\mu}{\alpha}W_1(t) + \frac{\mu}{\alpha}W_2(t)\right].$$

Using Equations (1) -(4) *and* $\varphi = min(d_1, d_2, \gamma_1, \gamma_2)$ and assuming that $N_1(t) \approx N_1(t-\Im)$ as $t \to \infty$, we get

$$\frac{dF(t)}{dt} \le r_n - \varphi F(t).$$

By using comparison theorem, we get as $\to \infty$: we get

$$F(t) \le \frac{r_n}{\varphi};$$

$$N_1(t) + N_2(t) + \frac{\mu}{\alpha}W_1(t) + \frac{\mu}{\alpha}W_2(t) \le \frac{r_n}{\varphi}.$$

$$So,\ 0 \leq N_1(t) + N_2(t) + \frac{\mu}{\alpha}W_1(t) + \frac{\mu}{\alpha}W_2(t) \leq \frac{r_n}{\varphi}\ \blacksquare$$

3.2.2 Positivity of the model

Since the model defines the dynamics of plant growth, it is important to show that all variables are positive for all time t. Positivity defines that the dynamic system of plant growth is sustain. From equation (1)-(4), we prove that all represented variables shows positive solutions, such that $N_1(0) > 0,\ N_2(0) > 0,\ W_1(0) > 0,\ W_2(0) > 0\ for\ all\ t > 0\ and\ N_1(t - \Im) = \text{Constant},\ \forall\ t \in [0,\ \Im]$, then the solution $N_1(t), N_2(t), W_1(t), W_2(t)$ of the model remains positive ∀ time t > 0.

From (3.2), $\frac{dN_2}{dt} = r\left(1 - \frac{N_2}{k}\right)N_2 - \mu W_2 N_2 - d_2 N_2;$

$$\frac{dN_2}{dt} \geq -(\mu W_2 + d_2)N_2;$$

$$N_2 \geq c^{e^{-(\mu W_2 + d_2)t}};$$

$$Hence, N_2 \geq 0\ as\ t \to \infty$$

From (3.3), we get, $\frac{dW_2}{dt} = (\alpha N_2 - \gamma_2)W_2 - \Delta_2 W_2^2;$

$$\frac{dW_2}{dt} \geq -(\gamma_2 - \Delta W_2)W_2;$$

$$W_2 \geq e^{-(\gamma_2 + \Delta W_2)t};$$

$$Hence, W_2 \geq 0\ as\ t \to \infty$$

From (3.4), we get, $\frac{dW_1}{dt} = -(\alpha N_1 - \gamma_1)W_1 - \Delta_2 W_1^2;$

$$\frac{dW_1}{dt} \geq -(\gamma_1 - \Delta_2 W_1)W_1;$$

$$W_1 \geq e^{-(\gamma_1 + \Delta_2 W_1)t};$$

$$\text{Hence}, W_1 \geq 0\ as\ t \to \infty$$

From (3.1), we get,

$$\frac{dN_1}{dt} = rN_1\left(1 - \frac{N_1}{k}\right) - \mu W_1 N_1(t - \Im) - d_1 N_1$$

$$\frac{dN_1}{dt} \geq -\left(\frac{r}{k} + d_1\right) N_1 - \mu W_1 N_1(t - \Im)$$

$$\frac{dN_1}{dt} + \left(\frac{r}{k} + d_1\right) N_1 \geq -\mu W_1 N_1(t - \Im)$$

$$\frac{dN_1}{dt} + \delta N_1 \geq -\mu W_1 N_1(t - \Im)$$

$$\frac{d\left(e^{\delta t} N_1\right)}{dt} \geq -\mu W_1 N_1(t - \Im) e^{\delta t}$$

$$N_1 \geq -\mu \int N_1(t - \Im) W_1 e^{-\delta(t-\Im)}\, dx$$

The solution of the above inequality N_1 will converge to *0 for* $t \to \infty$ *iff* $N_1(t - \Im) < \left(\frac{r}{k} + d_1\right)(t - \Im)\ for\ all\ t > \Im$.

3.2.3 Interior Equilibrium of the model

Here, we determine an interior equilibrium of the model, S_1 . There is one feasible solution to the system of equations, $S_1\ (N_1^*, N_2^*, W_1^*, W_2^*)$ where

$\frac{1}{\Delta_1}(\alpha N_1^* - \gamma_1) = W_1^* > 0$ provided $\alpha N_1^* > \gamma_1$

$\frac{1}{\Delta_2}(\alpha N_2^* - \gamma_2) = W_2^* > 0$ provided $\alpha N_2^* > \gamma_2$

$$N_1^* = \frac{\frac{\mu \gamma_1}{\Delta_1}\epsilon}{\frac{r}{k} + \frac{\mu\alpha}{\Delta_1}\epsilon + d_1}$$

$$N_2^* = \frac{-x_2 \pm \sqrt{x_2^2 - 4x_{1_*}x_3}}{2x_1}$$

where $x_1 = \frac{\mu\alpha}{\Delta_2}, x_2 = d - \frac{\mu\gamma_2}{\Delta_2}, x_3 = -r\left(1 - \frac{N_1^*}{k}\right)$

3.2.4 Study of Stability Analysis of Interior Equilibrium and Hopf – Bifurcation

In this, we examine dynamic behavior of the interior equilibrium point S_1 of the model. The following is the exponential characteristic equation for equilibrium S_1 :

$$\lambda^4 + A_1\lambda^3 + A_2\lambda^2 + A_3\lambda^1 + A_4 + de^{-\lambda\tau} = 0 \quad (3.5)$$

Here, $A_1 = (R_1 + R_5 + R_6 + R_9)$,

$A_2 = (R_6 R_9 + R_1 R_6 + R_1 R_9 + R_5 R_6 + R_5 R_9 + R_1 R_5 + R_8 R_7 + R_2 R_4)$,

$A_3 = (R_6R_9 R_1 + R_6R_9 R_5 + R_8R_7R_1 + R_8R_7R_5 + R_6R_1R_5 + R_6R_2R_4 + R_9R_1R_5 + R_9R_2R_4)$,

$A_4 = (R_1R_5R_6R_9 + R_2R_4R_6R_9 + R_2R_4R_8R_7 + R_1R_5R_8R_7)$

where $R_1 = \mu W_2 + d_2$, $R_2 = \mu N_2$, $R_3 = \frac{r}{k}$,

$$R_4 = -aW_2,\ R_5 = 2\Delta_2 W_2 - (\alpha N_2 - \gamma_2),$$

$$R_6 = 2\Delta_1 W_1 - (\alpha N_1 - \gamma_1), R_7 = -\alpha W_1,$$

$$R_8 = \mu N_1 e^{-\lambda\tau}, R_9 = \left(\frac{r}{k} + d_1\right)$$

Clearly $\lambda = i\omega$ is a root of Equation

$$(i\omega)^4 + A_1(i\omega)^3 + A_2(i\omega)^2 + A_3\omega + A_4 + de^{-(i\omega)\tau} = 0.$$

$$\omega^4 - iA_1\omega^3 - A_2\omega^2 + iA_3\omega + A_4 + d(cos\,\omega\tau - i\,sin\,\omega\tau) = 0.$$

Separating real and imaginary

$$\omega^4 - A_2\omega^2 + A_4 = -d\,cos\,\omega\tau \quad (3.6)$$

$$A_1\omega^3 - A_3\omega = -d\,sin\,\omega\tau \quad (3.7)$$

Squaring and Adding

$$\omega^8 + \left({A_1}^2 - 2A_2\right)\omega^6 + \left({A_2}^2 + 2A_1 - 2A^1A_3\right)\omega^4 \quad (3.8)$$
$$+\left({A_3}^2 - 2A_2A_1\right)\omega^2 + \left({A_4}^2 - d^2\right) = 0\ .$$

Let $\omega^2 = x\ and\ {A_1}^2 - 2A_2 = a, \left({A_2}^2 + 2A_4 - 2A_1A_3\right) = b, \left({A_3}^2 - 2A_2A_4\right) = c,$ $\left({A_4}^2 - d^2\right) = r,$

Equations become:

$$x^4 + ax^3 + bx^2 + cx + r = 0. \quad (3.9)$$

Lemma 2. If $r < 0$, there is at least one real root is positive in equation (9).

Proof**.** Let $p(x) = x^4 + ax^3 + bx^2 + cx + r$

Here $p(0) = r < 0$, $lim_{y\to\infty} p(x) = \infty$;

So, $\exists\ x_0 \in (0, \infty)$ such that $p(x_0) = 0$;

Proof completed. Also $p'(x) = 4x^3 + 3ax^2 + 2bx + c$;

Let $p'(x) = 0$;

$$4x^3 + 3ax^2 + 2bx = 0. \tag{3.10}$$

$$y^3 + qy + s = 0 \tag{3.11}$$

Where $y = x + \frac{3a}{4}$, $q = \frac{b}{2} - \frac{3a^2}{16}$, $s = \frac{c}{4} - \frac{ab}{8} + \frac{a^3}{32}$.

Assuming $y = (m + n)$ be the solution of equation (3.11), we get:

$$m^3 - \frac{p^3}{27m^3} + s = 0.$$

Assuming $m^3 = z$, we get $z^2 + sz - \frac{p^3}{27} = 0$.

Three roots are from equation (3.11):

$$y_1 = \left(-\frac{s}{2} + \sqrt{D}\right)^{1/3} + \left(-\frac{s}{2} - \sqrt{D}\right)^{1/3};$$

$$y_2 = \left(-\frac{s}{2} + \sqrt{D}\,\sigma\right)^{1/3} + \left(-\frac{s}{2} - \sqrt{D}\,\sigma^2\right)^{1/3};$$

$$y_3 = \left(-\frac{s}{2} + \sqrt{D}\,\sigma^2\right)^{1/3} + \left(-\frac{s}{2} - \sqrt{D}\,\sigma\right)^{1/3};$$

$$x_i = y_i - \frac{3a}{4}, \quad i = 1,2,3.$$

Where $D = \left(\frac{s}{2}\right)^2 + \left(\frac{q}{3}\right)^3$ and $\sigma = \frac{-1+\sqrt{3}i}{2}$.

Lemma 3. Let $r \geq 0$;

I. If $D \geq 0$, then positive roots are given by equation (3.9) iff $x_1 > 0$, $p(x_1) < 0$.

II. If $D < 0$, then positive roots are given by equation (3.9) iff there exists at least one $x^* \in (x_1, x_2, x_3)$ such that $x^* > 0$ and $p(x^*) \leq 0$.

III. If $D < 0$, then equation (3.11) has, three zeros only i.e $y_1,\ y_2, y_3$ accordingly equation (10) has also gives three roots $x_1,\ x_2, x_3$ such that at least one real root exists between them.

Proof: (I) If $D \geq 0,$ then equation (3.11) has a distinct real root y_1, which implies that equation (3.10) has a unique distinct real root x_1.

As consider $p(x)$ is a differentiable function and $lim_{x\to\infty}\, p(x) = \infty$, results x_1 be the unique critical point of $p(x)$, which comes out as the minimum point of $p(x)$.

Assumed equation (3.9) have positive roots. Generally, we represent that the four positive roots are denoted by ${x^*}_i, i = 1, 2, 3, 4$. Therefore equation (3.8) also gives four positive roots that is $\omega_j = \sqrt{{x^*}_i}, i = 1, 2, 3, 4$.

From (3.7) $\quad sin\,\omega\tau\ = \frac{A_3\omega - A_1\omega^3}{d}$.

That gives $\tau = \frac{1}{\omega}\left[sin^{-1}\left(\frac{A_3\omega - A_1\omega^3}{d}\right) + 2(j-1)\pi\right]\ ; j = 1,2,3,4 - -$

Let ${\tau_k}^{(j)} = \frac{1}{\omega_k}\left[sin^{-1}\left(\frac{A_3\omega - A_1\omega^3}{d}\right) + 2(j-1)\pi\right]\ ; k = 1, 2, 3, 4.; j = 1, 2, 3, 4 - -$

Then $\mp i\omega_k$ is a pair of complex roots i.e purely imaginary of equation (3.5)

Where $\tau = {\tau_k}^{(j)}, k = 1, 2, 3, 4.; j = 1, 2, 3, 4 - -$, we have $lim_{j\to\infty}\, {\tau_k}^{(j)} = \infty, k = 1, 2, 3, 4.$

Therefore, we can state $\tau_0 = {\tau_{k_0}}^{(j_0)} = min_{1\leq k\leq 4, j\geq 1}\left[{\tau_k}^{(j)}\right],\ \omega_0 = \omega_{k_0},\ y_0 = {y_{k_0}}^*$

Lemma 4. Suppose that $A_1 > 0,\ A_2 > 0,\ A_3 > 0, (A_4 + d\ ) > 0,\ A_1 A_2 - A_3 > 0,$ $A_1A_2A_3 - {A_3}^2 - {A_1}^2(A_4 + d) > 0.$

I. If any of the following condition satisfy: *(i)* $r < 0$ *(ii)* $r \geq 0,\ D \geq 0,\ x_1 > 0$, $p(x_1) \leq 0$ *(iii)* $r \geq 0,\ D < 0$ *and* $\exists$ *a* $x^* \in (x_1, x_2, x_3)$ such that $x^* > 0$ and $p(x^*) \leq 0$, there will be negative real part in all roots of equation (3.5), when $\Im \in [0, \Im_0)$.

II. From (I), if any condition (i) – (iii) are not concluded, then there will be roots with negative real parts of equation (3.5) $\forall, \tau \geq 0$.

Proof. Equation (3.5) defines with $\tau = 0$;

$$\lambda^4 + A_1\lambda^3 + A_2\lambda^2 + A_3\lambda + A_4 + d = 0 \quad (3.12)$$

All roots have negative real parts of equation (3.12) iff $A_1 > 0,\ A_2 > 0,\ A_3 > 0, (A_4 + d\ ) > 0,\ A_1A_2 - A_3 > 0,\ A_1A_2A_3 - {A_3}^2 - {A_1}^2(A_4 + d) > 0$.(using Routh-Hurwitz's criteria)

We discuss that if any conditions from (*i) - (iii*) are not satisfy, then none of the roots of equation (3.5) having zero as real part $\forall, \Im \geq 0$, From lemma *1 & 2*.

If any one of the states from lemma3, (i), (ii), (iii) holds, with $\Im \neq {\Im_k}^{(j)}, k = 1, 2, 3, 4.; j \geq 1$, then not any roots of the equation (3.5) having zero as real part. The least value of $\Im$ is $\Im_0$ by which equation (3.1) has purely complex roots.

Assume equation (3.5) has roots, $\lambda\ (\Im) =\ \alpha(\Im) + i\omega(\Im)$ satisfying:

$$\alpha(\Im_0) = 0, \omega(\Im_0) = \omega_0.$$

Lemma 5. Suppose $p'(x_0) \neq 0$. Then equation (3.5) has $\mp i\omega_0$ as set of simple and purely complex roots, if $\Im = \Im_0$. Also, If the lemma 3, conditions are satisfied, then $\frac{d}{d\tau}\big(Re\lambda(\Im_0)\big) > 0$.

Proof. The $i\omega_0$ should satisfy, whenever iω$_0$ is not a simple root:

$$\frac{d}{d\lambda}\left[\lambda^4 + A_1\lambda^3 + A_2\lambda^2 + A_3\lambda + A_4 + de^{-\lambda\Im}\right]_{\lambda = i\omega_0} = 0;$$

$$-4i{\omega_0}^3 - 3A_1{\omega_0}^2 + 2iA_2\omega_0 + A_3 - \Im d(cos\ \omega_0\Im - isin\ \omega_0\Im) = 0;$$

By separating real and imaginary parts of the above equation:

$$A_3 - 3A_1{\omega_0}^2 = \Im d\ cos\ \omega_0\Im\ ;$$

$$4{\omega_0}^3 - 2A_2\omega_0 = \Im d\ sin\ \omega_0\Im.$$

By dividing we obtain

$$tan\ \omega_0\Im = \frac{4{\omega_0}^3 - 2A_2\omega_0}{A_3 - 3A_1{\omega_0}^2}. \quad (3.13)$$

As Also,ω_0 must satisfy equation (3.2) and (3.3), from where we get:

$$tan\ \omega_0\Im = \frac{A_1{\omega_0}^3 - A_3\omega_0}{{\omega_0}^4 - A_2{\omega_0}^2 + A_4}. \quad (3.14)$$

Comparing (3.13) and (3.14) we get

$$4{\omega_0}^6 + 3\left({A_1}^2 - 2A_2\right){\omega_0}^4 + 2\left(2A_4 + {A_2}^2 - 2A_1A_3\right){\omega_0}^2 + \left({A_3}^2 - 2A_2A_4\right) = 0;$$

As we know ${\omega_0}^2 = x_0$,

$$4{x_0}^3 + 3\left({A_1}^2 - 2A_2\right){x_0}^2 + 2\left(2A_4 + {A_2}^2 - 2A_1A_3\right)x_0 + \left({A_3}^2 - 2A_2A_4\right) = 0;$$

$$4{x_0}^3 + 3l{x_0}^2 + 2mx_0 + n = 0.$$

Where $l = \left({A_1}^2 - 2A_2\right),\ m = \left(2A_4 + {A_2}^2 - 2A_1A_3\right),\ n = \left({A_3}^2 - 2A_2A_4\right).$

Which gives $p'(x) = 4x^3 + 3lx^2 + 2mx + n.$

Which is a contradiction as $p'(x_0) \neq 0.$

First part of the result is proved.

Differentiating equation (3.5) with respect to $\Im$, and obtain

$$\frac{d\lambda(\Im)}{d\Im} = \frac{d\lambda e^{-\lambda\Im}}{4\lambda^3 + 3A_1\lambda^2 + 2A_2\lambda + A_3 - d\Im e^{-\lambda\Im}};$$

Putting $\lambda = i\omega$,

$$\frac{d\lambda(\Im)}{d\Im} = \frac{di\omega(cos\,\omega - isin\,\omega\Im)}{(A_3 - 3A_1\omega^2 - d\Im\,cos\,\omega\Im) + i(2A_2 - 4\omega^3 + d\Im\,sin\,\omega\Im)};$$

When $\Im = \Im_0,\ \omega = \omega_0,\ x = x_0,$ we get

$$\frac{d\ Re\lambda(\Im_0)}{d\Im} = \frac{{\omega_0}^2}{\gamma}p'(x_0) \neq 0.$$

Where $\gamma = (A_3 - 3A_1\omega^2 - d\Im\,cos\,\omega\Im)^2 + (2A_2 - 4\omega^3 + d\Im\,sin\,\omega\Im)^2.$

If $\frac{d\ Re\lambda(\Im_0)}{d\tau} < 0$, equation (3.5) gives positive real part root for $\Im < \Im_0$ with the closeness of $\Im_0$ which contradicts, lemma 3. The proof is completed.

3.3 Numerical Stimulation

In this model MATLAB simulation is used to numerically consolidate the analytical findings. The system behaves as follows.

The values of these parameters are assumed after going through previous literature.

r = 3.71, k =3.02, μ = 4.01, d_1 = 0.00009, d_2 = 0.0009,

$\alpha = 1.5, \gamma_1 = 1.3, \gamma_2 = 1.3, \Delta_1 = 1.21, \Delta_2 = 1.21.$

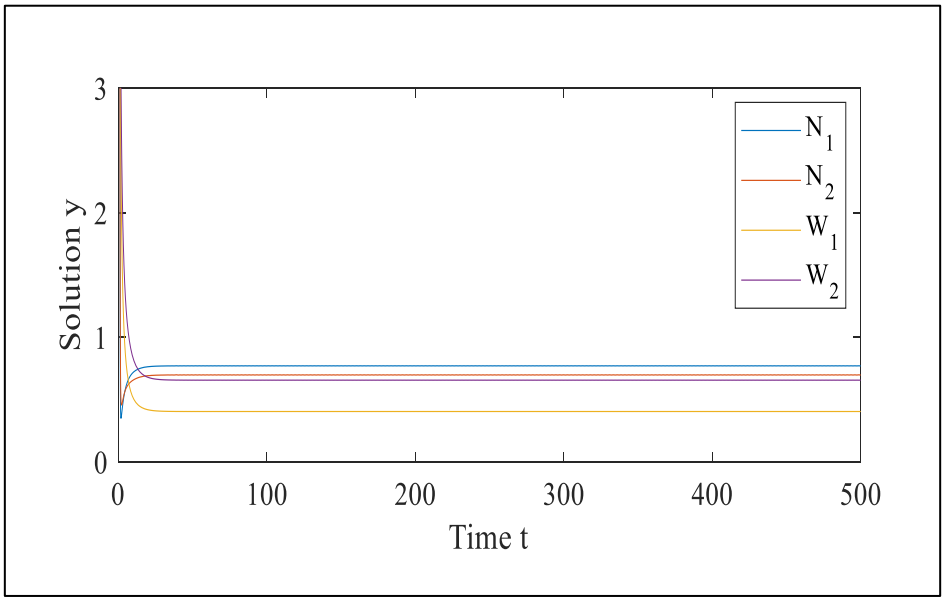

Figure 3.1 When there is absence of delay, $\Im = 0$, the system interior equilibrium point $\boldsymbol{S_1}$ is stable.

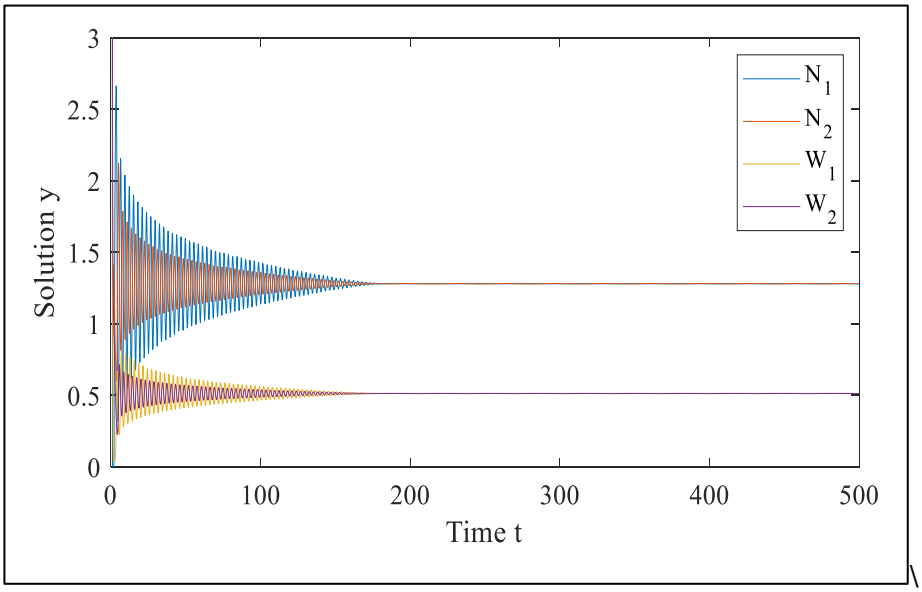

Figure 3.2 When there is delay that is $\Im < 2.15$, the system interior equilibrium point $\boldsymbol{S_1}$ is asymptotically stable.

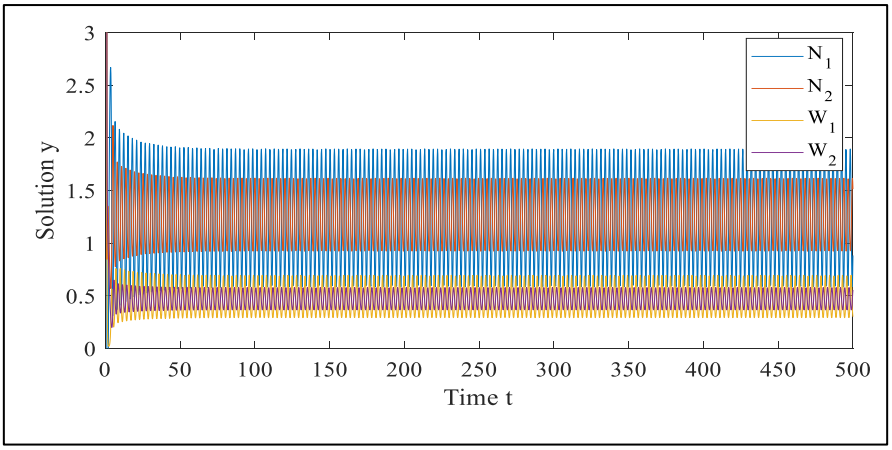

Figure 3.3 Shows that the interior equilibrium of the system loses stability and occurs the hopf bifurcation with delay $\Im > 1.25$.

3.4 Sensitivity Analysis

In this study, the model has fixed parameters. The "Direct Method" is used to figure out the global sensitivity coefficient. All of the parameters $(r, \alpha, \mu, \Delta_1, \Delta_2, \gamma_1, \gamma_2, d_1, d_2)$ contained in the system (1) - (4) are taken to be constants, then finding the partial derivatives of the solution for each parameter may be sufficient for the sensitivity analysis in this case. The following set of sensitivity equations can be created by taking the partially derivative of the solution (N_1, N_2, W_2, W_1) in respect to the variables:

$$\frac{dS_1}{dt} = rS_1 - \frac{2rN_1S_1}{k} - \mu\, S_4N_1\,(t-\Im) - \mu\, S_1(t-\Im)W_1 - d_1S_1. \tag{3.15}$$

$$\frac{dS_2}{dt} = rS_2 - \frac{2rN_2S_2}{k} - \mu\, S_3N_2 - \mu\, S_2W_2 - d_2S_2. \tag{3.16}$$

$$\frac{dS_3}{dt} = \alpha S_2W_2 + \alpha N_2S_3 - 2\Delta_2\, W_2S_3 - \gamma_2S_3. \tag{3.17}$$

$$\frac{dS_4}{dt} = \alpha S_1W_1 + \alpha N_1S_4 - 2\Delta_1\, W_1S_4 - \gamma_1S_4. \tag{3.18}$$

Where $S_1 = \frac{\partial N_1}{\partial \alpha}, S_2 = \frac{\partial N_2}{\partial \alpha}, S_3 = \frac{\partial W_2}{\partial \alpha}, S_4 = \frac{\partial W_1}{\partial \alpha}$.

The concentration of nutrients becomes unstable when α = 1.5 and Hopf -bifurcation occurs. But when the nutrients efficiency coefficient declines from α = 1.5 to α = 1.47, the graph becomes asymptotically stable, and it exhibits stability at α = 1.41 as shown in figure 4. Similarly, as α drops from α = 1.5 to α = 1.41, as shown in figure

3.5, figure 3.6, figure 3.7 the concentration of nutrients in shoot compartment and dry weight of root and shoot decreases respectively.

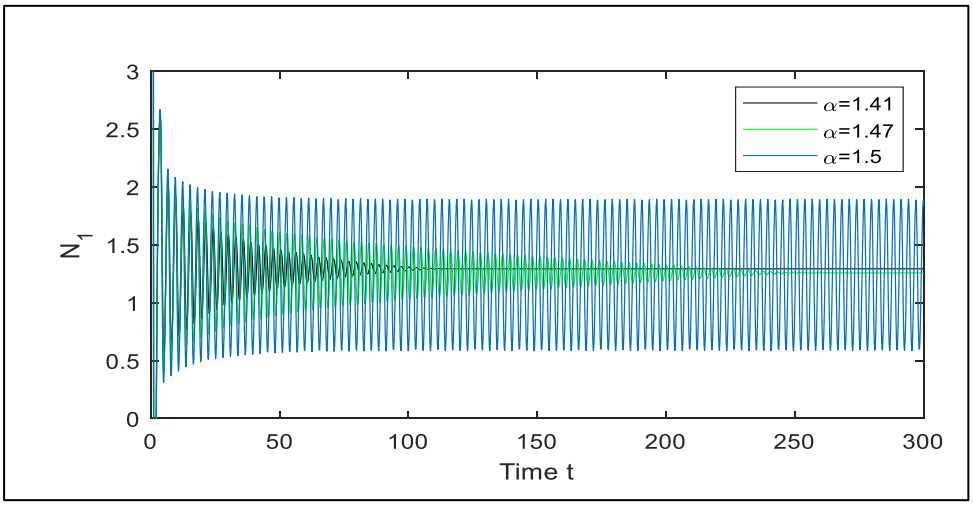

Figure 3.4 A time series graph shows the variation in the concentration of nutrients in roots for various values of the nutrients usage efficiency .

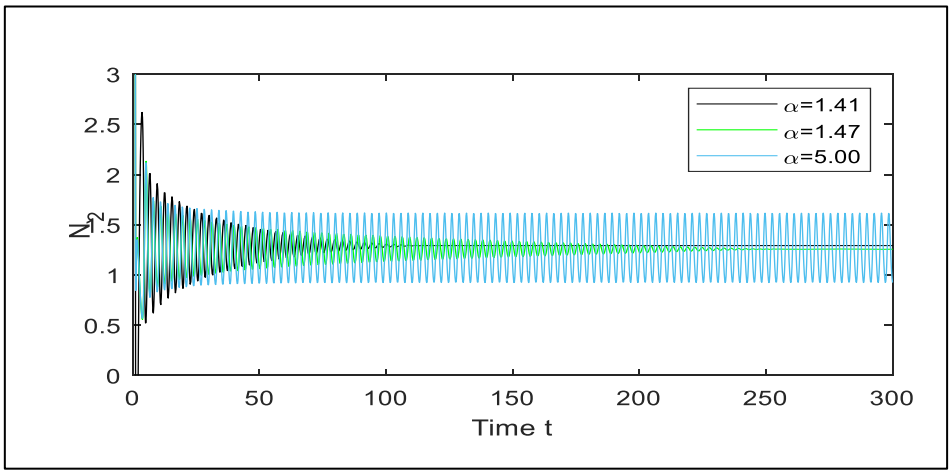

Figure 3.5 A time series graph shows the variation in the concentration of nutrients in shoot compartment for various values of the nutrients use efficiency .

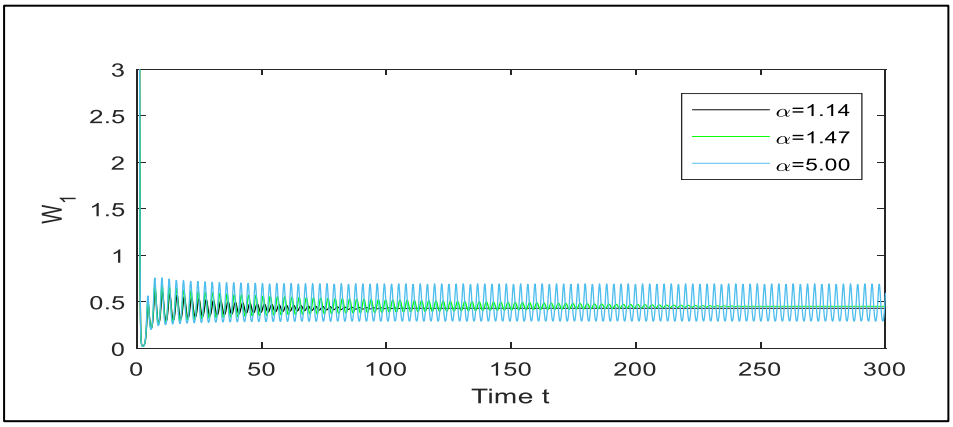

Figure 3.6 A time series graph shows the variation in the structural dry weight in roots for various values of the nutrients use efficiency .

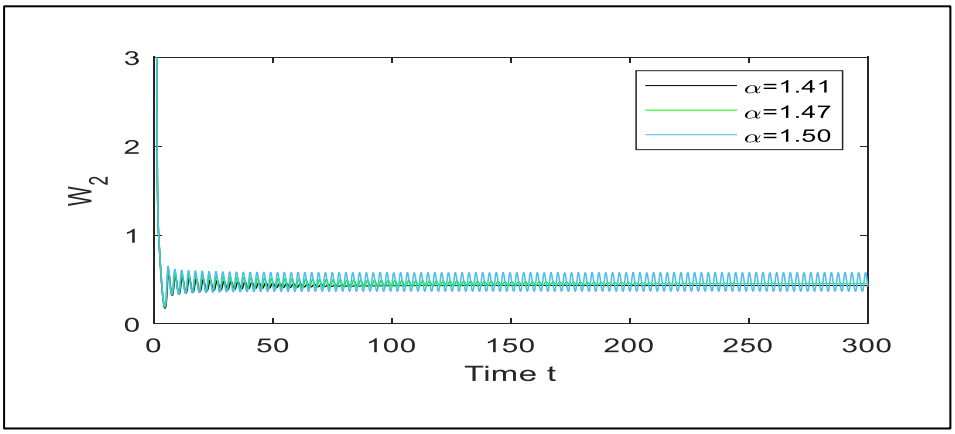

Figure 3.7 A time series graph shows the variation in the structural dry weight in shoot compartment for various values of the nutrients use efficiency .

3.5 Conclusion

The stability of the model has been examined about the IE S_1. When there is no delay ($\Im = 0$) in the model, as shown in Figure 3.1, the IE S_1 of the model is absolutely stable. This in accordance with lemma 4. The model has shown two distinct types of behaviour even after adding the delay. The IE S_1 is asymptotically stable, when the value of delay is less than 1.25 ($\Im < 1.25$) shown as Figure 3.2. The critical value of the parameter of delay is $\Im = 1.25$. When the value of delay parameter surpasses this critical value ($\Im > 1.25$), the equilibrium S_1 of the model shows oscillation that is HB as shown in the Figure 3.3. This behaviour of system is in agreement with lemma 2 & lemma 3. The sensitivity is calculated of state variable in the model (3.1) to (3.4) by changing the parameter α in DDEs (3.15) – (3.18). Figures (3.4) to (3.7) depicts the

phenomenon of sensitivity graphically that the state variable N_1, N_2, W_2 and W_1 changes the rate of oscillations with respect to the various values of α.

Chapter 4

A delay differential equation approach to investigate the impact of toxicity on plant growth patterns

4.1 Introduction

The plant uptakes nutrients from the soil for proper growth as part of plant-soil interaction process. Macronutrients and Micronutrients are the two major types of nutrients found in soil. The macronutrients found in soil, including phosphorus, potassium, nitrogen, calcium, hydrogen, and carbon, are advantageous resources that support plant growth. Nickel, zinc, and copper all play important roles in plant growth. These are often present in soil at extremely low concentrations. Heavy metals including chromium, cadmium, lead, mercury, nickel, etc., however, have a negative impact on soil quality [182], [183] . Excessive levels of heavy metals make soil more poisonous and gradually effect on plant growth [184]. Numerous elements, including geological, social, economic, and biological ones, contribute to the rise in toxic heavy elements in the soil. Additionally, nutrients play a significant influence in discrete plant growth, which has an impact on nonlinear population growth dynamics and, ultimately, on the yield of standing crops [4]. Metals or toxicity cause the soil's nutrition levels to become out of balance. The presence of toxicity affects both the biomass of trees and plants. Thornley was the first to experiment with mathematical modelling in plant physiology by taking into account various climatic change factors, such as humidity, temperature, rainfall, transpiration, respiration, rate of photosynthesis, guard cells of stomata, etc. However, these models were only taken into account for specific plant species under specific conditions [185],[186]. A simple mathematical model connecting toxic metal and soil chemistry that, toxic metals have a negative impact on tree biomass [187]. Biomass is negatively affected by the primary and secondary toxicity domains [188]. Also, nutrients have a crucial role in discrete plant growth, which has an impact on the dynamics of nonlinear population increase and, ultimately, on the yield of standing crops. Geographic location also affects crop yield and crop growth [189]. According to a mathematical model, a plant's rate of growth is a dynamic process that depends on factors like plant size, decrease growth rate, and nutrient mortality rate [180]. Delay was used to learn the

combined impact of acid and toxic metal on plant population [190]. The distribution of exponential polynomial roots is explained by Rouches's Theorem (1960). For their consideration of the distribution of exponential polynomial roots, Ruan and Wei (2001) used Rouches' theorem [175]. As plant biomass decreases under the influence of toxicity, the variable has oscillated for the delay value [83]. Delay was used to study the global stability in the collection of non-linear differential equations [165], [166]. It is possible to establish the direction of Hopf bifurcation as well as various numerical simulations, Using Hassard et al.'s manifold and normal form [191], [192]. The DDEs is used to construct the direct and adjoint approaches for sensitivity analysis in bioscience numerical modelling [193]. Direct method approach is used in the sensitivity analysis for nonlinear DE systems with time lags [181]. A generalised method for sensitivity analysis of DDE is purposed [194], [195]. In relation to the delays, theoretical conclusions for sensitivity are presented. The periodic responses to DDEs are studied using a parametric sensitivity analysis [150].

4.2 Mathematical Model

Assume, N be the plant nutrients concentration, the quantity of plant biomass B, and the amount of toxicity T concentration in the plant, all serve as three state variables, are used to model the dynamics of plant growth. The formulation of the model is as follows:

$$\frac{dN}{dt} = N_0 - \alpha_1 N(t-\Im)B - \alpha_2 N - \alpha_3 NT. \tag{4.1}$$

$$\frac{dB}{dt} = rB\left(1 - \frac{B}{K}\right) + \beta_1 N(t-\Im)B - \beta_2 B. \tag{4.2}$$

$$\frac{dT}{dt} = T_o - \gamma_1 NT - \gamma_2 T. \tag{4.3}$$

Initially: $N(0) > 0, B(0) > 0, T(0) > 0 \; \forall \;\; t$ and $N(t-\Im) =$ constant for $t \in [-\Im, 0]$.

These are the parameters: N_0 is the fixed amount of nutrients that are available, and T_0 is the fixed amount of toxicity that are available in soil because of the presence of toxic metals. r represents the growth rate of plant and K as the carrying capacity . α_1 is the rate of consumption of nutrients by biomass, α_3 is considered as rate of decay of nutrients due to its interaction with toxicity. β_1 is utilisation coefficient of nutrients. γ_1 is rate of decay of toxicity due to interaction with nutrients. The rates of natural

decay for N, B and T are α_2, β_2, γ_2 respectively. Here, it is assumed that all of the parameters $\alpha_1, \alpha_2, \alpha_3, \beta_1, \beta_2, \gamma_1, \gamma_{2,} N, B, T$ are positive.

4.2.1 Boundedness

4.2.1.1 *Lemma 1*: Consider the function, $\boldsymbol{W = N + B + T;}$

such that, $\frac{dW}{dt} = \frac{dN}{dt} + \frac{dB}{dt} + \frac{dT}{dt}$.

Using Equations (4.1) - (4.3), $\frac{dW(t)}{dt} = No - \alpha_1 NB - \alpha_2 N - \alpha_3 NT + r\left(1 - \frac{B}{K}\right) + \beta_1 NB - \beta_2 B + To - \gamma_1 NT - \gamma_2 T$ and $min(\alpha_1, \alpha_2, \alpha_3, \beta_1, \beta_2, \gamma_1, \gamma_2) = \delta$ and assuming $N \approx N(t - \Im)$ as $\to \infty$, $\frac{dW(t)}{dt} \leq (N_o + T_o)$

By Comparison theorem as $t \to \infty$, $W \leq \frac{N_o + T_o}{\delta}$,So $0 \leq (N + B + T) \leq \frac{N_o + T_o}{\delta}$.

4.2.2 Positivity of Solutions

Positivity of system defines that model's solution, with initial data, will eventually be positive $\forall\, t$ exceeding some finite value. One must demonstrate that every solution provided by the equations is positive solution. (4.1) - (4.3), where initial condition is $N(0) > 0, B(0) > 0, T(0) > 0 \;\forall\, t \; and \; N(t - \Im) = constant \; for \; t \in [-\Im, 0]$, the model solution (N, B, T) remain positive $\forall$ time $t > 0$.

From equation (4.3): $\frac{dT}{dt} \geq -\delta(N + 1)T$ i.e. $\frac{dT}{dt} \geq -\big((N_o + T_o) + \delta\big)T$, $T \geq c_1 e^{-((N_o + T_o) + \delta)t}$, here c_1 is constant of integration. So, T $> 0 \;\forall\, t$.

For N and B, the same argument is valid.

4.2.3 Interior Equilibrium Point

A mathematical model under consideration has an equilibrium point that defines a constant solution. We identify the internal equilibrium E^* of the model. For the set of equations (4.1)-(4.3), there is only one possible equilibrium at $E^*(N^*, B^*, T^*)$,

$$N^* = \frac{-b \mp \sqrt{b^2 - 4ac}}{2a};$$

$$T^* = \frac{T_o}{\gamma_1 N^* - \gamma_2};$$

$$B^* = \frac{K}{r}(r - \beta_1 N^* - \beta_2).$$

where a = $\alpha_1 K\beta_1\gamma_1$, b = $\alpha_1\gamma_1 K\, r - \alpha_1 K\beta_2\gamma_1 - \alpha_1 K\beta_1\gamma_2 + \alpha_2\gamma_1 r$, c = $\alpha_1 K\, r + \alpha_1 K\beta_2\gamma_1 - \alpha_2\gamma_2 r + \alpha_3 T_o$.

4.2.4 Analysis of Hopf- bifurcation

This section analyses, the dynamical internal equilibrium point behaviour $E^*(N^*, B^*, T^*)$ of model (4.1) -(4.3). In relation to equilibrium E^*, the exponential

$$\lambda^3 + P_1\lambda^2 + P_2\lambda + P_3 + (Q_1\lambda^2 + Q_2\lambda + Q_3)e^{-\lambda\tau} = 0; \tag{4.4}$$

characteristic equation is provided by:

Where $P_1 = \alpha_2 + \alpha_3 T + \frac{r}{k} + \beta_2 + \gamma_1 N + \gamma_2$,

$$P_2 = \frac{r}{k}\alpha_2 + \frac{r}{k}\alpha_3 T + \beta_2\alpha_2 + \beta_2\alpha_3 T + \frac{r}{k}\gamma_1 N + \frac{r}{k}\gamma_2 + \beta_2\gamma_1 N + \beta_2 N_2 + \alpha_2\gamma_1 N + \gamma_1 N\alpha_3 + \gamma_2\alpha_2 + \gamma_2\alpha_3 T,$$

$P_3 = \frac{r}{k}\alpha_2\gamma_1 N + \frac{r}{k}\alpha_2\gamma_2 + \alpha_2\beta_2\gamma_1 N + \alpha_2\beta_2\gamma_2 + \frac{r}{k}\alpha_3\gamma_1 NT + \frac{r}{k}\alpha_3\gamma_2 T + \alpha_3\beta_2\gamma_1 NT + \alpha_3\beta_2\gamma_2 T - \gamma_1\alpha_3 TN$,

$$Q_1 = \alpha_1 B,$$

$$Q_2 = \frac{r}{k}\alpha_1 B + \beta_2\alpha_1 B + \gamma_1\alpha_1 N + \gamma_2\alpha_1 B,$$

$$Q_3 = \frac{r}{k}\alpha_1\gamma_1 BN + \frac{r}{k}\alpha_1\gamma_2 B + \alpha_2\beta_2\gamma_1 BN + \alpha_1 B_2\gamma_2 B.$$

Clearly $P_1, P_2, P_3, Q_1, Q_2, Q_3$ all are positive.

Equation (4) can only be solved if and only if $\lambda = i\omega$ is true.

$$(i\omega)^3 + P_1(i\omega)^2 + P_2(i\omega) + P_3 + (Q_1(i\omega)^2 + Q_2(i\omega) + Q_3)e^{-i\omega\Im} = 0. \tag{4.5}$$

Separating real and imaginary parts:

$$P_3 - P\omega^2 + (Q_3 - Q_1\omega^2)cos\ \omega\Im + Q_2\omega \sin\omega\Im = 0. \tag{4.6}$$

$$P_2\omega - \omega^3 + Q_2\omega\ cos\ \omega\Im - (Q_3 - Q_1\omega^2)\sin\omega\Im = 0. \tag{4.7}$$

Which gives: (4.8)

$$\omega^6 + \left({P_1}^2 - {Q_1}^2 - 2P_2\right)\omega^4 + \left({P_2}^2 - {Q_2}^2 + 2Q_1Q_3 - 2P_1P_3\right)\omega^2 + \left({P_3}^2 - {Q_3}^2\right) = 0.$$

Let

$$u = \left({P_1}^2 - {Q_1}^2 - 2P_2\right), v = \left({P_2}^2 - {Q_2}^2 + 2Q_1Q_3 - 2P_1P_3\right), z = \left({P_3}^2 - {Q_3}^2\right). \quad (4.9)$$

Let $\omega^2 = x$, then equation (4.8) is: $x^3 + ux^2 + vx + z = 0$.

Claim 1: If $z < 0$, eq. (4.9) has one real +ve zero.

Proof: Consider $s(x) = x^3 + ux^2 + vx + z$;

Here $(0) = z < 0$, $\lim_{x\to\infty} s(x) = \infty$ So, $\exists\ z_0 \in (0, \infty)$ such that $s(x_0) = 0$. ■

Claim 2: If $z \geq 0$, $D = u^2 - 3v \geq 0$ is a necessary condition for the existence of positive real roots in equation (4.9).

Proof: Since, $s(x) = x^3 + ux^2 + vx + z$ therefore $s'(x) = 3x^2 + 2ux + v$;

$s'(x) = 0$ implies $3x^2 + 2ux + v = 0$; (4.10)

The roots of equation (10) can be written as

$$x_{1,2} = \frac{-2u \mp \sqrt{4u^2 - 12v}}{6} = \frac{-u \mp \sqrt{D}}{3}. \quad (4.11)$$

There are no real roots in equation (10) if $D < 0$. As a result, the function $s(x)$ is an increasing monotone function in x. Since $k(0) = z \geq 0$, therefore positive real roots cannot exist in equation (9). It has been proven.

Clearly if $D \geq 0$, then $x_1 = \frac{-u+\sqrt{D}}{3}$ is local minima of $s(x)$. Hence, the following assertion.

Claim 3: If $z \geq 0$, and only if $x_1 > 0$ and $s(x_1) \leq 0$, equation (4.9) has positive real.

Proof. It is clear that there is enough. There is only one requirement: necessity. If not, assume that $s(x) > 0$ and either $x_1 \leq 0$ or $x_1 > 0$. Consequently $s(x)$ has no positive

real zeros if $x_1 \leq 0$ since $s(x)$ is rising for $x \geq x_1$ and $s(0) = c \geq 0$. Since $x_2 = \frac{-u-\sqrt{D}}{3}$ is the local maximum value if $x_1 > 0$ and $s(x_1) > 0$, it follows that $s(x_1) \leq s(x_2)$. Because $s(x)$ lacks positive real roots, $s(0) = c \geq 0$. Proof is now complete.

4.2.4.1 ***Lemma 2*****:** Assume that equation (11) defines $\boldsymbol{x_1}$.

i. If $z < 0$,at least a positive real zero exists in eq. (4.9).

ii. If $z \geq 0$ and $D = u^2 - 3v < 0$, no positive zeros can be found for eq. (4.9).

iii. If $z \geq 0$, there are positive zeros in eq. (4.9) iff $x_1 > 0$ and $s(x_1) \leq 0$.

Proof: Assume that equation (4.9) has roots that are positive. Suppose it has three constructive roots without losing generality, signified by x_1, x_2 , x_3. Then equation (4.48) has three positive roots, say $\omega_1 = \sqrt{x_1}$, $\omega_2 = \sqrt{x_2}$, $\omega_3 = \sqrt{x_3}$.

From (4.7) $\sin \omega\tau = \frac{P_2\omega - \omega^3}{d}$Which gives $\tau = \frac{1}{\omega}\left[sin^{-1}\left(\frac{P_2\omega-\omega^3}{d}\right) + 2(j-1)\pi\right]$; $j = 1,2,3,-$

Let $\tau_k{}^{(j)} = \frac{1}{\omega_k}\left[sin^{-1}\left(\frac{P_2\omega_k-{\omega_k}^3}{d}\right) + 2(j-1)\pi\right]$; $k = 1,2,3.$; $j = 0,1,2,---$

Then $\mp i\omega_k$ is a pair of equation (8), roots that are entirely imaginary.

Where $\Im = \Im_k{}^{(j)}, k = 1,2,3.; j = 0,1,2,3,--,$ $\lim_{j\to\infty} \Im_k{}^{(j)} = \infty \, where \, k = 1,2,3.$

Thus, define

$$\Im_0 = \Im_{k_0}{}^{(j_0)} = \min_{1\leq k\leq 3, j\geq 1}\left[\Im_k{}^{(j)}\right], \qquad \omega_0 = \omega_{k_0}, \qquad x_0 = x_{k_0}{}^{j} \tag{4.12}$$

4.2.4.2 Lemma 3: Suppose that $\boldsymbol{P_1 > 0}, \boldsymbol{(P_3 + d) > 0}, \ \boldsymbol{P_1P_2 - (P_3 + d) > 0}$.

i. The real part of very root of equation (4) is negative $\forall$ $\Im \geq 0$ if $z \geq 0$ and $D = u^2 - 3v < 0$.

ii. The real part of every root of equation (4) is negative $\forall\, \Im \in [0, \Im_0)$ if $z < 0$ o $z \geq 0$, $x_1 > 0$ and $s(x_1) \leq 0$.

Proof: When $\Im = 0$, equation (4.4) changes to

$$\lambda^3 + (P_1 + Q_1)\lambda^2 + (P_2 + Q_2)\lambda + (P_3 + Q_3) = 0. \tag{4.13}$$

Using Routh-Hurwitz's criteria, (H1): $if\ (P_3 + Q_3) > 0, (P_1 + Q_1)(P_2 + Q_2) - (P_3 + Q_3) > 0$, then all the roots in equation (4.4) have negative real part.

If $z \geq 0$ and $D = u^2 - 3v < 0$, equation (4) does not have any roots with a real part of zero $\forall \Im \geq 0$ according to Lemma 2 (II). When $z < 0$ or $z \geq 0$, $x > 0$ and $s(x_1) \leq 0$, Lemma 2 (I) and (III) implies that when $\Im \neq \Im_k{}^{(j)}, k = 1, 2, 3.; j \geq 1$, Since $\Im_0$ is the smallest value of $\Im$ and equation (4.4) just has imaginary roots, it does not have any real roots with any real parts. The result is obtained using the theorem 1.

$$\lambda(\Im) = \psi(\Im) + i\omega(\Im). \tag{4.14}$$

Suppose

being the roots of the equation (4.4) holds: $\psi(\Im_0) = 0,\ \omega(\Im_0) = \omega_0$.

Assume that $s'(x_0) \neq 0$, to ensure that $\mp\omega_0$ simple and purely imaginary roots of equation (4.4), as $\Im = \Im_0$ and $\lambda(\Im)$ meets satisfies the transversality requirement.

4.2.4.3 Lemma 4: Suppose $\boldsymbol{x_0 = \omega_0{}^2}$. If $\boldsymbol{\Im = \Im_0}$, Then Sign $[\boldsymbol{\psi'(\Im_0)}]$ =Sign $[\boldsymbol{s'(x_0)}]$

Proof. Differentiating w.r.t $\Im$ and inserting $\lambda(\Im)$ into equation (4) results in the following.

$\frac{d\lambda}{d\Im}\left[3\lambda^2 + 2P_1\lambda + Q_2 + \left((Q_1\lambda^2 + Q_2\lambda + Q_3)(-\Im) + (2Q_1\lambda + Q_2)\right)e^{-\lambda\Im}\right] =$
$\lambda(Q_1\lambda^2 + Q_2\lambda + Qn_3)e^{-\lambda\Im}$.

Then $\left(\frac{d\lambda}{d\Im}\right)^{-1} = \frac{(3\lambda^2+2P_1\lambda+P_2)e^{\lambda\Im}}{\lambda(Q_1\lambda^2+Q_2\lambda+Q_3)} + \frac{(2Q_1\lambda+Q_2)}{\lambda(Q_1\lambda^2+Q_2\lambda+Q)} - \frac{\Im}{\lambda}$

From equations (6) -(8):

$\mu'(\Im_0) = Re\left[\frac{(3\lambda^2+2P_1\lambda+P_2)e^{\lambda\Im}}{\lambda(Q_1\lambda^2+Q_2\lambda+Q_3)}\right] + Re\left[\frac{(2Q_1\lambda+Q_2)}{\lambda(Q_1\lambda^2+Q_2\lambda+Q_3)}\right] = \frac{1}{\Delta}[3{\omega_0}^6 + 2u{\omega_0}^4 + v{\omega_0}^2]$

Where $\Delta = [(Q_3 - Q\omega^2)^2 + (Q_2\omega)^2]$. In this case $\Delta > 0$ and $\omega_0 > 0$.

Consequently, it is proved that Sign $[\psi'(\Im_0)]$ =Sign $[s'(x_0)]$.

4.2.5 Direction Analysis and stability analysis of the HB Solution

Theorem 1: Let Assume, $y_1 = N - N^*, y_2 = B - B^*, y_3 = T - T^*$ and time scaling, as well as normalising the delay $\Im$, $t \to \frac{t}{\Im}$, equation (4.1) – (4.3) are:

$$\frac{dy_1}{dt} = -\alpha_2 y_1 - \alpha_1 B^* y_1(t-1) - \alpha_1 y_1(t-1) y_2 - \alpha_3 T^* y_1 - \alpha_3 N^* y_3 - \alpha_3 y_1 y_3; \quad (4.15)$$

$$\frac{dy_2}{dt} = \frac{r}{k} y_2 - \beta_2 y_2 + \beta_1 N^* y_1(t-1) + \beta_1 y_1(t-1) y_2; \quad (4.16)$$

$$\frac{dy_3}{dt} = -\gamma_1 T^* y_1 - \gamma_1 N^* y_3 - \gamma_2 y_3 - \gamma_1 y_1 y_3; \quad (4.17)$$

Thus, work can be done in the phase $C = C\left((-1,0), {R_+}^3\right)$. Without loss of generality, denote the critical value $\Im_j$ by $\Im_0$. Let $\Im = \Im_0 + \mu$, then $\mu = 0$ is a Hb value of the system given by equations (15) -(17). Rewrite this system as follows for notational simplicity:

$$y'(t) = L_\mu(y_t) + F(\mu, y_t). \quad (4.18)$$

Where $y(t) = (y_1(t), y_2(t), y_3(t))^T \in R^3, y_t(\theta) \in C$ is defined by $y_t(\theta) = y_t(t+\theta)$, and

$L_\mu: C \to R$, $F: R \times C \to R$ are provided, respectively by

$$L_\mu \delta = (\tau_0 + \mu) \begin{bmatrix} -(\alpha_2 + \alpha_3 T^*) & 0 & -\alpha_3 N^* \\ 0 & -\left(\frac{r}{k} + \beta_2\right) & 0 \\ -\gamma_1 T^* & 0 & -(\gamma_1 N^* + \gamma_2) \end{bmatrix} \begin{bmatrix} \delta_1(0) \\ \delta_2(0) \\ \delta_3(0) \end{bmatrix} + (\Im_0 + \mu)$$

$$\begin{bmatrix} -\alpha_1 B^* & 0 & 0 \\ -\beta_1 B^* & 0 & 0 \\ 0 & 0 & 0 \end{bmatrix} \begin{bmatrix} \delta(-1) \\ \delta(-2) \\ \delta(-3) \end{bmatrix} \text{s.}$$

And $F(\mu, \delta) = (\Im_0 + \mu) \begin{bmatrix} F_1 \\ F_2 \\ F_3 \end{bmatrix}$ respectively where $F_1 = -\alpha_1 \delta_1(-1)\delta_2(0)$,

$F_2 = \beta_1 \delta_1(-1)\delta_2(0), F_3 = -\gamma_1 \delta_1(0)\delta_3(0)$,

$\delta(\theta) = \left(\delta_1(\theta), \delta_2(\theta), \delta(\theta)\right)^T \in C\left((-1,0), R\right)$.

According to the Riesz theorem, a function $\eta(\theta, \mu)$ is constrained variation for $\theta \in [-1,0]$, such that $L_\mu \delta = \int_{-1}^{0} d\,\eta(\theta, 0)\delta(\theta)$ for $\delta \in C$.

Choose in reality

$$\eta(\theta,\mu) = (\Im_0 + \mu)\begin{bmatrix} -(\alpha_2 + \alpha_3 T^*) & 0 & -\alpha_3 N^* \\ 0 & -\left(\frac{r}{k} + \beta_2\right) & 0 \\ -\gamma_1 T^* & 0 & -(\gamma_1 N^* + \gamma_2) \end{bmatrix}\delta(\theta) +$$

$$(\tau_0 + \mu)\begin{bmatrix} -\alpha_1 B^* & 0 & 0 \\ -\beta_1 B^* & 0 & 0 \\ 0 & 0 & 0 \end{bmatrix}\delta(\theta + 1).$$

Here $\in C\left([-1,0], {R_+}^3\right)$, define

$$A(\mu)\delta = \begin{cases} \frac{d\delta(\theta)}{d\theta}, & \theta \in [-1,0) \\ \int_{-1}^{0} d\,\eta(\theta,0)\delta(\theta), & \theta = 0. \end{cases}$$ And

$$R(\mu)\delta = \begin{cases} 0, & \theta \in [-1,0) \\ F(\mu,\delta) & \theta = 0. \end{cases}$$

The system (18) then corresponds to:

$$y'(t) = A(\mu)\delta + R(\mu)y_t. \tag{4.19}$$

For $\psi \in C^1\left([-1,0], {R_+}^3\right)$, state

$$A^*\psi(h) = \begin{cases} -\frac{d\psi(h)}{ds}, & h \in [-1,0) \\ \int_{-1}^{0} d\,\eta^T(-t,0)\psi(-t), & h = 0. \end{cases}$$ And bilinear inner product

$$< \psi(h), \delta(\theta) > = \overline{\psi(0)}\delta(0) - \int_{-1}^{0}\int_{\xi=\theta}^{\theta} \overline{\psi}(\xi - \theta)d\eta(\theta)\delta(\xi)\,d\xi. \tag{4.20}$$

Sine A^* and $A = A(0)$ are adjoint operators and $i\omega_0$ are eigen values of $A(0)$. Thus they are eigen values of A^*. Assume that $q(\theta) = q(0)e^{i\omega_0\theta}$ is an eigen vector of $A(0)$ corresponding to the eigen value $i\omega_0$. Then $A(0) = i\omega_0\, q(\theta)$. When $\theta = 0$,

$\left[i\omega_0 I - \int_{-1}^{0} d\eta(\theta)e^{i\omega_0\theta}\right] q(0) = 0$, that outcome $q(0) = (1, \sigma_1, \rho_1)^T$

$$\sigma_1 = \frac{(\alpha_1 B^* + (\alpha_2 + \alpha_3 T^*) - i\omega_0)}{\alpha_3 N^*} \;\; and \;\; \rho_1 = \frac{\beta_1 B^*\left(\left(\frac{r}{k} + \beta_2\right) - i\omega_0\right)}{\left(\frac{r}{k} + \beta_2\right)^2 + {\omega_0}^2}.$$

The same can be confirmed that $q^*(s) = D(1, \sigma_2, \rho_2)e^{i\omega_0\tau_0 s}$ is the eigen value of A^* that corresponds to $-i\omega_0$, where

$$\sigma_1 = \frac{(\alpha_1 B^* + (\alpha_2 + \alpha_3 T^*) - i\omega_0)}{\alpha_3 N^*} \;\; and \;\; \rho_1 = \frac{\beta_1 B^*\left(\left(\frac{r}{k} + \beta_2\right) - i\omega_0\right)}{\left(\frac{r}{k} + \beta_2\right)^2 + {\omega_0}^2}.$$

To ensure $< q^*(s), q(\theta) > = 1$, it is necessary to calculate the value of D.

From equation (22), $< q^*(s), q(\theta) >$

$=$

$\overline{D}(1, \overline{\sigma_2}, \overline{\rho_2})(1, \sigma_1, \rho_1)^T -$

$\int_{-1}^{0} \int_{\xi=\theta}^{\theta} \overline{D}(1, \overline{\sigma_2}, \overline{\rho_2}) e^{-i\omega_0 \Im_0 (\xi-\theta)} d\eta(\theta)(1, \sigma_1, \rho_1)^T e^{i\omega_0 \Im_0} \, d\xi$

$= \overline{D} \left\{ 1 + \sigma_1 \overline{\sigma_2} + \rho_1 \overline{\rho_2} - \int_{-1}^{0} (1, \overline{\sigma_2}, \overline{\rho_2}) \, \theta e^{i\omega_0 \Im_0 \theta} (1, \sigma_1, \rho_1)^T \right\}$

$= \overline{D} \{ 1 + \sigma_1 \overline{\sigma_2} + \rho_1 \overline{\rho_2} + \tau_0 \overline{\sigma_2} W^* (\beta_1 \rho_1 - \alpha_1 \sigma_1) e^{i\omega_0 \Im_0} \}$

Hence, select $\overline{D} = \frac{1}{\left(1 + \sigma_1 \overline{\sigma_2} + \rho_1 \overline{\rho_2} + \Im_0 \overline{\sigma_2} B^* (\beta_1 \rho_1 - \alpha_1 \sigma_1) e^{i\omega_0 \Im_0}\right)}$.

That way $< q^*(s), q(\theta) > = 1, < q^*(s), \overline{q(\theta)} > = 0$.

The coordinates characterising the centre manifold C_0 at μ=0 are computed by applying the algorithm described in [16] and using their notations. Assume y_t as solution of equation (4.18) at $\mu = 0$. Therefore

$z(t) =< q^*(s), y_t(\theta) >, \; W(t, \theta) = y_t(\theta) - 2Re(z(t)q(\theta)).$ (4.21)

On the centre manifold C_0, $W(t, \theta) = W\left(z(t), \overline{z(t)}, \theta\right)$;

Where $W(z, \overline{z}, \theta) = W_{20}(\theta) \frac{z^2}{2} + W_{11}(\theta) z\overline{z} + W_{02}(\theta) \frac{\overline{z}^2}{2} + \cdots,$

Local coordinates for the centre of the manifold C_0 are z and $\overline{z}$ towards q^* and $\overline{q^*}$. Consider that W is real if y_t is real. The only real solutions should be taken into consideration. For the solution $y_t \in C_0$ of equation (20), since $\mu = 0$,

$$z'(t) = i\omega_0 \tau_0 z + < \overline{q^*}(\theta), F\big(0, B(z, \overline{z}, \theta) + 2Re\big(z(t)q(\theta)\big)\big) >$$

$$= i\omega_0 \tau_0 z + \overline{q^*}(0) \, F\big(0, W(z, \overline{z}, 0) + 2Re\big(z(t)q(\theta)\big)\big).$$

$$\equiv i\omega_0 \tau_0 z + \overline{q^*}(0) F_0(z, \overline{z}).$$

Rewrite this equation as

$$z'(t) = i\omega_0 \tau_0 z(t) + g(z, \overline{z}); \quad (4.22)$$

Where $g(z, \overline{z}) = \overline{q^*}(0) F_0(z, \overline{z}) = g_{20}(\theta) \frac{z^2}{2} + g_{11}(\theta) z\overline{z} + g_{02}(\theta) \frac{\overline{z}^2}{2} +$ (4.23)

$$g_{21}(\theta) \frac{z^2 \overline{z}}{2} + \cdots;$$

As $y_t(\theta) = (y_{1t}, y_{2t}, y_{3t}\ ) = W(t,\theta) + z\,q(\theta) + \overline{z}\overline{q(\theta)}$ and $q(0) =$, so

$$(1, \sigma_1, \rho_1)^T e^{i\omega_0 \Im_0 \theta}.$$

$$y_{1t}(0) = z + \overline{z} + {W_{20}}^{(1)}(0)\frac{z^2}{2} + {W_{11}}^{(1)}(0)\, z\overline{z} + {W_{02}}^{(1)}(0)\frac{\overline{z}^2}{2} + \cdots,$$

$$y_{2t}(0) = \sigma_1 z + \overline{\sigma_1}\,\overline{z} + {W_{20}}^{(2)}(0)\frac{z^2}{2} + {W_{11}}^{(2)}(0)\, z\overline{z} + {W_{02}}^{(2)}(0)\frac{\overline{z}^2}{2} + \cdots,$$

$$y_{3t}(0) = \rho_{1_1} z + \overline{\rho_{1_1}}\,\overline{z} + {W_{20}}^{(3)}(0)\frac{z^2}{2} + {W_{11}}^{(3)}(0)\, z\overline{z} + {W_{02}}^{(3)}(0)\frac{\overline{z}^2}{2} + \cdots,$$

$$y_{1t}(-1) = ze^{-i\omega_0\Im_0} + \overline{z}e^{i\omega_0\Im_0} + {W_{20}}^{(1)}(-1)\frac{z^2}{2} + {W_{11}}^{(1)}(-1)\, z\overline{z} +$$

$${W_{02}}^{(1)}(-1)\frac{\overline{z}^2}{2} + \cdots,$$

$$y_{2t}(-1) = \sigma_1 e^{-i\omega_0\Im_0} z + \overline{\sigma_1}\, e^{i\omega_0\Im_0}\,\overline{z} + {W_{20}}^{(2)}(-1)\frac{z^2}{2} + {W_{11}}^{(2)}(-1)\, z\overline{z} +$$

$${W_{02}}^{(2)}(-1)\frac{\overline{z}^2}{2} + \cdots,$$

Thus, comparing coefficients to equation (4.23) provides:

$$g_{20} = \overline{D}(1, \sigma_1, \rho_1) f_{z^2},\ g_{02} = \overline{D}(1, \overline{\sigma_1}, \overline{\rho_2}\,) f_{\overline{z}^2},$$

$$g_{11} = \overline{D}(1, \overline{\sigma_1}, \overline{\rho_2}\,) f_{z\overline{z}}, g_{21} = \overline{D}(1, \overline{\sigma_1}, \overline{\rho_2}\,) f_{z^2\overline{z}}.$$

For clarification g_{21}, Computation must be the main focus of $W_{20}(\theta)$ and $W_{11}(\theta)$. From equations (4.19) and (4.21):

$$W' = {u_t}' - z'q - \overline{z}'q = \begin{cases} AW - 2Re\left[\overline{q^*}(0)F_0 q(\theta)\right], & \theta \in [-1,0) \\ AW - 2Re\left[\overline{q^*}(0)F_0 q(0)\right] + F_0, & \theta = 0 \end{cases}$$

Let $W' = AW + H(z, \overline{z}, \theta)$ (4.24)

Where $H(z, \overline{z}, \theta) = H_{20}(\theta)\frac{z^2}{2} + H_{11}(\theta) z\overline{z} + H_{02}(\theta)\frac{\overline{z}^2}{2} + H_{21}(\theta)\frac{z^2\overline{z}}{2} + \cdots,$ (4.25)

As opposed to that, on C_0 at the origin $W' = W_z z' + W_z \overline{z}'$.

The above series is expanded, the coefficients are calculated, and the result is

$$[A - 2i\omega_0 I] W_{20}(\theta) = -H_{20}(\theta),\ \ AW_{11}(\theta) = -H_{11}(\theta). \quad (4.26)$$

By equation (4.22), for $\theta \in [-1,0)$,

$$H(z, \overline{z}, \theta) = -\overline{q^*}(0)\overline{F_0} q(\theta) - \overline{q^*}(0)\overline{F_0}\,\overline{q}(\theta) = -gq(\theta) - \overline{g}\ \overline{q}(\theta)\ .$$

Comparing the coefficients with (4.23) for $\theta \in [-1,0]$ that

$$H_{20}(\theta) = -g_{20} q(\theta) - \overline{g_{02}}\,\overline{q}(\theta),\ H_{11}(\theta) = -g_{11} q(\theta) - \overline{g_{11}}\,\overline{q}(\theta).$$

From equation (4.422), (4.25) and definition of A are obtained

$$W_{20}(\theta) = 2i\omega_0\Im_0 W_{20}(\theta) + g_{20}q(\theta) + \overline{g_{02}}\,\overline{q}(\theta).$$

Solving for $W_{20}(\theta)$:

$$W_{20}(\theta) = \frac{ig_{20}}{\omega_0\Im_0}q(0)e^{i\omega_0\Im_0\theta} + \frac{i\overline{g_{02}}}{3\omega_0\tau_0}\overline{q}(0)e^{-i\omega_0\Im_0\theta} + E_1e^{2i\omega_0\Im_0\theta},$$

And similarly

$$W_{11}(\theta) = \frac{-ig_{11}}{\omega_0\Im_0}q(0)e^{i\omega_0\Im_0\theta} + \frac{i\overline{g_{11}}}{\omega_0\Im_0}\overline{q}(0)e^{-i\omega_0\Im_0\theta} + E_2\ .$$

Where E_1 and E_2 are both three dimensional vectors, and can be determined by setting $\theta = 0$ in H. In fact since $H(z,\overline{z},\theta) = -2Re\left[\overline{q^*}(0)F_0q(0)\right] + F_0$, So

$$H_{20}(\theta) = -g_{20}q(\theta) - \overline{g_{02}}\,\overline{q}(\theta) + F_{z^2},$$

$$H_{11}(\theta) = -g_{11}q(\theta) - \overline{g_{11}}\,\overline{q}(\theta) + F_{z\overline{z}}.$$

Where $F_0 = F_{z^2}\frac{z^2}{2} + F_{z\overline{z}}z\overline{z} + F_{\overline{z}^2}\frac{\overline{z}^2}{2} + \cdots$

Hence combining the definition of A,

$\int_{-1}^{0} d\,\eta(\theta)W_{20}(\theta) = 2i\omega_0\Im_0 W_{20}(0) + g_{20}q(0) + \overline{g_{02}}\,\overline{q}(0) - F_{z^2}$ and

$\int_{-1}^{0} d\,\eta(\theta)W_{11}(\theta) = g_{11}q(0) - \overline{g_{11}}\,\overline{q}(0) - F_{z\overline{z}}.$

Notice that

$\left[i\omega_0\Im_0 I - \int_{-1}^{0} e^{i\omega_0\Im_0\theta}d\eta(\theta)\right]q(0) = 0$ and $\left[-i\omega_0\Im_0 I - \int_{-1}^{0} e^{-i\omega_0\Im_0\theta}d\eta(\theta)\right]\overline{q}(0) = 0$.

implies

$\left[2i\omega_0\Im_0 I - \int_{-1}^{0} e^{2i\omega_0\Im_0\theta}d\eta(\theta)\right]E_1 = F_{z^2}$ and $-\left[\int_{-1}^{0} d\eta(\theta)\right]E_2 = F_{z\overline{z}}.$

Hence,

$$\begin{bmatrix} \left(2i\omega_0 + \alpha_2 + \alpha_3 T^* + \alpha_1 B^* e^{-2i\omega_0 \Im_0}\right) & 0 & -\alpha_3 N^* \\ -\beta_1 W^* e^{-2i\omega_0 \Im_0} & \left(2i\omega_0 + \frac{r}{K} + \beta_2\right) & 0 \\ \gamma_1 T^* & 0 & (2i\omega_0 + \gamma_1 N^* + \gamma_2) \end{bmatrix} E_1 =$$

$$-2\begin{bmatrix} \alpha_1 \sigma_1 e^{-i\omega_0 \Im_0 \theta} \\ \beta_1 \sigma_1 e^{-i\omega_0 \Im_0 \theta} \\ -\gamma_1 \rho_1 \end{bmatrix} \text{ and}$$

$$\begin{bmatrix} (\alpha_2 + \alpha_3 T^* + \alpha_1 B^*) & 0 & -\alpha_3 N^* \\ -\beta_1 W^* & (\frac{r}{K} + \beta_2) & 0 \\ \gamma_1 T^* & 0 & (\gamma_1 N^* + \gamma_2) \end{bmatrix} E_2 = -2\begin{bmatrix} \alpha_1 Re\{\sigma_1\} e^{i\omega_0 \Im_0 \theta} \\ -\beta_1 Re\{\sigma_1\} e^{i\omega_0 \Im_0 \theta} \\ -\gamma_1 Re\{\rho_1\} \end{bmatrix}$$

As a result, the parameters can express g_{21}.

Using the parameters, each g_{ij} can be determined based on the study mentioned above. Consequently, the following values can be calculated:

$$C_1(0) = \frac{i}{2\omega_0 \Im_0}\left(g_{11}g_{20} - 2|g_{11}|^2 - \frac{|g_{02}|^2}{3}\right) + \frac{g_{21}}{2} \quad , \quad \mu_2 = -\frac{Re\{C_1(0)\}}{Re\{\lambda'(\Im_0)\}}, \quad \beta_2 = \quad (4.27)$$

$2Re\{C_1(0)\}$,

$T_2 = -\frac{Im\{C_1(0)\} + \mu_2 Im\{\lambda'(\Im_0)\}}{\omega_0 \Im_0}$.

Theorem 2: The value of μ_2 can be determines by the direction of the Hb: if $\mu_2 > 0 (\mu_2 < 0)$, then the Hopf bifurcation is supercritical (subcritical) and the bifurcating periodic solutions exists for $\Im > \Im_0$ $(\Im < \Im_0)$. The value of β_2 can determines the stability of bifurcating solutions: the bifurcating periodic solutions are orbitally asymptotically stable (unstable) if $\beta_2 < 0$ $(\beta_2 > 0)$. The bifurcating periodic solutions is determined by the value of T_2: the period increases (decreases) if $T_2 > 0$ $(T_2 < 0)$.

4.3 Numerical Stimulation

MATLAB simulation is used to numerically consolidate the analytical findings. The system behaves as follows:

$N_o = 3.17, \alpha_1 = 0.22, \alpha_2 = 0.001, \alpha_3 = 0.0009, r = 1.89, \beta_1 = 0.2, \beta_2 = 0.001, T_o = 2.06, \gamma_1 = 0.06, \gamma_2 = 0.001$.

The Figure 4.1. shows that when there is no delay $\Im$, the system is absolutely stable. Plant nutrients concentration N, plant biomass B, and toxicity T shows no fluctuation in their natural growth. Figure 4.2 and Figure 4.3. shows when the delay $\Im$ increased

from 0 to 1.24 the system shows limit cycles or perturbation early on but finally stabilize called asymptotically behaviour. Figure 4.4 and Figure 4.5. shows one the delay parameter τ crosses the critical value 1.25 the limit cycle of same period and same direction continue together, HB occurs.

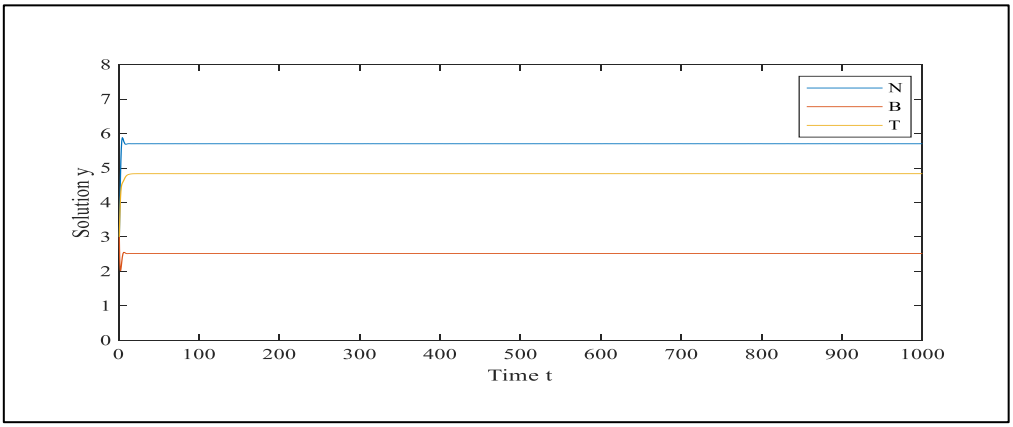

Figure 4.1 When there is absence of delay, $\mathfrak{I} = 0$, the system interior equilibrium point $\boldsymbol{E_1}$ is stable.

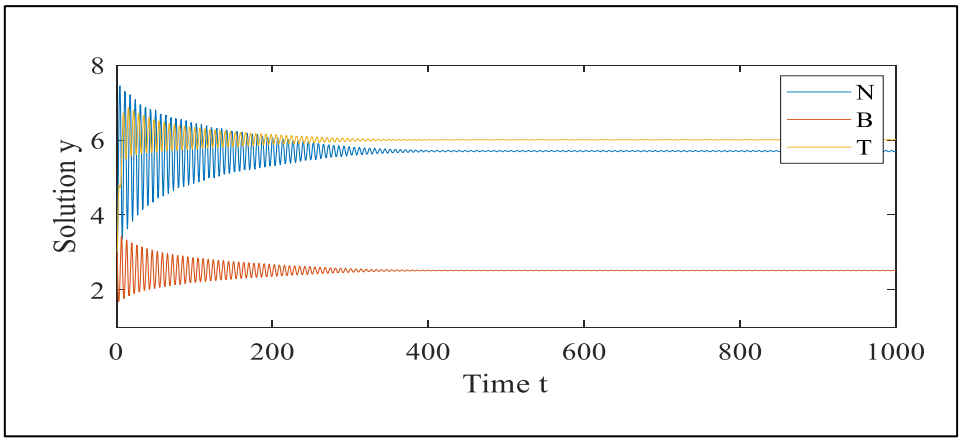

Figure 4.2 When there is delay that is $\mathfrak{I} < 1.25$, the system interior equilibrium point $\boldsymbol{E_1}$ is asymptotically stable.

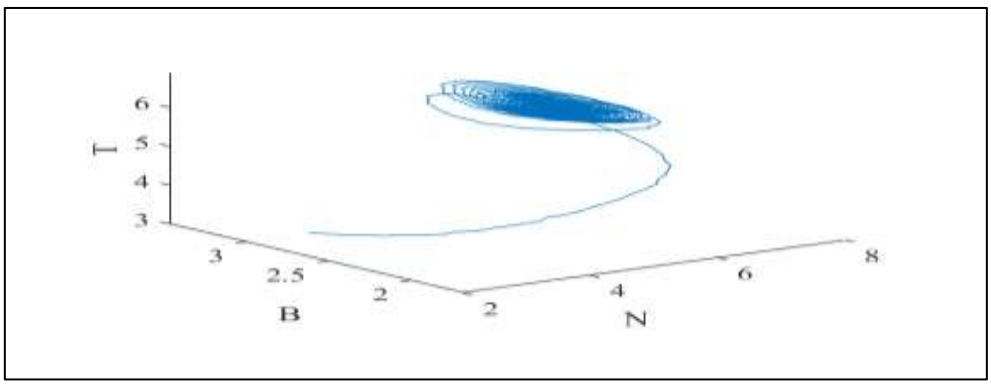

Figure 4.3 The phase space representation of toxicity T, plant biomass B, and nutrients N with a delay of $\mathfrak{I} < \mathbf{1.25}$.

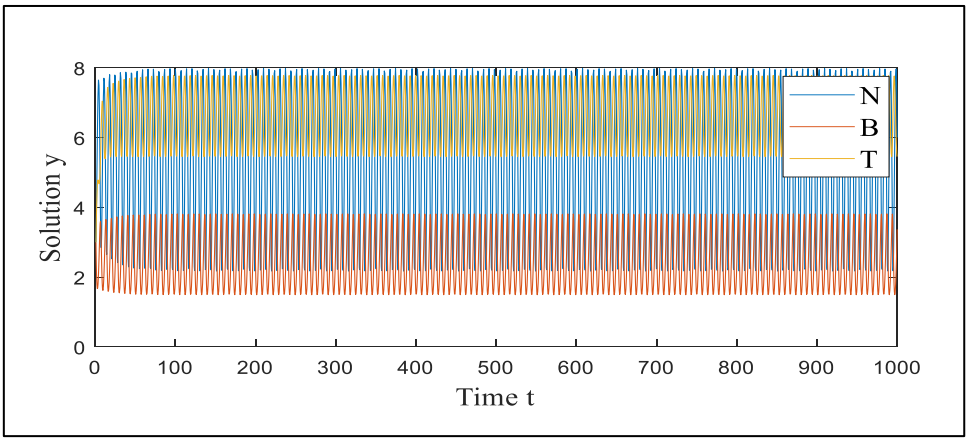

Figure 4.4 When there is delay that is $\mathfrak{I}$ >1.25, the system's IE point $\boldsymbol{E_1}$ losses its stability and shown HB.

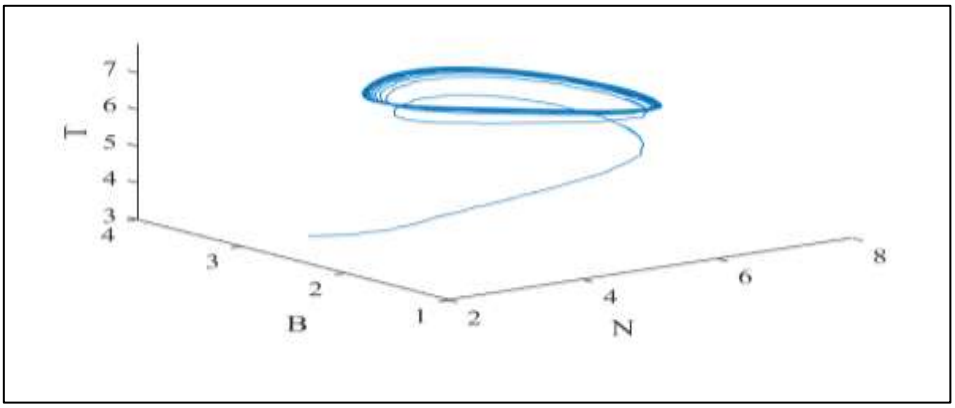

Figure 4. 5 The phase space representation of toxicity T, plant biomass B, and nutrients N with a delay of $\mathfrak{I} > \mathbf{1.25}$. Asymptotically and orbitally stable is the bifurcating periodic solution.

4.3.1 Sensitivity Analysis

The model has constant parameters in this study. To calculate the global sensitivity coefficient, the "Direct Method" is utilised. For each parameter the partial derivatives of the solution can be found, may be all that is required for sensitivity analysis in this situation if all of the parameters $(\alpha_1, \alpha_2, \alpha_3, \beta_1, \beta_2, \gamma_1, \gamma_2)$ present in the system (1) – (3) are assumed to be constants. taking derivative partially of the solution $(N, B\ and\ T)$ in relation to the β_1, produce the set of sensitivity equations shown below:

$$\frac{dS_1}{dt} = -\alpha_1 N(t-\tau)S_2 - \alpha_1 BS_1(t-\tau) - \alpha_2 S_1 + \alpha_3 NS_3 - \alpha_3 TS_1; \quad (4.28)$$

$$\frac{dS_2}{dt} = -\frac{r}{k}S_2 + \beta_1 N(t-\tau)S_2 - \beta_1 BS_1(t-\tau) - \beta_2 S_2; \quad (4.29)$$

$$\frac{dS_3}{dt} = -\gamma_1 NS_3 - \gamma_1 TS_1 - \gamma_2 S_3; \quad (4.30)$$

Where $S_1 = \frac{\partial N}{\partial \beta_1}, S_2 = \frac{\partial W}{\partial \beta_1}, S_3 = \frac{\partial M}{\partial \beta_1}$.

The nutrient concentration becomes unstable when $\beta_1 = 0.2$ and Hopf -bifurcation occurs. But when the utilisation coefficient declines from $\beta_1 = 0.2$ to $\beta_1 = 0.18$, the graph becomes asymptotically stable, and it exhibits stability at $\beta_1 = 0.12$ as shown in figure 4.6. Similarly, as β_1 drops from $\beta_1 = 0.2$ to $\beta_1 = 0.12$, as shown in figure 8 and figure 4.9, the amount of plant biomass produced and the toxicity decreases respectively.

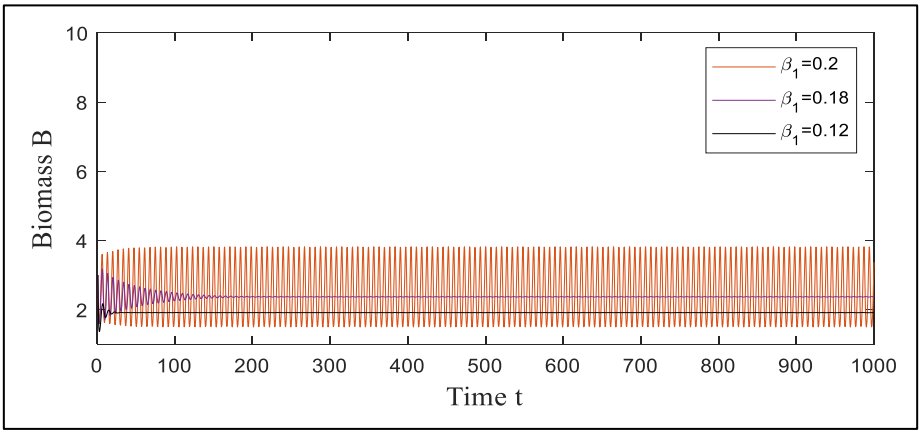

Figure 4.6 For various values of the utilisation coefficient $\boldsymbol{\beta_1}$, a time series graph shows the relationship between small variations in nutrients concentration $\boldsymbol{N}$.

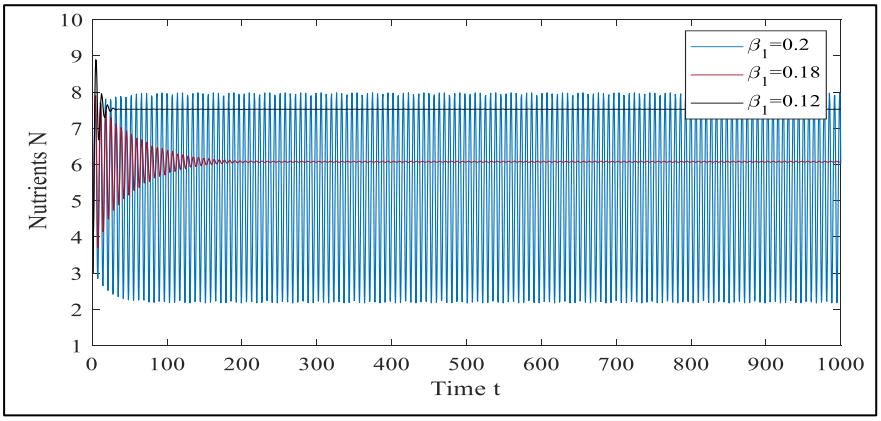

Figure 4.7 For various values of the utilisation coefficient β_1, time series graph shows the relationship between small variations in biomass B.

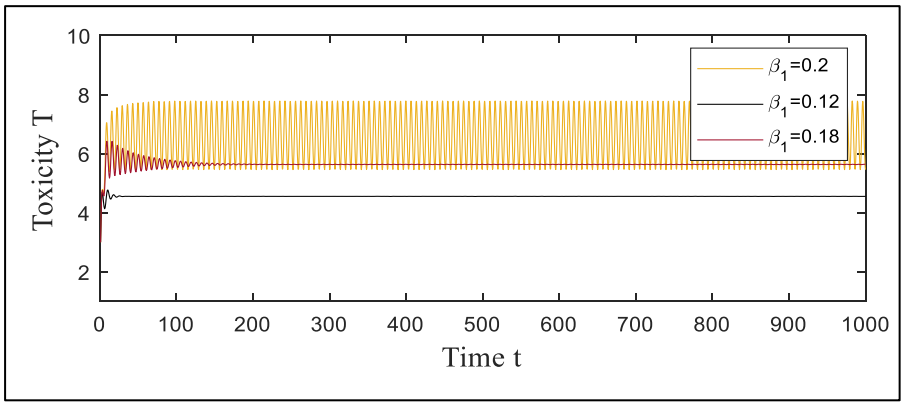

Figure 4.8 For various values of the utilisation coefficient $\boldsymbol{\beta_1}$, a time series graph shows the relationship between small variations in toxic metal $\boldsymbol{T}$.

4.4 Conclusion

In this paper, we investigated the impact of delay on the dynamics of plant growth when toxic metals are present. Stable equilibrium, HB, periodic oscillations, sensitivity analysis, directional analysis and other dynamical phenomena are all seen. Based on some numerical simulations, we draw the conclusion that for some parameter values, the stability and HB about interior equilibrium E^* can occur. It has been verified that interior equilibrium E^* is stable in the absence of a delay, as seen in (figure 4.1). The DP is found to have a critical value below ($\tau \leq 1.25$), which the system is asymptotically stable as seen in (figure 4.2 and figure 4.3). The proposed model become unstable and show oscillations when $\tau \geq 1.25$ as in (figure 4.4 and figure 4.5). It results that after taking time lag into account, limit cycles are observed for interior equilibrium points when time delay exceeds a certain critical value. For state variables at the interior equilibrium with respect to the system parameters, sensitivity indices are calculated in the mathematical model (4.1) – (4.3). The "direct method" is used to evaluate sensitivity of state variables by changing the parameter β_1 included in delay differential systems (4.28) – (4.30). Analysis of sensitivity demonstrate that the state variable $N, B \; and \; T$ significantly change their rate of

oscillations for various values of the parameter β_1 . Figures (4.6) to (4.8) depicts this phenomenon of sensitivity graphically.

Chapter 5

Analyzing the competitive dynamics of two plant populations under the influence of toxic decay.

5.1 Introduction

In plant ecology, there are many factors that effect on a plant growth. The physical environment, availability of biomass and presence of toxicity changes with time, the densities of plant growth also varied. The study of plant physiology includes fluctuations in density of plant growth under mutual competition. It has been noted that an excessive rise in first plant population growth may have a negative impact on the growth of another plant [196]. It is explained that the growth rate of plant biomass is a dynamic process that depends on variables such as the nutrients mortality rate, the size of the plant, and the growth rate of toxicity [180]. The environment pollution toxicity-related substances are constant present in species, this has an impact on population plant growth [83]. Thornley was the first to experiment with mathematical modelling in plant physiology by taking into account various climatic change factors, such as humidity, temperature, rainfall, transpiration, respiration, rate of photosynthesis, guard cells of stomata, etc. However, these models were only taken into account for specific plant species under specific conditions [6],[186]. There are various factors, including geological, social, economic, and biological, that contributes to increase in toxic heavy metals in the soil, this has an effect on the dynamic growth of nonlinear population [4]. The balance of the soil nutrients is upset by metals or toxicity which has an impact on plant and tree biomass. Accumulation of heavy metals make soil poisonous which gives adversely effect on growth of plants [197]. All plants are generally introduced to modified the parameters for the uptake of metals from the soil [198]. As a result, in the dynamics, the delay term is included. Using a system of non-linear DDEs, the effect of the delay parameter on the dynamics of plant growth that are affected by toxicants has been studied [169],[167],[199]. Delay was used to study the global stability in the collection of non-linear DEs [115],[166]. Rouches' Theorem provides an explanation for the distribution of exponential polynomial roots (1960) and further used by Ruan and Wei [200]. Using

the manifold and normal form proposed by Hassard et al., it is possible to determine the direction of the HB as well as numerous numerical simulations [191],[192]. In numerical modelling, the sensitivity analysis for nonlinear DEs systems with time lags utilising direct methods when the comprising model parameters were changed with respect to time, not only remain constant [197], [198]. Traditional and generalised sensitivity functions discussed for a set of non-linear DDEs in general [201],[20]. In relation to the delays, theoretical conclusions for sensitivity are presented. The periodic responses to DDEs are studied using a parametric sensitivity analysis[150] .

5.2 Mathematical model

Let P_1 and P_2 represent the two competing plants, where P_1 is considered as the first plant biomass and P_2 as the second plant biomass. The concentration of toxicity T has an adverse impact on the growth of plant populations. Both the plant population P_1 and P_2 assume to follow logistic growth. The toxicity does not affect the plant biomass immediately but takes incubation time denoted by delay parameter $\Im$ .The formulation of the model is as follows:

$$\frac{dP_1}{dt} = r_1 P_1 \left(1 - \frac{P_1(t-\Im)}{K}\right) - \alpha_1 P_1 P_2 - \beta_1 P_1 T - \gamma_1 P_1; \tag{5.1}$$

$$\frac{dP_2}{dt} = r_2 P_2 \left(1 - \frac{P_2(t-\Im)}{K}\right) - \alpha_2 P_1 P_2 - \beta_2 P_2 T - \gamma_2 P_2; \tag{5.2}$$

$$\frac{dT}{dt} = T_0 - \delta_1 P_1 T - \delta_2 P_2 T - \varepsilon T; \tag{5.3}$$

Initially: $P_1(0) > 0$, $P_2(0) > 0$, $(0) > 0$ for all t and $N\ (t - \Im)$ = constant for $t \in [-\tau, 0]$.

Table 5.1 Abbreviations used to specify the terms used in the Chapter

Parameters	Description
P_1	Plant biomass of first plant
P_2	Plant biomass of second plant
T	Toxic metal
r_1	Natural growth rate of plant P_1
r_2	Natural growth rate of plant P_2
K	Carrying capacity
α_1	Rate of decay of P_1due to mutual competition of

	P_2
α_2	Rate of decay of P_2due to mutual competition of P_1
β_1	Rate of decay of P_1due to toxicity
β_2	Rate of decay of P_2 due to toxicity
γ_1	Rate of natural decay of P_1
γ_2	Rate of natural decay of P_2
T_0	Constant rate inflow of toxicity
δ_1	Decay of toxicity due to absorption by P_1
δ_2	Decay of toxicity due to absorption by P_2
ε	Natural decay of toxicity

5.2.1 Positivity of Solutions

Positivity of system defines that model's solution, with initial data, will eventually be positive $\forall\, t$ exceeding some finite value. One must demonstrate that every solution provided by the equations is positive solution. (1) - (3), where initial condition is $P_1(0) > 0, P_2(0) > 0, T(0) > 0 \;\forall\; t \; and \; P_1(t - \Im) = constant \; for \; t \in [-\Im, 0]$, the model solution (P_1, P_2, T) remain positive $\forall$ time $t > 0$.

$$\frac{dP_1}{dt} = r_1P_1 - \alpha_1P_1P_2 - \beta_1P_1\,T - \gamma_1P_1;$$

$$\frac{dP_1}{dt} \geq (-\alpha_1P_2 - \beta_1T - \gamma_1)P_1;$$

$$\int \frac{dp_1}{dt} \geq (-\alpha_1P_2 - \beta_1T - \gamma_1)P_1;$$

$$P_1 \geq e^{-\alpha_1P_2} + e^{-\beta_1 T\Im} + e^{-\gamma_1 t}.$$

$as \; t \to \infty \; \therefore \; e^{-\infty} \to 0$

$Hence \; P_1 \geq 0, Similarly \; P_2 \geq 0 \; and \; T \geq 0.$

5.2.2 Interior Equilibrium Point

A mathematical model under consideration has an equilibrium point that defines a constant solution. We identify the internal equilibrium E^* of the model. For the set of

equations (5.1)-(5.3), there is only one possible equilibrium at $E^*(P_1^*, P_2^*, T^*)$,$P_1(t-\Im) \cong P_1$ and $P_2(t-\Im) \cong P_2$

$$P_{1=}^* \frac{-k}{r_1}(\alpha_1 P_2 + \beta_1 + \gamma_1 - r_1) \rightarrow P_1^* = f(P_2);$$

$also,$

$$P_2^* = \frac{-k}{r_2}(\alpha_2 P_1 + \beta_2 + \gamma_2 - r_2).$$

$Put\ P_1^*\ in\ P_2^*, \quad than, P_2^* = \frac{u}{v}\ , where\ v = \left(1 - \frac{\alpha_1 \alpha_2 k^2}{r_1 r_2}\right) and\ u = \frac{\alpha_2 k^2}{r_1 r_2}\ \beta_1 + \frac{\alpha_2 k^2}{r_1}\ \gamma_1 - \frac{\alpha_2 k^2}{r_2} - \frac{k\beta^2}{r_2} - \frac{k\,\gamma_2}{r_2} + k\ .\ Similarly\ for\ P_1^*, T^*.$

5.2.3 Analysis of Hopf- bifurcation

This section analyses, the dynamical internal equilibrium point behaviour $E^*(P_1^*, P_2^*, T^*)$ of model (5.1) -(5.3). In relation to equilibrium E^*, the exponential characteristic equation is provided by:

$$\lambda^3 + a_1\lambda^2 + a_2\lambda + a_3 + (b_1\lambda^2 + b_2\lambda + b_3)e^{-\lambda\tau} = 0.$$

$a_1 = -\delta_1 P_1 + \delta_2 P_2 + \varepsilon - r_2 + \alpha_2 P_1 + \beta_2 T + \delta_2 - r_1\ ,$

$b_1 = \frac{r_2}{k}\ P_2 + \frac{r_1}{k}\ P_1,$

$a_2 = -r_2\delta_1 P_1 - r_2\delta_2 P_2 - r_2\,\varepsilon + \alpha_2\delta_1 P_1^2 + \alpha_2\delta_2 P_1 P_2 + \alpha_2\varepsilon P_1 + \beta_2\delta_1 P_1 T + \beta_2\delta_2 P_2$
$+\beta_2\varepsilon T + \delta_1 r_2 P_1 + \gamma_2\delta_2 P_2 + \gamma_2\varepsilon - r_1\delta_1 P_1 - \delta_2 r_1 P_2 - \varepsilon r_1 + r_1 r_2 - r_1\alpha_2 P_1 -$
$r_1\beta_2 T - r_1\,\gamma_2 - \beta_2\delta_2 T P_2,$

$b_2 = \frac{r_2}{k}\delta_1 P_1 P_2 + \frac{r_2}{k}\ P_2\varepsilon + \delta_1 P_1^2\frac{r_1}{k} + \delta_2\frac{r_1}{k}P_1 P_2 + \frac{r_2}{k}P_2\varepsilon + \frac{r_1}{k}P_1\varepsilon - \frac{r_2}{k}r_1 P_2 - \frac{r_1}{k}r_2 P_1$
$+\frac{r_1}{k}\alpha_2 P_1^2 - \frac{r_1}{k}\beta_2 P_1 T + \frac{r_1}{k}\ \gamma_2 P_1,$

$a_3 = r_1\beta_2\delta_2 T P_2 - \alpha_1\alpha_2\delta_1 P_1^2 P_2 - \alpha_1\alpha_2\delta_2 P_1 P_2^2 - \alpha_1\alpha_2 P_1 P_2\varepsilon - \alpha_2\beta_1\delta_2 P_1\,P_2 T$
$-\delta_1\alpha_1\beta_2 T P_1 P_2 + r_2\delta_1\beta_1 T P_1 - \delta_1\beta_1 T P_1^2\alpha_2 - \delta_1\beta_1\beta_2 T^2 P_1 - \delta_1\beta_1\,\gamma_2 T P_1 + r_1 r_2\delta_1 P_1$
$+r_1 r_2\delta_2 P_2 + r_1 r_2\varepsilon - \alpha_2 r_1 P_1^2\delta_1 - \alpha_1 r_1 p_1\delta_2 P_2 - \alpha_2 r_1 P_1\varepsilon - \beta_2 r_1 T\delta_1 P_1 - \beta_2 r_1 T\delta_2 P_2$
$-\beta_2 r_1 T\varepsilon - \gamma_2 r_1\delta_1 P_1 - \gamma_2 r_1\delta_2 P_2 - \gamma_2 r_1\varepsilon,$

$b_3 = -\delta_1\frac{r}{k}r_2 P_2 P_1 - r_1\frac{r_2}{k}P_2^2 - \varepsilon r_1\frac{r_2}{k}P_2 - r_1\frac{r_2}{k}P_1^2\delta_1 - \frac{r_1}{k}r_2 P_1 P_2\delta_2 - \frac{r_1}{k}r_2 P_1$
$+\frac{r_1}{k}\delta_1\alpha_2 P_1^3$

$+\delta_2 \frac{r_1}{k}\alpha_2 P_1^2 P_2 + \frac{r_1}{k}\alpha_2 P_1^2 \varepsilon + \frac{r_1}{k} P_1^2 \beta_2 T\delta_1 - \frac{r_1}{k} P_1 P_2 \beta_2 T\delta_2 + \frac{r_1}{k} P_1 \beta_2 T\varepsilon + \frac{r_1}{k} P_1^2\, \gamma_2 \delta_1$

$+ \frac{r_1}{k} P_1 P_2\, \gamma_2 \delta_2 + \frac{r_1}{k} P_1\, \gamma_2 \varepsilon - \frac{r_2}{k}\delta_1 \beta_1 T P_1 P_2 - r_1 \frac{r_2}{k} P_2 P_1 \delta_1.$

Clearly $a_1, a_2, a_3, b_1, b_2, b_3$ all are positive.

Equation (5.4) can only be solved if and only if $\lambda = i\omega$ is true.

$(i\omega)^3 + a_1(i\omega)^2 + a_2(i\omega) + a_3 + (b_1(i\omega)^2 + b_2(i\omega) + b_3)e^{-i\omega\Im} = 0$.

(5.5)

Separating real and imaginary parts:

$a_3 - a_1\omega^2 + (b_3 - b_1\omega^2)cos\ \omega\Im + b_2\omega \sin \omega\Im = 0$.

(5.6)

$a_2\omega - \omega^3 + b_2\omega\ cos\ \omega\Im - (b_3 - b_1\omega^2) \sin \omega\Im = 0$.

(5.7)

Which gives: $\omega^6 + \left({a_1}^2 - {b_1}^2 - 2a_2\right)\omega^4 + \left({a_2}^2 - {b_2}^2 + 2b_1b_3 - 2a_1a_3\right)\omega^2 + \left({a_3}^2 - {b_3}^2\right) = 0$.

(5.8)

$q = \left({a_1}^2 - {b_1}^2 - 2a_2\right), r = \left({a_2}^2 - {b_2}^2 + 2b_1b_3 - 2a_1a_3\right), s = \left({a_3}^2 - {b_3}^2\right).$

Let $\omega^2 = x$, then equation (5.8) is: $x^3 + qx^2 + rx + s = 0.$

(5.9)

Claim 1: If $s < 0$, eq. (5.9) has one real +ve zero.

Proof: Consider $h(x) = x^3 + qx^2 + rx + s$.

Here $h\ (0) = s < 0$, $\lim_{x\to\infty} h(x) = \infty$ So, $\exists\ z_0 \in (0, \infty)$ such that $h(x_0) = 0$.

Claim 2: If $s \geq 0$, $D = q^2 - 3r \geq 0$ is a necessary condition for the existence of positive real roots in equation (5.9).

Proof: Since, $h(x) = x^3 + qx^2 + rx + s$ therefore $h'(x) = 3x^2 + 2qx + r$

$h'(x) = 0$ implies $3x^2 + 2qx + r = 0.$ (5.10)

The roots of equation (5.10) can be written as $x_{1,2} = \frac{-2q \mp \sqrt{4q^2 - 12r}}{6} = \frac{-q \mp \sqrt{D}}{3}$ (5.11)

There are no real roots in equation (5.10) if $D < 0$. As a result, the function $h(x)$ is an increasing monotone function in x. Since $h(0) = s \geq 0$, therefore positive real roots cannot exist in equation (5.9). It has been proven.

Clearly if $D \geq 0$, then $x_1 = \frac{-q+\sqrt{D}}{3}$ is local minima of $h(x)$. Hence, the following assertion.

Claim 3: If $s \geq 0$, and only if $x_1 > 0$ and $h(x_1) \leq 0$, equation (5.9) has positive real.

Proof. It is clear that there is enough. There is only one requirement: necessity. If not, assume that $h(x) > 0$ and either $x_1 \leq 0$ or $x_1 > 0$. Consequently $h(x)$ has no positive real zeros if $x_1 \leq 0$ since $h(x)$ is rising for $x \geq x_1$ and $h(0) = c \geq 0$. Since $x_2 = \frac{-q-\sqrt{D}}{3}$ is the local maximum value if $x_1 > 0$ and $h(x_1) > 0$, it follows that $h(x_1) \leq h(x_2)$. Because $h(x)$ lacks positive real roots, $h(0) = c \geq 0$. Proof is now complete.

5.2.3.1 ***Lemma 1*****:** Assume that equation (5.11) defines $\boldsymbol{x_1}$.

I. If $s < 0$,at least a positive real zero exists in eq. (5.9).

II. If $s \geq 0$ and $D = q^2 - 3r < 0$, no positive zeros can be found for eq. (5.9).

III. If $s \geq 0$, there are positive zeros in eq. (5.9) iff $x_1 > 0$ and $h(x_1) \leq 0$.

Proof: Assume that equation (5.9) has roots that are positive. Suppose it has three positive roots without losing generality, signified by x_1, x_2 , x_3. As a result equation (5.8) has three positive roots, say $\omega_1 = \sqrt{x_1}$, $\omega_2 = \sqrt{x_2}$, $\omega_3 = \sqrt{x_3}$.

From (5.7) $\sin \omega\Im = \frac{a_2\omega-\omega^3}{d}$Which gives $\Im = \frac{1}{\omega}\left[sin^{-1}\left(\frac{a_2\omega-\omega^3}{d}\right) + 2(j-1)\pi\right]$; $j = 1,2,3,-$

Let $\Im_k{}^{(j)} = \frac{1}{\omega_k}\left[sin^{-1}\left(\frac{a_2\omega_k-{\omega_k}^3}{d}\right) + 2(j-1)\pi\right]$; $k = 1,2,3.$; $j = 0,1,2,---$

Then $\mp i\omega_k$ is a pair of equation (5.8), roots that are entirely imaginary.

Where $\Im = \Im_k{}^{(j)}, k = 1,2,3,4.$; $j = 0,1,2,3,--$, $\lim_{j\to\infty} \Im_k{}^{(j)} = \infty, k = 1,2,3,4.$

Thus, define

$$\Im_0 = \Im_{k_0}{}^{(j_0)} = \min_{1\leq k\leq 3, j\geq 1}\left[\Im_k{}^{(j)}\right],\ \omega_0 = \omega_{k_0},\ x_0 = {x_{k_0}}^j. \tag{5.12}$$

5.2.3.2 Lemma 2: Suppose that $\boldsymbol{a_1 > 0, (a_3 + d) > 0,\ a_1 a_2 - (a_3 + d) > 0}$.

I. The real part of very root of equation (5.4) is negative $\forall\ \tau \geq 0$ if $s \geq 0$ and $D = q^2 - 3r < 0$.

II. The real part of every root of equation (5.4) is negative $\forall\ \tau \in [0, \tau_0)$ if $s < 0$ o $s \geq 0, x_1 > 0$ and $h(x_1) \leq 0$.

Proof: When $\tau = 0$, equation (5.4) changes to

$$\lambda^3 + (a_1 + b_1)\lambda^2 + (a_2 + b_2)\lambda + (a_3 + b_3) = 0. \tag{5.13}$$

Using Routh-Hurwitz's criteria, **(H1):** $if\ (a_3 + b_3) > 0, (a_1 + b_1)(a_2 + b_2) - (a_3 + b_3) > 0$, then all the roots in equation (5.4) have negative real part.

If $s \geq 0$ and $D = q^2 - 3r < 0$, equation (5.4) does not have any roots with a real part of zero $\forall\ \tau \geq 0$ according to Lemma 2 (II). When $s < 0$ or $s \geq 0$, $x > 0$ and $h(x_1) \leq 0$, Lemma 2 (I) and (III) implies that when $\Im \neq \Im_k{}^{(j)}, k = 1, 2, 3.; j \geq 1$, Since $\Im_0$ is the smallest value of $\Im$ and equation (5.4) just has imaginary roots, it does not have any real roots with any real parts. The result of the lemma is obtained by using Theorem 1.

Let $\lambda(\Im) = \psi(\Im) + i\omega(\Im)$. (5.14)

be the roots of equation (5.4) satisfying: $\psi(\Im_0) = 0,\ \omega(\Im_0) = \omega_0$

Assume that $h'(x_0) \neq 0$, to ensure that $\mp\omega_0$ simple and purely imaginary roots of equation (5.4), with $\Im = \Im_0$ and $\lambda(\Im)$ meets satisfies transversality requirement.

5.2.3.3 Lemma 3: Suppose $\boldsymbol{x_0 = \omega_0{}^2}$. If $\boldsymbol{\Im = \Im_0}$, Then sign $[\boldsymbol{\psi'(\Im_0)}]$ =Sign $[\boldsymbol{h'(x_0)}]$

Proof. Differentiating w.r.t $\Im$ and inserting $\lambda(\Im)$ into equation (5.54) results in the following.

$$\frac{d\lambda}{d\Im}\left[3\lambda^2 + 2a_1\lambda + b_2 + \left((b_1\lambda^2 + b_2\lambda + b_3)(-\Im) + (2b_1\lambda + b_2)\right)e^{-\lambda\tau}\right] =$$

$$\lambda(b_1\lambda^2 + b_2\lambda + b_3)e^{-\lambda\Im}\ .$$

Then $\left(\frac{d\lambda}{d\Im}\right)^{-1} = \frac{(3\lambda^2 + 2a_1\lambda + a_2)e^{\lambda\Im}}{\lambda(b_1\lambda^2 + b_2\lambda + b_3)} + \frac{(2b_1\lambda + b_2)}{\lambda(b_1\lambda^2 + b_2\lambda + b_3)} - \frac{\Im}{\lambda}$.

From equations (6) -(8):

$$\mu'(\Im_0) = Re\left[\frac{(3\lambda^2+2a_1\lambda+a_2)e^{\lambda\Im}}{\lambda(b_1\lambda^2+b_2\lambda+b_3)}\right] + Re\left[\frac{(2b_1\lambda+b_2)}{\lambda(b_1\lambda^2+b_2\lambda+b_3)}\right] = \frac{1}{\Delta}[3{\omega_0}^6 + 2q{\omega_0}^4 + r{\omega_0}^2].$$

Where $\Delta = [(b_3 - b_1\omega^2)^2 + (b_2\omega)^2]$. In this case $\Delta > 0$ and $\omega_0 > 0$.

Consequently, it is proved that Sign $[\psi'(\Im_0)]$ =Sign $[h'(x_0)]$.

5.3 Direction analysis and stability analysis of the hopf bifurcation solution

Let Assume, $y_1 = P_1 - {P_1}^*, y_2 = P_2 - {P_2}^*, y_3 = T - T^*$ and time scaling, as well as normalising the delay $\Im$, $t \to \frac{t}{\Im}$, equation (5.1) – (5.3) are:

$$\frac{dy_1}{dt} = -\gamma_1 y_1 - r_1 y_1 - \alpha_1 {P_2}^* y_1 - \alpha_1 {P_1}^* y_2 - \beta_1 {P_1}^* y_3 - \beta_1 T^* y_1 - \frac{r_1}{k}{P_1}^* y_1(t-1) - \frac{r_1}{k}{P_1}^*(t-1)y_1 - \frac{r_1}{k}y_1(t-1)y_1 - \alpha_1 y_1 y_2 - \beta_1 y_1 y_2; \quad (5.15)$$

$$\begin{aligned}\frac{dy_2}{dt} = {} & -\gamma_2 y_2 - r_2 y_2 - \alpha_2 {P_2}^* y_1 - \alpha_2 {P_1}^* y_2 - \beta_2 {P_2}^* y_3 - \beta_2 T^* y_2 \\ & - \frac{r_2}{k}{P_2}^* y_2(t-1) - \frac{r_2}{k}{P_2}^*(t-1)y_2 \\ & - \frac{r_2}{k}y_2(t-1)y_2 - \alpha_2 y_1 y_2 \\ & - \beta_2 y_1 y_3;\end{aligned} \quad (5.16)$$

$$\frac{dy_3}{dt} = -\varepsilon y_3 - \delta_1 {P_1}^* y_3 - \delta_1 y_1 T^* - \delta_2 {P_2}^* y_3 - \delta_2 y_2 T^* - \delta_1 y_1 y_3 - \delta_2 y_2 y_3; \quad (5.17)$$

Thus, work can be done in the phase $C = C\left((-1,0), {R_+}^3\right)$. Without loss of generality, denote the critical value $\Im_j$ by $\Im_0$. Let $\Im = \Im_0 + \mu$, then $\mu = 0$ is a Hb value of the system given by equations (5.15) -(5.17). Rewrite this system as follows for notational simplicity:

$$y'(t) = L_\mu(y_t) + F(\mu, y_t). \quad (5.18)$$

Where $y(t) = (y_1(t), y_2(t), y_3(t))^T \in R^3, y_t(\theta) \in C$ is defined by $y_t(\theta) = y_t(t+\theta)$, and

$L_\mu: C \to R$, $F: R \times C \to R$ are provided, respectively by

$$L_\mu\delta = (\Im_0 + \mu)$$

$$\begin{bmatrix} -(\gamma_1 + \alpha_1 {P_2}^* + \beta_1 T^*) & -\alpha_1 {P_1}^* & -\beta_1 {P_1}^* \\ -\alpha_2 {P_2}^* & -(\gamma_2 + \alpha_2 {P_1}^* + \beta_2 T^*) & -\beta_2 {P_2}^* \\ -\delta_1 T^* & -\delta_2 T^* & -(\delta_1 {P_1}^* + \delta_2 {P_2}^*) \end{bmatrix} \begin{bmatrix} \delta_1(0) \\ \delta_2(0) \\ \delta_3(0) \end{bmatrix} +$$

$$(\tau_0 + \mu) \begin{bmatrix} -\frac{r_1}{k} {P_1}^* & 0 & 0 \\ -\frac{r_2}{k} {P_2}^* & 0 & 0 \\ 0 & & \end{bmatrix} \begin{bmatrix} \delta(-1) \\ \delta(-2) \\ \delta(-3) \end{bmatrix}.$$

And $F(\mu, \delta) = (\tau_0 + \mu) \begin{bmatrix} F_1 \\ F_2 \\ F_3 \end{bmatrix}$ respectively where $F_1 = -\alpha_1 \delta_1(-1)\delta_2(0)$,

$F_2 = \beta_1 \delta_1(-1)\delta_2(0), F_3 = -\gamma_1 \delta_1(0)\delta_3(0)$,

$\delta(\theta) = \big(\delta_1(\theta), \delta_2(\theta), \delta(\theta)\big)^T \in C\big((-1{,}0), R\big)$.

According to the Riesz theorem, a function $\eta(\theta, \mu)$ is constrained variation for $\theta \in [-1{,}0]$, such that $L_\mu\delta = \int_{-1}^{0} d\,\eta(\theta, 0)\delta(\theta)$ for $\delta \in C$.

Choose in reality

$$\eta(\theta, \mu)$$
$$= (\Im_0$$
$$+ \mu) \begin{bmatrix} -(\gamma_1 + \alpha_1 {P_2}^* + \beta_1 T^*) & -\alpha_1 {P_1}^* & -\beta_1 {P_1}^* \\ -\alpha_2 {P_2}^* & -(\gamma_2 + \alpha_2 {P_1}^* + \beta_2 T^*) & -\beta_2 {P_2}^* \\ -\delta_1 T^* & -\delta_2 T^* & -(\delta_1 {P_1}^* + \delta_2 {P_2}^*) \end{bmatrix} \delta(\theta)$$
$$+ \ (\Im_0 + \mu) \begin{bmatrix} -\frac{r_1}{k} {P_1}^* & 0 & 0 \\ -\frac{r_2}{k} {P_2}^* & 0 & 0 \\ 0 & & \end{bmatrix} \delta(\theta + 1)$$

Here $\in C\big([-1{,}0], {R_+}^3\big)$, define

$$A(\mu)\delta = \begin{cases} \frac{d\delta(\theta)}{d\theta}, & \theta \in [-1{,}0) \\ \int_{-1}^{0} d\,\eta(\theta, 0)\delta(\theta), & \theta = 0. \end{cases}$$ And

$$R(\mu)\delta = \begin{cases} 0, & \theta \in [-1{,}0) \\ F(\mu, \delta) & \theta = 0. \end{cases}$$

The system (5.18) then corresponds to:

$$y'(t) = A(\mu)\delta + R(\mu)y_t \,. \tag{5.19}$$

For $\psi \in C^1([-1,0], {R_+}^3)$, state

$$A^*\psi(h) = \begin{cases} -\frac{d\psi(h)}{ds}, & h \in [-1,0) \\ \int_{-1}^{0} d\,\eta^T(-t,0)\psi(-t), & h = 0. \end{cases}$$ And bilinear inner product

$$< \psi(h), \delta(\theta) > = \overline{\psi(0)}\delta(0) - \int_{-1}^{0}\int_{\xi=\theta}^{\theta} \overline{\psi}(\xi-\theta)d\eta(\theta)\delta(\xi)\,d\xi. \tag{5.20}$$

Sine A^* and $A = A(0)$ are adjoint operators and $i\omega_0$ are eigen values of $A(0)$. Thus they are eigen values of A^*. Assume that $q(\theta) = q(0)e^{i\omega_0\theta}$ is an eigen vector of $A(0)$ corresponding to the eigen value $i\omega_0$. Then $A(0) = i\omega_0\, q(\theta)$. When $\theta = 0$,

$\left[i\omega_0 I - \int_{-1}^{0} d\eta(\theta)e^{i\omega_0\theta}\right] q(0) = 0$, that outcome $q(0) = (1, \sigma_1, \rho_1)^T$

$\sigma_1 = \frac{(\alpha_1 B^* + (\alpha_2 + \alpha_3 T^*) - i\omega_0)}{\alpha_3 N^*}$ and $\rho_1 = \frac{\beta_1 B^*\left(\left(\frac{r}{k}+\beta_2\right) - i\omega_0\right)}{\left(\frac{r}{k}+\beta_2\right)^2 + {\omega_0}^2}$.

The same can be confirmed that $q^*(s) = D(1, \sigma_2, \rho_2)e^{i\omega_0\tau_0 s}$ is the eigen value of A^* that corresponds to $-i\omega_0$, where

$\sigma_1 = \frac{(\alpha_1 B^* + (\alpha_2 + \alpha_3 T^*) - i\omega_0)}{\alpha_3 N^*}$ and $\rho_1 = \frac{\beta_1 B^*\left(\left(\frac{r}{k}+\beta_2\right) - i\omega_0\right)}{\left(\frac{r}{k}+\beta_2\right)^2 + {\omega_0}^2}$.

To ensure $< q^*(s), q(\theta) > = 1$, it is necessary to calculate the value of D.

From equation (5.22), $< q^*(s), q(\theta) >$

$=$

$\overline{D}(1, \overline{\sigma_2}, \overline{\rho_2})(1, \sigma_1, \rho_1)^T -$

$\int_{-1}^{0}\int_{\xi=\theta}^{\theta} \overline{D}(1, \overline{\sigma_2}, \overline{\rho_2})e^{-i\omega_0\Im_0(\xi-\theta)}d\eta(\theta)(1, \sigma_1, \rho_1)^T e^{i\omega_0\Im_0}\,d\xi$;

$= \overline{D}\left\{1 + \sigma_1\overline{\sigma_2} + \rho_1\overline{\rho_2} - \int_{-1}^{0}(1, \overline{\sigma_2}, \overline{\rho_2})\,\theta e^{i\omega_0\Im_0\theta}(1, \sigma_1, \rho_1)^T\right\}$;

$= \overline{D}\{1 + \sigma_1\overline{\sigma_2} + \rho_1\overline{\rho_2} + \tau_0\overline{\sigma_2}W^*(\beta_1\rho_1 - \alpha_1\sigma_1)e^{i\omega_0\Im_0}\}$.

Hence, select $\overline{D} = \frac{1}{(1+\sigma_1\overline{\sigma_2}+\rho_1\overline{\rho_2}+\Im_0\overline{\sigma_2}B^*(\beta_1\rho_1-\alpha_1\sigma_1)e^{i\omega_0\Im_0})}$.

That way $< q^*(s), q(\theta) > = 1, < q^*(s), \overline{q(\theta)} > = 0$.

The coordinates characterising the centre manifold C_0 at μ=0 are computed by applying the algorithm described in [1] and using their notations. Assume y_t as solution of equation (5.18) at $\mu = 0$. Therefore,

$$z(t) =< q^*(s), y_t(\theta) >,\ W(t,\theta) = y_t(\theta) - 2Re(z(t)q(\theta)). \tag{5.21}$$

On the centre manifold C_0, $W(t,\theta) = W\left(z(t), \overline{z(t)}, \theta\right)$

Where $W(z,\overline{z},\theta) = W_{20}(\theta)\frac{z^2}{2} + W_{11}(\theta)z\overline{z} + W_{02}(\theta)\frac{\overline{z}^2}{2} + \cdots,$

Local coordinates for the centre of the manifold C_0 are z and $\overline{z}$ towards q^* and $\overline{q^*}$. Consider that W is real if y_t is real. The only real solutions should be taken into consideration. For the solution $y_t \in C_0$ of equation (20), since $\mu = 0$,

$$z'(t) = i\omega_0\Im_0 z + < \overline{q^*}(\theta), F\big(0, B(z,\overline{z},\theta) + 2Re\big(z(t)q(\theta)\big)\big) >$$

$$= i\omega_0\Im_0 z + \overline{q^*}(0)\ F\big(0, W(z,\overline{z},0) + 2Re\big(z(t)q(\theta)\big)\big);$$

$$\equiv i\omega_0\Im_0 z + \overline{q^*}(0)F_0(z,\overline{z}).$$

Rewrite this equation as

$$z'(t) = i\omega_0\Im_0 z(t) + g(z,\overline{z}). \tag{5.22}$$

Where $g(z,\overline{z}) = \overline{q^*}(0)F_0(z,\overline{z}) = g_{20}(\theta)\frac{z^2}{2} + g_{11}(\theta)z\overline{z} + g_{02}(\theta)\frac{\overline{z}^2}{2} +$ (5.23)

$g_{21}(\theta)\frac{z^2\overline{z}}{2} + \cdots$

As $y_t(\theta) = (y_{1t}, y_{2t}, y_{3t}\ ) =\ W(t,\theta) + z\ q(\theta) + \overline{z}\overline{q(\theta)}$ and $q(0) = (1, \sigma_1, \rho_1)^T e^{i\omega_0\Im_0\theta}$, so

$$y_{1t}(0) = z + \overline{z} + W_{20}{}^{(1)}(0)\frac{z^2}{2} + W_{11}{}^{(1)}(0)\ z\overline{z} + W_{02}{}^{(1)}(0)\frac{\overline{z}^2}{2} + \cdots,$$

$$y_{2t}(0) = \sigma_1 z + \overline{\sigma_1}\,\overline{z} + W_{20}{}^{(2)}(0)\frac{z^2}{2} + W_{11}{}^{(2)}(0)\ z\overline{z} + W_{02}{}^{(2)}(0)\frac{\overline{z}^2}{2} + \cdots,$$

$$y_{3t}(0) = \rho_{1_1} z + \overline{\rho_{1_1}}\,\overline{z} + W_{20}{}^{(3)}(0)\frac{z^2}{2} + W_{11}{}^{(3)}(0)\ z\overline{z} + W_{02}{}^{(3)}(0)\frac{\overline{z}^2}{2} + \cdots,$$

$y_{1t}(-1) =$

$$ze^{-i\omega_0\Im_0} + \overline{z}e^{i\omega_0\Im_0} + W_{20}{}^{(1)}(-1)\frac{z^2}{2} + W_{11}{}^{(1)}(-1)\ z\overline{z} + W_{02}{}^{(1)}(-1)\frac{\overline{z}^2}{2} + \cdots,$$

$$y_{2t}(-1) = \sigma_1 e^{-i\omega_0\Im_0} z + \overline{\sigma_1}\, e^{i\omega_0\Im_0}\, \overline{z} + W_{20}{}^{(2)}(-1)\frac{z^2}{2} + W_{11}{}^{(2)}(-1)\, z\overline{z} +$$

$$W_{02}{}^{(2)}(-1)\frac{\overline{z}^2}{2} + \cdots,$$

Thus, comparing coefficients to equation (5.23) provides:

$$g_{20} = \overline{D}(1, \sigma_1, \rho_1) f_{z^2},\ g_{02} = \overline{D}(1, \overline{\sigma_1}, \overline{\rho_2}) f_{\overline{z}^2},$$

$$g_{11} = \overline{D}(1, \overline{\sigma_1}, \overline{\rho_2}) f_{z\overline{z}}, g_{21} = \overline{D}(1, \overline{\sigma_1}, \overline{\rho_2}) f_{z^2\overline{z}}$$

For clarification g_{21}, Computation must be the main focus of $W_{20}(\theta)$ and $W_{11}(\theta)$. From equations (5.19) and (5.21):

$$W' = u_t{}' - z'q - \overline{z}'q = \begin{cases} AW - 2Re\left[\overline{q^*}(0)F_0 q(\theta)\right], & \theta \in [-1,0) \\ AW - 2Re\left[\overline{q^*}(0)F_0 q(0)\right] + F_0, & \theta = 0 \end{cases}$$

Let $W' = AW + H(z, \overline{z}, \theta)$ (5.24)

Where $H(z, \overline{z}, \theta) = H_{20}(\theta)\frac{z^2}{2} + H_{11}(\theta) z\overline{z} + H_{02}(\theta)\frac{\overline{z}^2}{2} + H_{21}(\theta)\frac{z^2\overline{z}}{2} + \cdots,$ (5.25)

As opposed to that, on C_0 at the origin $W' = W_z z' + W_{\overline{z}}\overline{z}'$.

The above series is expanded, the coefficients are calculated, and the result is

$$[A - 2i\omega_0 I] W_{20}(\theta) = -H_{20}(\theta),\ \ AW_{11}(\theta) = -H_{11}(\theta) \quad (5.26)$$

By equation (5.22), for $\theta \in [-1,0)$,

$$H(z, \overline{z}, \theta) = -\overline{q^*}(0)\overline{F_0} q(\theta) - \overline{q^*}(0)\overline{F_0}\, \overline{q}(\theta) = -gq(\theta) - \overline{g}\ \overline{q}(\theta)$$

Comparing the coefficients with (5.23) for $\theta \in [-1,0]$ that

$$H_{20}(\theta) = -g_{20} q(\theta) - \overline{g_{02}}\, \overline{q}(\theta),\ H_{11}(\theta) = -g_{11} q(\theta) - \overline{g_{11}}\, \overline{q}(\theta).$$

From equation (5.22), (5.25) and definition of A are obtained

$$W_{20}(\theta) = 2i\omega_0 \Im_0 W_{20}(\theta) + g_{20} q(\theta) + \overline{g_{02}}\, \overline{q}(\theta);$$

Solving for $W_{20}(\theta)$:

$$W_{20}(\theta) = \frac{ig_{20}}{\omega_0\Im_0} q(0) e^{i\omega_0\Im_0\theta} + \frac{i\overline{g_{02}}}{3\omega_0\Im_0}\overline{q}(0) e^{-i\omega_0\Im_0\theta} + E_1 e^{2i\omega_0\Im_0\theta},$$

And similarly

$$W_{11}(\theta) = \frac{-ig_{11}}{\omega_0\Im_0} q(0) e^{i\omega_0\Im_0\theta} + \frac{i\overline{g_{11}}}{\omega_0\Im_0}\overline{q}(0) e^{-i\omega_0\Im_0\theta} + E_2\ .$$

Where E_1 and E_2 are both three dimensional vectors, and can be determined by setting $\theta = 0$ in H.

In fact since $H(z,\overline{z},\theta) = -2Re\left[\overline{q^*}(0)F_0 q(0)\right] + F_0$, So

$H_{20}(\theta) = -g_{20}q(\theta) - \overline{g_{02}}\,\overline{q}(\theta) + F_{z^2}$;

$H_{11}(\theta) = -g_{11}q(\theta) - \overline{g_{11}}\,\overline{q}(\theta) + F_{z\overline{z}}$;

Where $F_0 = F_{z^2}\frac{z^2}{2} + F_{z\overline{z}}z\overline{z} + F_{\overline{z}^2}\frac{\overline{z}^2}{2} + \cdots$

Hence combining the definition of A,

$\int_{-1}^{0} d\,\eta(\theta)W_{20}(\theta) = 2i\omega_0\tau_0 W_{20}(0) + g_{20}q(0) + \overline{g_{02}}\,\overline{q}(0) - F_{z^2}$ and

$\int_{-1}^{0} d\,\eta(\theta)W_{11}(\theta) = g_{11}q(0) - \overline{g_{11}}\,\overline{q}(0) - F_{z\overline{z}}$;

Notice that

$\left[i\omega_0\Im_0 I - \int_{-1}^{0} e^{i\omega_0\Im_0\theta}d\eta(\theta)\right]q(0) = 0$ and $\left[-i\omega_0\Im_0 I - \int_{-1}^{0} e^{-i\omega_0\Im_0\theta}d\eta(\theta)\right]\overline{q}(0) = 0$;

implies

$\left[2i\omega_0\Im_0 I - \int_{-1}^{0} e^{2i\omega_0\Im_0\theta}d\eta(\theta)\right]E_1 = F_{z^2}$ and $-\left[\int_{-1}^{0} d\eta(\theta)\right]E_2 = F_{z\overline{z}}$;

Hence,

$$\begin{bmatrix} -\left(2i\omega_0 + \gamma_1 + \alpha_1 P_2^{\,*} + \beta_1 T^* + \frac{r_1}{k}P_1^{\,*}e^{-2i\omega_0\Im_0}\right) & -\alpha_1 P_1^{\,*} & -\beta_1 P_1^{\,*} \\ -(\alpha_2 P_2^{\,*} + \frac{r_2}{k}P_2^{\,*}e^{-2i\omega_0\Im_0}) & -(2i\omega_0 + \gamma_2 + \alpha_2 P_1^{\,*} + \beta_2 T^*) & -\beta_2 P_2^{\,*} \\ -\delta_1 T^* & -\delta_2 T^* & -(2i\omega_0 + \delta_1 P_1^{\,*} + \delta_2 P_2^{\,*}) \end{bmatrix} E_1 =$$

$$-2\begin{bmatrix} \alpha_1\sigma_1 e^{-i\omega_0\Im_0\theta} \\ \beta_1\sigma_2 e^{-i\omega_0\Im_0\theta} \\ -\gamma_1\rho_1 \end{bmatrix}$$; and

$$\begin{bmatrix} -(\gamma_1 + \alpha_1 P_2^{\,*} + \beta_1 T^*) & -\alpha_1 P_1^{\,*} & -\beta_1 P_1^{\,*} \\ -\alpha_2 P_2^{\,*} & -(\gamma_2 + \alpha_2 P_1^{\,*} + \beta_2 T^*) & -\beta_2 P_2^{\,*} \\ -\delta_1 T^* & -\delta_2 T^* & -(\delta_1 P_1^{\,*} + \delta_2 P_2^{\,*}) \end{bmatrix} E_2 =$$

$$-2\begin{bmatrix} \alpha_1 Re\{\sigma_1\}e^{i\omega_0\Im_0\theta} \\ \beta_1 Re\{\sigma_1\}e^{i\omega_0\Im_0\theta} \\ -\gamma_1 Re\{\rho_1\} \end{bmatrix}.$$

As a result, the parameters can express g_{21}.

Using the parameters, each g_{ij} can be determined based on the study mentioned above. Consequently, the following values can be calculated:

$$C_1(0) = \frac{i}{2\omega_0\Im_0}\left(g_{11}g_{20} - 2|g_{11}|^2 - \frac{|g_{02}|^2}{3}\right) + \frac{g_{21}}{2} \quad , \quad \mu_2 = -\frac{Re\{C_1(0)\}}{Re\{\lambda'(\tau_0)\}}, \quad \beta_2 = \quad (5.27)$$

$2Re\{C_1(0)\}$,

$T_2 = -\frac{Im\{C_1(0)\}+\mu_2 Im\{\lambda'(\Im_0)\}}{\omega_0\Im_0}$.

Theorem2: The value of μ_2 can be determines by the direction of the Hb: if $\mu_2 > 0(\mu_2 < 0)$, then Hb is supercritical (subcritical) and the bifurcating periodic solutions exists for $\Im > \Im_0$ $(\Im < \Im_0)$. The value of β_2 can determines the stability of bifurcating solutions: the bifurcating periodic solutions are orbitally asymptotically stable (unstable) if $\beta_2 < 0$ $(\beta_2 > 0)$. The bifurcating periodic solutions is determined by the value of T_2: the period increases (decreases) if $T_2 > 0$.

5.4 Numerical Stimulation

MATLAB simulation is used to numerically consolidate the analytical findings. The system behaves as follows:

$r_1 = 0.89, r_2 = 1.7, \alpha_1 = 1.001, \alpha_2 = 0.04, \beta_1 = 0.001, \beta_2 = 1.6, T_o = 3.7, \gamma_1 = 0.09, \gamma_2 = 0.9, \delta_1 = 6.04, \delta_2 = 2.94, \varepsilon = 0.009.$

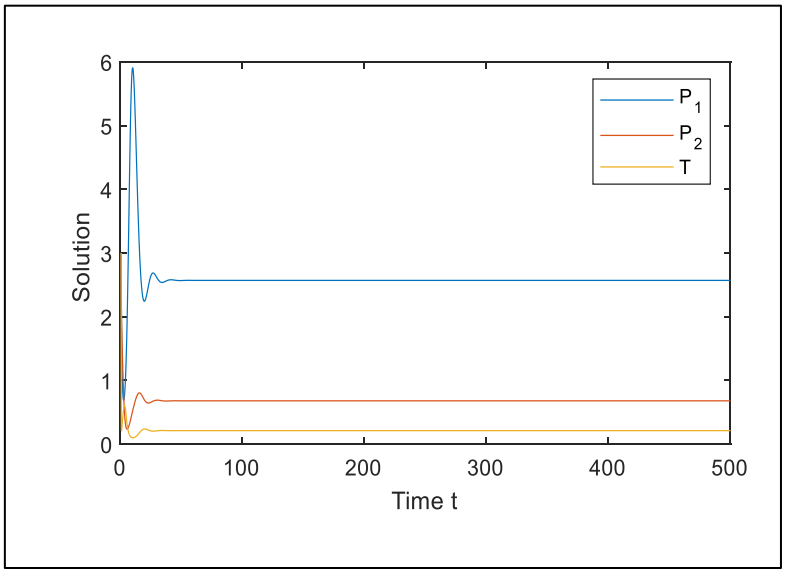

Figure 5.1 When there is absence of delay, $\Im$ = 0, the system interior equilibrium point $\boldsymbol{E_1}$ is stable.

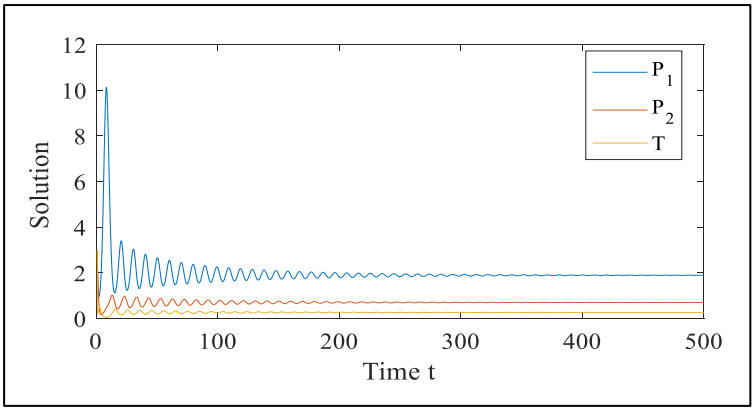

Figure 5.2 When there is delay that is $\Im < 2.18$, the system interior equilibrium point $\boldsymbol{E_1}$ is asymptotically stable.

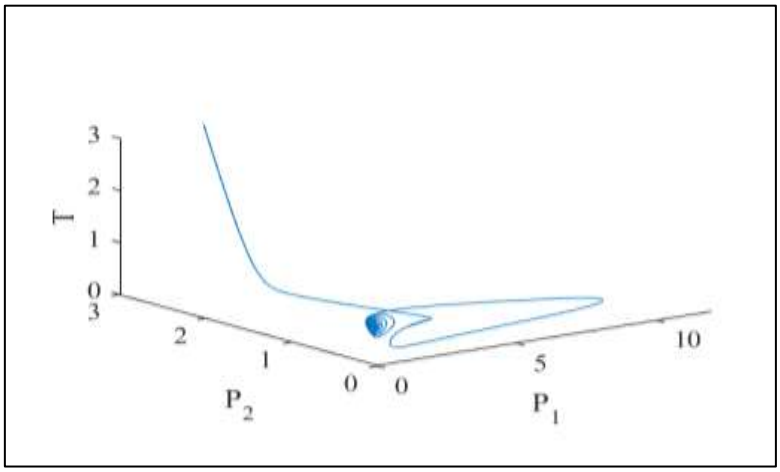

Figure 5.3 The phase space representation of toxicity T, plant biomass B, and nutrients N with a delay of $< \mathbf{1.25}$.

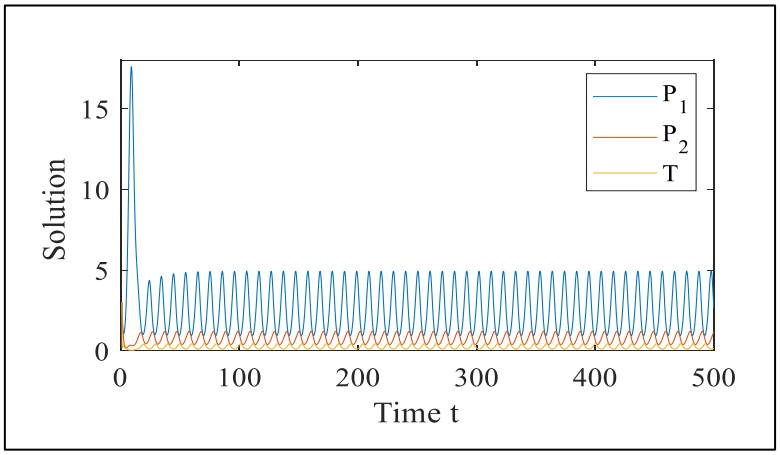

Figure 5.4 When there is delay that is $\Im$ >2.18, the system's interior equilibrium point $\boldsymbol{E_1}$ losses its stability and shown Hopf – bifurcation.

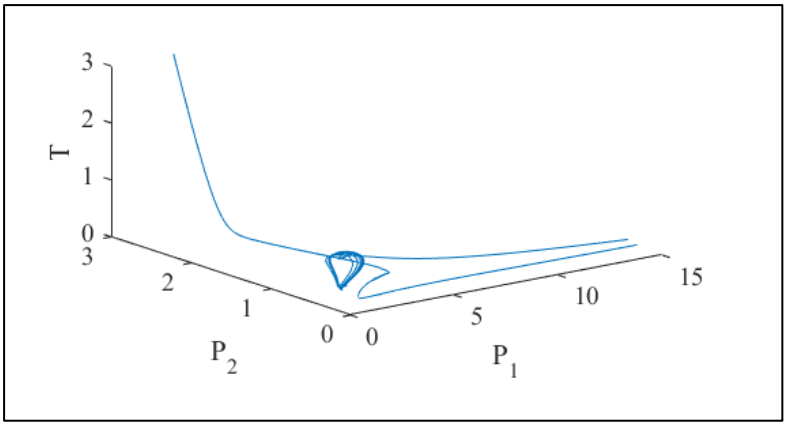

Figure 5.5 The phase space representation of toxicity T, plant biomass B, and nutrients N with a delay of $\mathfrak{J} > 2.18$. Asymptotically and orbitally stable is the bifurcating periodic solution.

5.4.1 Sensitivity Analysis

The model has constant parameters in this study. To calculate the global sensitivity coefficient, the "Direct Method" is utilised. For each parameter the partial derivatives of the solution can be found, may be all that is required for sensitivity analysis in this situation if all of the parameters $(\alpha_1, \alpha_2, \beta_1, \beta_2, \gamma_1, \gamma_2, \delta_1, \delta_2)$ present in the system (1) – (3) are assumed to be constants. Taking derivative partially of the solution $(P_1, P_2\ and\ T)$ in relation to the β_2, produce the set of sensitivity equations shown below:

$$\frac{dS_1}{dt} = r_1 S_1 - \frac{2r_1 S_1(t-\mathfrak{J})}{K} - \alpha_1 S_1 P_2 - \alpha_1 P_1 S_2 - \beta_1 P_1 S_3 - \beta_1 S_1 T - \gamma_1 S_1; \quad (5.28)$$

$$\frac{dS_2}{dt} = r_2 S_2 - \frac{2r_2 S_2(t-\mathfrak{J})}{K} - \alpha_2 P_1 S_2 - \alpha_2 S_1 P_2 - \beta_2 P_2 S_3 - \beta_2 S_2 T - \gamma_2 S_2; \quad (5.29)$$

$$\frac{dS_3}{dt} = -\delta_1 P_1 S_3 - \delta_1 T S_1 - \delta_2 P_2 S_3 - \delta_2 T S_2 - \varepsilon S_3. \quad (5.30)$$

Where $S_1 = \frac{\partial P_1}{\partial \beta_2}, S_2 = \frac{\partial P_2}{\partial \beta_2}, S_3 = \frac{\partial T}{\partial \beta_2}$.

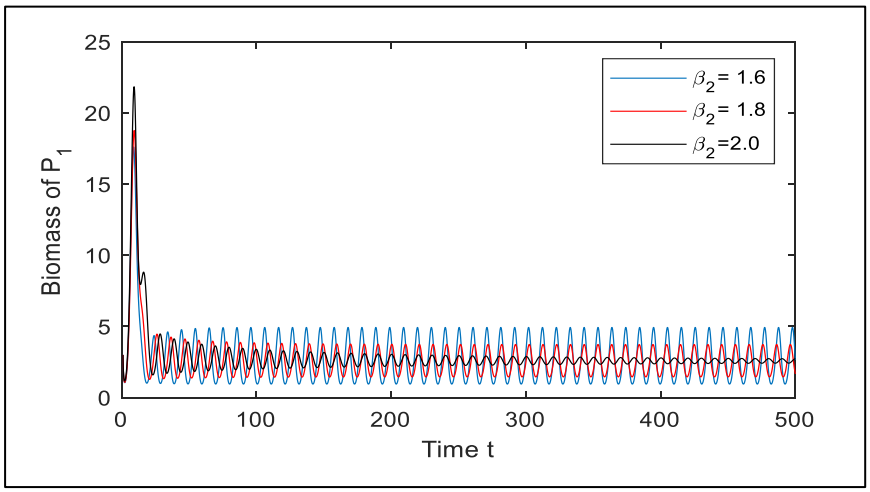

Figure 5.5 For various values of the utilisation coefficient $\boldsymbol{\beta_2}$, a time series graph shows the relationship between small variations in biomass of plant $\boldsymbol{P_1}$.

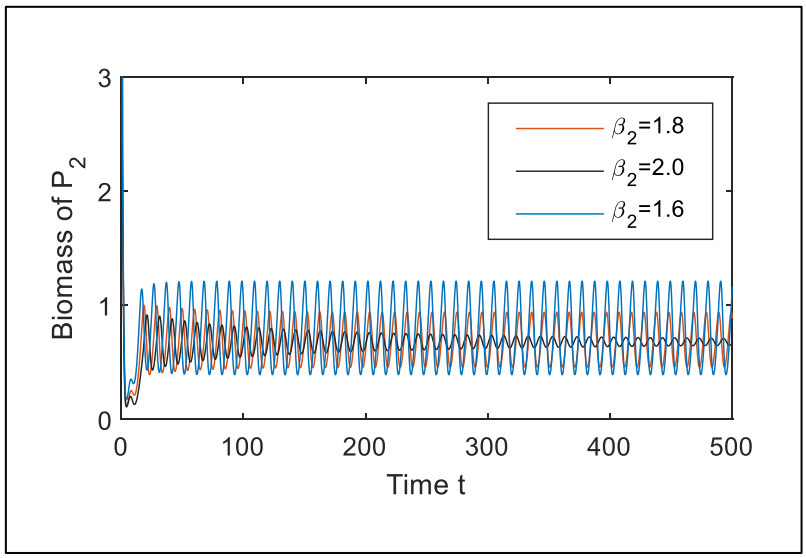

Figure 5.6 For various values of the utilisation coefficient $\boldsymbol{\beta_2}$, time series graph shows the relationship between small variations in biomass of plant $\boldsymbol{P_2}$.

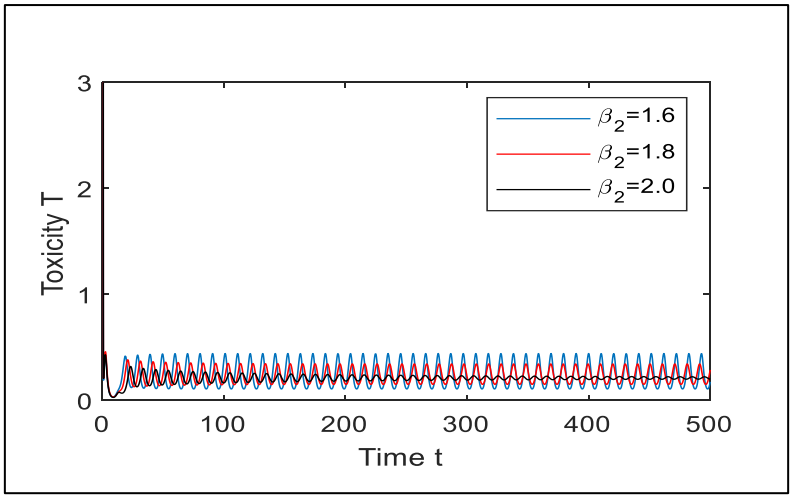

Figure 5.7 For various values of the utilisation coefficient $\boldsymbol{\beta_2}$, a time series graph shows the relationship between small variations in toxic metal $\boldsymbol{T}$.

5.5 Conclusion

In this paper, we investigated the impact of delay on the dynamics of mutual competitive plant growth when toxic metals are present. Other dynamical phenomena such as stable equilibrium, Hopf bifurcation, periodic oscillations, sensitivity analysis, and directional analysis are also observed. We conclude from some numerical simulations that for specific parameter values, the stability and Hopf bifurcation about interior equilibrium E* can happen. The stability of interior equilibrium E* in the absence of a delay has been demonstrated, as seen in (figure 5.51). The parameter delay is found to have a critical value below ($\tau \leq 1.95$), which the system exhibits asymptotic stability as seen in (figure 5.2 and figure 5.3). The proposed model oscillates and becomes unstable, when $\tau \geq 1.95$ as in (figure 5.4 and figure 5.5). As a result, when time lag surpasses a specific critical value, limit cycles for interior equilibrium points are detected after accounting for time lag.

References

[1] L. Hiltner, “Uber Neure Erfahrungen Und Problem Auf Dem Gebiete der Bodenbakteriologie Und Unter Besonderer Berukscichtigung der Grundungung Und Brache.,” *Arb.Dtsch, Landwirt.Ges*, pp. 59–78, 1904.

[2] F. Dalton and W. Gardner, “Simultaneous Uptake and Water by Plant Roots.,” *Argon. J*, vol. 67, p. 334–339., 1975.

[3] J. Thornley, *Mathematical Models in Plant Physiology*. Academic Press, London, 1976.

[4] A. R. Watkinson, “Density-dependence in single-species populations of plants,” *J. Theor. Biol.*, 1980.

[5] R. M. Gifford and L. T. Evans, “Photosynthesis, Carbon Partitioning, and Yield,” *Annu. Rev. Plant Physiol.*, 1981.

[6] H. Miler, *Dynamics of nutrient cycling in population ecosystem in nutrition of plantation forests*. 1984.

[7] J. F. Reynolds and B. Acock, “Predicting the response of plants to increasing carbon dioxide: A critique of plant growth models,” *Ecol. Modell.*, 1985.

[8] H. T. Valentine, “Tree-growth models: Derivations employing the pipe-model theory,” *J. Theor. Biol.*, 1985.

[9] A. Mäkelä, “Partitioning coefficients in plant models with turn-over,” *Ann. Bot.*, 1986.

[10] A. Pugliese, “Optimal resource allocation in perennial plants: A continuous-time model,” *Theor. Popul. Biol.*, 1988.

[11] R. N. Kickert and S. V. Krupa, “Modeling plant response to tropospheric ozone: A critical review,” *Environ. Pollut.*, 1991.

[12] T. Czaran and S. Bartha, “Spatiotemporal dynamic models of plant populations and communities.,” *Trends Ecol. Evol.*, 1992.

[13] J. H. M. Thornley, “Shoot: Root allocation with respect to C, N and P: An investigation and comparison of resistance and teleonomic models,” *Ann. Bot.*, 1995.

[14] J. Thornley, “Modelling allocation with Transport/Conversion process,” *Silva Fenn.*, vol. 31, no. 3, pp. 341–355, 1997.

[15] J. Thornley, “Modelling Shoot: Root Relations: the only way forward?,” *Ann. Bot.*, vol. 81, pp. 165–171, 1998.

[16] J. Thornley, “Modelling stem height and diameter growth in plants,” *Ann. Bot.*, vol. 84, pp. 195–205, 1999.

[17] C. Deleuze and F. Houllier, “A transport model for tree ring width,” *Silva Fenn.*, vol. 31, no. 3, pp. 239–250, 1997.

[18] O. Diekmann *et al.*, “On the formulation and analysis of general deterministic structured population models. II. Nonlinear theory.,” *J Math Biol*, 1998.

[19] F. Somma, J. W. Hopmans, and V. Clausnitzer, “Transient three-dimensional modeling of soil water and solute transport with simultaneous root growth, root water and nutrient uptake,” *Plant Soil*, 1998.

[20] G. S. Khush, “Green revolution: preparing for the 21st century,” *Genome*, 1999.

[21] A. Lacointe, “Carbon allocation among tree organs: A review of basic processes and representation in functional-structural tree models,” *Ann. For. Sci.*, 2000.

[22] P. Tinker and P. Nye, *Solute Movement in The Rhizosphere*. Oxford University Press,UK, 2000.

[23] L. GarcÍa-Barrios, D. Mayer-Foulkes, M. Franco, G. Urquijo-Vásquez, and J. Franco-Pérez, “Development and validation of a spatially explicit individual-based mixed crop growth model,” *Bull. Math. Biol.*, 2001.

[24] B. M. Bolker, S. W. Pacala, and C. Neuhauser, “Spatial Dynamics in Model Plant Communities: What Do We Really Know?,” *Am. Nat.*, 2003.

[25] P. Hedden, “The genes of the Green Revolution,” *Trends in Genetics*. 2003.

[26] I. Ioslovich and P.-O. Gutman, “On the botanic model of plant growth with intermediate vegetative-reproductive stage.,” *Theor. Popul. Biol.*, 2005.

[27] H. T. Valentine and A. Mäkelä, “Bridging process-based and empirical approaches to modeling tree growth,” in *Tree Physiology*, 2005.

[28] A. W. M. Verkroost and M. J. Wassen, “A simple model for nitrogen-limited plant growth and nitrogen allocation,” *Ann. Bot.*, 2005.

[29] R. R. Vance and A. L. Nevai, “Plant population growth and competition in a light gradient: A mathematical model of canopy partitioning,” *J. Theor. Biol.*, 2007.

[30] A. R. Overman, “A memoir on mthematical models of crop growth and yield: Effect of geographic location,” 2008.

[31] N. P. Harberd, E. Belfield, and Y. Yasumura, “The Angiosperm Gibberellin-GID1-DELLA Growth Regulatory Mechanism: How an ‘Inhibitor of an Inhibitor’

Enables Flexible Response to Fluctuating Environments," *plant cell online*, 2009.

[32] A. C. Fowler, O. Clary, and T. Roose, "A dynamic model of annual foliage growth and carbon uptake in trees," *J. R. Soc. Interface*, 2009.

[33] Z. Liu, "Spatial organization in plant model," 2010.

[34] K. Asano *et al.*, "Artificial selection for a green revolution gene during japonica rice domestication," *Proc. Natl. Acad. Sci.*, 2011.

[35] P. Pingali, "Green revolution: impacts, limits, and the path ahead.," *Proc. Natl Acad. Sci.*, vol. 109, no. 31, pp. 12302–12308, 2012.

[36] R. S. Quilliam, K. A. Marsden, C. Gertler, J. Rousk, T. H. DeLuca, and D. L. Jones, "Nutrient dynamics, microbial growth and weed emergence in biochar amended soil are influenced by time since application and reapplication rate," *Agric. Ecosyst. Environ.*, 2012.

[37] T. Clough, L. Condron, C. Kammann, and C. Müller, "A Review of Biochar and Soil Nitrogen Dynamics," *Agronomy*, vol. 3, no. 2, pp. 275–293, 2013.

[38] J. S. Clark, J. Melillo, J. Mohan, and C. Salk, "The seasonal timing of warming that controls onset of the growing season," *Glob. Chang. Biol.*, 2014.

[39] M. J. Hawkesford, "Reducing the reliance on nitrogen fertilizer for wheat production," *Journal of Cereal Science*. 2014.

[40] M. C. Vanderwel and D. W. Purves, "How do disturbances and environmental heterogeneity affect the pace of forest distribution shifts under climate change?," *Ecography (Cop.).*, 2014.

[41] K. W. King *et al.*, "Phosphorus Transport in Agricultural Subsurface Drainage: A Review," *J. Environ. Qual.*, 2015.

[42] A. Serrano-Mislata, S. Bencivenga, M. Bush, K. Schiessl, S. Boden, and R. Sablowski, "DELLA genes restrict inflorescence meristem function independently of plant height," *Nat. Plants*, 2017.

[43] D. Poxson and D. Simon, "Guding plant growth electronically," *Plant Biol.*, 2017.

[44] J. Sanderman, C. Creamer, W. T. Baisden, M. Farrell, and S. Fallon, "Greater soil carbon stocks and faster turnover rates with increasing agricultural productivity," *Soil*, 2017.

[45] T. Dahiru, "Plant Growth Substances in Crop Production: A Review.," Adamawa State University Mubi, Nigeria., 2018.

[46] I. Ciereszko, "Regulatory roles of sugars in plant growth and development,"

Acta Soc. Bot. Pol., vol. 87, no. 2, 2018.

[47] F. A. Bazzaz, G. L. Rolfe, and R. W. Carlson, "Effect of Cd on Photosynthesis and Transpiration of Excised Leaves of Corn and Sunflower," *Physiol. Plant.*, vol. 32, no. 4, pp. 373–376, 1974.

[48] F. A. Bazzaz, R. W. Carlson, and G. L. Rolfe, "Inhibition of Corn and Sunflower Photosynthesis by Lead," *Physiol. Plant.*, vol. 34, no. 4, pp. 326–329, 1975.

[49] E. J. Hewitt, "Principles of plant nutrition," *Nature*, 1979.

[50] K. Rodecap and D. Tigey, "Stress Etylene: A biomass for rhizosphere applied phytotoxicants," *Environ. Monit. Assess.*, vol. 1, pp. 119–127, 1981.

[51] T. G. Hallam, C. E. Clark, and G. S. Jordan, "Effects of toxicants on population: A qualitative approach II.First order kinetic," *J. Math. Biol.*, vol. 18, pp. 25–37, 1983.

[52] T. G. Hallam, C. E. Clark, and R. R. Lassiter, "Effects of toxicants on populations: a qualitative approach I. Equilibrium environmental exposure," *Ecol. Modell.*, 1983.

[53] T. G. Hallam and J. T. de Luna, "Effects of toxicants on populations: A qualitative. Approach III. Environmental and food chain pathways," *J. Theor. Biol.*, 1984.

[54] J. T. De Luna and T. G. Hallam, "Effects of toxicants on populations: A qualitative approach IV. Resource-consumer-toxicant models," *Ecol. Modell.*, 1987.

[55] M. Gatto and S. Rinaldi, "Some models of catastrophic behavior in exploited forests," *Vegetatio*, 1987.

[56] J. B. Shukla, H. I. Freedman, V. M. Pal, O. P. Misra, M. Agarwal, and A. Shukla, "Degradation and subsequent regeneration of a forestry resource: A mathematical model," *Ecol. Modell.*, 1989.

[57] J. Wolf, C. T. De Wit, and H. Van Keulen, "Modeling long-term crop response to fertilizer and soil nitrogen - I. Model description and application," *Plant Soil*, vol. 120, no. 1, pp. 11–22, 1989.

[58] H. I. Freedman and J. B. Shukla, "Models for the effect of toxicant in single-species and predator-prey systems," *J. Math. Biol.*, 1991.

[59] G. De Leo, L. Del Furia, and M. Gatto, "The interaction between soil acidity and forest dynamics: A simple model exhibiting catastrophic behavior," *Theor. Popul. Biol.*, 1993.

[60] A. Brune and K. J. Dietz, “A Comparative analysis of element composition of roots and leaves of barley seedlings grown in the presence of toxic cadmium, molybdenum, nickel, and zinc concentrations1,” *J. Plant Nutr.*, 1995.

[61] J. B. Shukla, B. Dubey, and H. I. Freedman, “Effect of changing habitat on survival of species,” *Ecol. Modell.*, 1996.

[62] P. S. Curtis and X. Wang, “A meta-analysis of elevated CO_2 effects on woody plant mass, form, and physiology,” *Oecologia*. 1998.

[63] M. Bonnet, O. Camares, and P. Veisseire, “Effects of zinc and influence of Acremonium lolii on growth parameters, chlorophyll a fluorescence and antioxidant enzyme activities of ryegrass (Lolium perenne L. cv Apollo),” *J. Exp. Bot.*, 2000.

[64] T. Mossor-Pietraszewska, “Effect of aluminium on plant growth and metabolism.,” *Acta Biochim. Pol.*, 2001.

[65] V. N. Pishchik *et al.*, “Experimental and mathematical simulation of plant growth promoting rhizobacteria and plant interaction under cadmium stress,” *Plant Soil*, 2002.

[66] B. Dubey, R. K. Upadhyay, and J. Hussain, “Effects of industrialization and pollution on resource biomass: A mathematical model,” *Ecol. Modell.*, 2003.

[67] M. K. Van Ittersum, P. A. Leffelaar, H. Van Keulen, M. J. Kropff, L. Bastiaans, and J. Goudriaan, “On approaches and applications of the Wageningen crop models,” in *European Journal of Agronomy*, 2003.

[68] M. Shenker, O. E. Plessner, and E. Tel-Or, “Manganese nutrition effects on tomato growth, chlorophyll concentration, and superoxide dismutase activity,” *J. Plant Physiol.*, 2004.

[69] F. Dercole, K. Niklas, and R. Rand, “Self-thinning and community persistence in a simple size-structured dynamical model of plant growth,” *J. Math. Biol.*, 2005.

[70] A. R. Sheldon and N. W. Menzies, “The effect of copper toxicity on the growth and root morphology of Rhodes grass (Chloris gayana Knuth.) in resin buffered solution culture,” *Plant Soil*, vol. 278, no. 1–2, pp. 341–349, 2005.

[71] D. Thomas, L. Vandemuelebroeke, and A. Yamaguchi, “A mathematical evolution model of phytoremediation of metals,” *Discret. Contin. Dyn. Syst. Ser. B*, vol. 5, no. 2, pp. 411–422, 2005.

[72] R. Naresh, S. Sundar, and J. B. Shukla, “Modeling the effect of an intermediate toxic product formed by uptake of a toxicant on plant biomass,” *Appl. Math. Comput.*, 2006.

[73] A. Läuchli and S. R. Grattan, “Plant growth and development under salinity stress,” in *Advances in Molecular Breeding Toward Drought and Salt Tolerant Crops*, 2007.

[74] P. Verma, K. V. George, H. V. Singh, and R. N. Singh, “Modeling cadmium accumulation in radish, carrot, spinach and cabbage,” *Appl. Math. Model.*, 2007.

[75] C. L. Wu, K. W. Chau, and J. S. Huang, “Modelling coupled water and heat transport in a soil-mulch-plant-atmosphere continuum (SMPAC) system,” *Appl. Math. Model.*, 2007.

[76] X. Liu and Q. Zhang, “Stabilization and persistance of N species food chain feedback control system in polluted environment,” *Int. J. Inf. Syst. Sci.*, vol. 4, pp. 479–487, 2008.

[77] J. B. Shukla, S. Sharma, B. Dubey, and P. Sinha, “Modeling the survival of a resource-dependent population: Effects of toxicants (pollutants) emitted from external sources as well as formed by its precursors,” *Nonlinear Anal. Real World Appl.*, vol. 10, no. 1, pp. 54–70, 2009.

[78] Q. Hayat, S. Hayat, M. Irfan, and A. Ahmad, “Effect of exogenous salicylic acid under changing environment: A review,” *Environmental and Experimental Botany*. 2010.

[79] P. C. Nagajyoti, K. D. Lee, and T. V. M. Sreekanth, “Heavy metals, occurrence and toxicity for plants: A review,” *Environ. Chem. Lett.*, 2010.

[80] R. P. Singh and M. Agrawal, “Effect of different sewage sludge applications on growth and yield of Vigna radiata L. field crop: Metal uptake by plant,” *Ecol. Eng.*, 2010.

[81] S. Sinha, O. P. Misra, and J. Dhar, “A two species competition model under the simultaneous effect of toxicant and disease,” *Nonlinear Anal. Real World Appl.*, 2010.

[82] T. Tsonev and F. J. C. Lidon, “Zinc in plants - An overview,” *Emirates Journal of Food and Agriculture*. 2012.

[83] O. P. Misra and P. Kalra, “Modelling Effect of Toxic Metal On the Individual Plant Growth: A Two Compartment Model,” *Am. J. Comput. Appl. Math.*, vol. 2, no. 6, pp. 276–289, 2012.

[84] A. Ahmad, I. Khan, and H. Diwan, “Chromium toxicity and tolerance in crop plants,” in *Crop Improvement Under Adverse Conditions*, 2013.

[85] Y.-B. Guo, H. Feng, C. Chen, C.-J. Jia, F. Xiong, and Y. Lu, “Heavy Metal

Concentrations in Soil and Agricultural Products Near an Industrial District," *Polish J. Environ. Stud.*, 2013.

[86] G. M. Pavel V.L., Sobariu D.L., Diaconu M., Statescu F., "Effects of heavy metals on Lepidium sativum germination and growth.," *Environ. Eng. Manag. journal.*, vol. 12, no. 4, pp. 727–733, 2013.

[87] O. P. Misra and P. Kalra, "Effect of Toxic Metal on the Structural Dry," vol. 6, no. 5, pp. 1–27, 2013.

[88] J. B. Shukla, S. Sundar, S. Shivangi, and R. Naresh, "Modeling and analysis of the acid rain formation due to precipitation and its effect on plant species," *Nat. Resour. Model.*, 2013.

[89] D. K. Gupta, S. Chatterjee, S. Datta, V. Veer, and C. Walther, "Role of phosphate fertilizers in heavy metal uptake and detoxification of toxic metals," *Chemosphere*. 2014.

[90] S. Bedbabis *et al.*, "Long-terms effects of irrigation with treated municipal wastewater on soil, yield and olive oil quality," *Agric. Water Manag.*, 2015.

[91] Boros M.N. and V. Micle, "Copper influence on germination and growth of sunflower (Helianthus Annuus)," *Stud. UBB Ambient. LX.*, vol. 1, no. 2, pp. 23–30, 2015.

[92] S. Sundar and R. Naresh, "Modelling and analysis of the survival of biological species in a polluted environement: Effect of environmental tax," *Comput. Ecol. Softw.*, vol. 5, no. 2, pp. 201–221, 2015.

[93] N. Cu, "Effect of heavy metals on plant growth and ability to use fertilizing substances to reduce heavy metals accumulation by Brassica Jencea L. Czern," *Glob. J. Sci. Front. Res. D Agric. Vet.*, vol. 15, no. 3, 2015.

[94] C. Peng, M. Wang, and W. Chen, "Modelling cadmium contamination in paddy soils under long-term remediation measures: Model development and stochastic simulations," *Environ. Pollut.*, vol. 216, pp. 146–155, 2016.

[95] G. Mustafa and S. Komatsu, "Toxicity of heavy metals and metal-containing nanoparticles on plants," *Biochim. Biophys. Acta - Proteins Proteomics*, 2016.

[96] A. Kumar, A. Agrawal, A. Hasan, and A. Misra, "Modelling the effect of toxicant on the deformity in a subclass of a biological species," *Model. Earth Syst. Environ.*, vol. 2, no. 40, 2016.

[97] S. Sundar, N. Swaroop, and R. Naresh, "Modeling the Effect of Population and Population Augmented Industrialization on Forestry Resources," *Eur. J. Eng. Res.*

Sci., 2017.

[98] Y. Yan, L. Zhang, L. Feng, D. Sun, and Y. Dang, "Comparison of varying operating parameters on heavy metals ecological risk during anaerobic co-digestion of chicken manure and corn stover," *Bioresour. Technol.*, 2018.

[99] "Delay-Differential Equations," *Math. Sci. Eng.*, 1966.

[100] M. C. Mackey and L. Glass, "Oscillation and chaos in physiological control systems," *Science (80-.).*, 1977.

[101] L. Glass and M. C. Mackey, "A simple model for phase locking of biological oscillators.," *J. Math. Biol.*, 1979.

[102] K. L. Cooke and Z. Grossman, "Discrete delay, distributed delay and stability switches," *J. Math. Anal. Appl.*, 1982.

[103] L. J. Donald L, DeAngelis and Gross, *Individual based models and approaches in ecology, population, communities and ecosystem*. Chapman and Hall, New York, London, 1992.

[104] K. Gopalsamy, *Stability and Oscillations in Delay Differential Equations of Population Dynamics*. 1992.

[105] Y. Kuang, *Delay differential equations with applications in population dynamics*. 1993.

[106] J. Bélair, M. C. Mackey, and J. M. Mahaffy, "Age-structured and two-delay models for erythropoiesis," *Math. Biosci.*, 1995.

[107] M. Roussel, "The use of delay differential equations in chemical kinetics," *J. Phys. Chem.*, 1996.

[108] J. He, "Variational iteration method for delay differential equations," *Commun. Nonlinear Sci. Numer. Simul.*, 1997.

[109] X. Li, S. Ruan, and J. Wei, "Stability and bifurcation in delay-differential equations with two delays," *J. Math. Anal. Appl.*, 1999.

[110] K. Engelborghs, T. Luzyanina, and D. Roose, "Numerical bifurcation analysis of delay differential equations," *J. Comput. Appl. Math.*, 2000.

[111] G. A. Bocharov and F. A. Rihan, "Numerical modelling in biosciences using delay differential equations," *J. Comput. Appl. Math.*, 2000.

[112] S. Ruan and J. Wei, "On the zeros of a third degree exponential polynomial with applications to a delayed model for the control of testosterone secretion.," *IMA J. Math. Appl. Med. Biol.*, 2001.

[113] L. F. Shampine and S. Thompson, "Solving DDEs in MATLAB," *Appl.*

Numer. Math., 2001.

[114] K. Engelborghs, T. Luzyanina, and D. Roose, "Numerical bifurcation analysis of delay differential equations using DDE-BIFTOOL," *ACM Trans. Math. Softw.*, 2002.

[115] I. Kubiaczyk and S. H. Saker, "Oscillation and stability in nonlinear delay differential equations of population dynamics," *Math. Comput. Model.*, vol. 35, no. 3–4, pp. 295–301, 2002.

[116] Y. Kuznetsov, *Elements of applied bifurcation theory*. Springer, 2004.

[117] Y. Lenbury and D. V. Giang, "Nonlinear delay differential equations involving population growth," *Math. Comput. Model.*, 2004.

[118] X. Li and J. Wei, "On the zeros of a fourth degree exponential polynomial with applications to a neural network model with delays," *Chaos, Solitons and Fractals*, 2005.

[119] S. Ruan, "Delay Differential Equations in Single Species Dynamics," in *Delay Differential Equations and Applications.*, Springer, Berlin, 2006, pp. 477–517.

[120] T. Erneux, *Applied Delay Differential Equations*. 2007.

[121] D. Roose and R. Szalai, "Continuation and bifurcation analysis of delay differential equations," *Numer. Contin. methods Dyn. ...*, 2007.

[122] B. Balachandran, T. Kalmár-Nagy, and D. E. Gilsinn, *Delay differential equations: Recent advances and new directions*. 2009.

[123] T. Zhang, H. Jiang, and Z. Teng, "On the distribution of the roots of a fifth degree exponential polynomial with application to a delayed neural network model," *Neurocomputing*, 2009.

[124] H. Smith, *An Introduction to Delay Differential Equations with Applications to the Life Sciences*. 2011.

[125] J. Mallet-Paret and R. D. Nussbaum, "Stability of periodic solutions of state-dependent delay-differential equations," *J. Differ. Equ.*, 2011.

[126] J. Sieber and R. Szalai, "Characteristic Matrices for Linear Periodic Delay Differential Equations," *SIAM J. Appl. Dyn. Syst.*, 2011.

[127] M. Wolfrum, S. Yanchuk, P. Hövel, and E. Schöll, "Complex dynamics in delay-differential equations with large delay," *European Physical Journal: Special Topics*. 2011.

[128] Y. Kuang, "Delay differential equations," *Encycl. Theor. Ecol.*, 2012.

[129] G. Huang, A. Liu, and U. Foryś, "Global Stability Analysis of Some Nonlinear

Delay Differential Equations in Population Dynamics," *J. Nonlinear Sci.*, vol. 26, no. 1, pp. 27–41, 2016.

[130] L. Berezansky and E. Braverman, "Boundedness and persistence of delay differential equations with mixed nonlinearity," *Appl. Math. Comput.*, vol. 279, no. September, pp. 154–169, 2016.

[131] T. Hopf, "Hopf bifurcation," 知识点. 1942.

[132] J. E. Marsden, M. McCracken, P. R. Sethna, and G. R. Sell, "The Hopf Bifurcation and Its Applications," *J. Appl. Mech.*, 1978.

[133] S. B. Hsu and T. W. Hwang, "Hopf bifurcation analysis for a predator-prey system of Holling and Leslie type," *Taiwan. J. Math.*, 1999.

[134] D. V. Ramana Reddy, A. Sen, and G. L. Johnston, "Time delay effects on coupled limit cycle oscillators at Hopf bifurcation," *Phys. D Nonlinear Phenom.*, 1999.

[135] P. Manfredi and L. Fanti, "Cycles in dynamic economic modelling," *Econ. Model.*, 2004.

[136] J. Wei and M. Y. Li, "Hopf bifurcation analysis in a delayed Nicholson blowflies equation," *Nonlinear Anal. Theory, Methods Appl.*, 2005.

[137] R. P. Gupta and P. Chandra, "Bifurcation analysis of modified Leslie-Gower predator-prey model with Michaelis-Menten type prey harvesting," *J. Math. Anal. Appl.*, 2013.

[138] M. Xiao, W. X. Zheng, and J. Cao, "Bifurcation and control in a neural network with small and large delays," *Neural Networks*, 2013.

[139] L. Zhang and S. Guo, "Hopf bifurcation in delayed van der Pol oscillators," *Nonlinear Dyn.*, 2013.

[140] Y. Wang, H. Wang, and W. Jiang, "Hopf-transcritical bifurcation in toxic phytoplankton-zooplankton model with delay," *J. Math. Anal. Appl.*, 2014.

[141] R. P. Dickinson and R. J. Gelinas, "Sensitivity analysis of ordinary differential equation systems-A direct method," *J. Comput. Phys.*, 1976.

[142] C. T. H. Baker and F. A. Rihan, "Sensitivity Analysis of Parameters inModelling with Delay Differential Equations," 1999.

[143] H. C. Frey and S. R. Patil, "Identification and review of sensitivity analysis methods," in *Risk Analysis*, 2002.

[144] F. A. Rihan, "Sensitivity analysis for dynamic systems with time-lags," *J.*

Comput. Appl. Math., 2003.

[145] H. Caswell, "Sensitivity analysis of transient population dynamics," *Ecology Letters*. 2007.

[146] J. Kepler, "Sensitivity Analysis: The Direct and Adjoint Method," *Mathematik.Jku.At*, 2010.

[147] T. M. Perumal and R. Gunawan, "Understanding dynamics using sensitivity analysis: Caveat and solution," *BMC Syst. Biol.*, 2011.

[148] F. A. Rihan, "Delay differential equations in biosciences: Parameter estimation and sensitivity analysis," in *Proceedings of the 2013 international conference on applied mathematics and computational methods*, 2013, pp. 50–58.

[149] Q. Wu, "Sensitivity Analysis for Functional Structural Plant Modelling," Ecole Centrale Paris, 2014.

[150] B. Ingalls, M. Mincheva, and M. R. Roussel, "Parametric Sensitivity Analysis of Oscillatory Delay Systems with an Application to Gene Regulation," *Bull. Math. Biol.*, 2017.

[151] B. Dubey and J. Hussain, "Models for the effect of environmental pollution on forestry resources with time delay," *Nonlinear Anal. Real World Appl.*, 2004.

[152] J. Pastor and R. Durkee Walker, "Delays in nutrient cycling and plant population oscillations," *Oikos*. 2006.

[153] S. Naresh, R., Sharma, D., & Sundar, "Modeling the effect of toxicant on plant biomass with time delay," *Int. J. Nonlinear Sci.*, vol. 17, pp. 254–267, 2014.

[154] L. J. Gross, *Mathematical Modeling in Plant Biology: Implications of Physiological Approaches for Resource Management.* Springer Verlag, Berlin, 1990.

[155] H. Smith, *An Introduction to Delay Differential Equations With Applications tothe Life Sciences*. 2010.

[156] S. Ahmad and M. Rao, *Theory of Ordinary Differential Equations*. New Delhi: Affiliated Eat-West Press Private Limited, 2014.

[157] S. Ruan and J. Wei, "On the zeros of transcendental functions with applications to stability of delay differential equations with two delays," *Dyn. Contin. Discret. Impuls. Syst. Ser. A Math. Anal.*, 2003.

[158] J. Dieudonne, *Foundations of Modern Analysis*. New York. Academic Press, 1960.

[159] R. K. Pandey, N. Kumar, and R. N. Mohaptra, "An Approximate Method for Solving Fractional Delay Differential Equations," *Int. J. Appl. Comput. Math.*, 2016.

[160] P. Kalra and P. Kumar, " The study of time lag on plant growth under the effect of toxic metal," A mathematical mode Pertanika J.Sci.& Technol., 26(3), 1131-1154, 2018.

[161] P. Kalra and P. Kumar , "The Study of Combined Effect of Delay Induced by Acid and Toxic Metal on Plant Population," A Modeling Approach J. Phys.: Conf. Ser. 1531 012067, 2020.

[162] B.D. Hassard B.D, N.D Kazarino and Y.H. Wan, Theory and Application of Hopf -Bifurcation CUP, Archive.

[163] C. Godin, J. Hanan, W. Kurth, A. Lacointe and A. Takenaka, P. Prusinkiewicz, "Proceedings of the 4th International Workshop on Functional-Structural Plant Models", Montpellier, France, UMR AMAP, 2004.

[164] P. Kumar, "Hopf Bifurcation Induced by Delay Parameter in Depletion of Forest Biomass Due To Wood Based Industries," European Journal of Molecular & Clinical Medicine Vol 7(7), 2020.

[165] Gopalsamy and G.Ladas, "On the oscillation and asymptotic behavior of fi(t) = N(t)[a + bN(t - T) -cN2(t - T)]'," Qurt. Appl. Math. 3, 433-440, 1990.

[166] G. Ladas G and C. Qian C, "Oscillation and global stability in a delay logistic equation," Dyn. and Stabl. of Systems 9, 153-162, 1994.

[167] P. Kalra and P. Kumar, "The study of effect of toxic metal on plant growth dynamics with time lag: A two-compartment model," J.Math.Fund.Sci., 50(3): 233-256, 2018.

[168] L. R. Benjamin and R. C. Hardwick, Sources of variation and measures of variability in even-aged stands of plants, *Ann. Bot.* **58** (1986) 757–778.

[169] P. Kalra and P. Kumar "Role of delay in plant growth dynamics: A two compartment mathematical model," American Institute of Physics.,doi: 10.1063/1.4990344.

[170] C. D. Foy, Physiological effects of hydrogen, aluminium and manganese toxicities in acid soil, in Soil Acidity and Liming, eds. R. W. Pearson and F. Adams (American Society of Agronomy, Wisconsin, 1984), pp. 57–97.

[171] R. Tucker, D. H. Hardy and C. E. Stokes, *Heavy Metals in North Carolina Soils, Occurrence and Significance* (N.C. Department of Agriculture and Consumer Services, Agronomics division, Raleigh, 2003).

[172] S. Trivedi and L. Erdei, Effects of cadmium and lead on the accumulation of *Ca*2+ and *K*+ and on the influx and translocation of *K*+ status, *Physiol. Plant* **84**

(1992) 94–100.

[173] T. Roose, & A. Fowler, “A mathematical model for water and nutrients uptake by roots,” J. Theor. Biol. 228, 173-184, (doi:10.1016/j.jtbi.2003.12.013).

[174] J. Dieudonne, Foundations of Modern Analysis, (New York. Academic Pres4s,1960)

[175] S. Ruan and J. Wei, 2001, IMA Journal of Mathematics Applications in Medical Biology; 18:41-52 (2001).

[176] I. Kubiaczyk and S.H. Saker, Mathematical and Computer Modelling 35: 295-301(2002).

[177] L. Berezansky and E. Braverman, “Boundedness and persistence of delay differential equations with mixed nonlinearity,” Appl. Math. Comput., vol. 279, 2016, doi: 10.1016/j.amc.2016.01.015.

[178] G. Ladas and C. Qian, “Oscillation and global stability in a delay logistic equation,” Dyn. Stab. Syst., vol. 9, no. 2, 1994, doi: 10.1080/02681119408806174.

[179] J. Wei and M. Y. Li, “Hopf bifurcation analysis in a delayed Nicholson blow flies equation,” Nonlinear Anal. Theory, Methods Appl., 2005, doi: 10.1016/j.na.2003.04.002.

[180] D. Kaur and P. Kumar, “Bifurcation induced by delay parameter in plant growth dynamics” journal of physics, volume 2267.

[181] F. A. Rihan, “Sensitivity analysis for dynmics systems with time-lags,” *J. Comput. Appl. Math.*, vol. 151, no. 2, 2003, doi: 10.1016/S0377-0427(02)00659-3.

[182] S. Trvedi and L. Erdei, “Effects of cadmium and lead on the accumulation of Ca2+ and K+ and on the influx and translocation of K+ in wheat of low and high K+ status,” *Physiol. Plant.*, vol. 84, no. 1, 1992, doi: 10.1111/j.1399-3054.1992.tb08770.x.

[183] D. H. Hardy, J. Myers and C. Stokes, *Heavy metals in North Carolina soils : occurrence & significance*. N.C. Department of Agriculture and Consumer Services, Agronomic Division.

[184] O. P. Misra and P. Kalra, “Effect of toxic metal on the structural dry weight of a plant: A Model,” Int. J. Biomath., vol. 6, no. 5, 2013, doi: 10.1142/S1793524513500289.

[185] J. H. M. Thornley, “Mathematical Models in Plant Physiology. A Quantitative Approach to Problems in Plant and Crop Physiology.,” Acad. Press. London, 1976.

[186] A. Lacointe, “Carbon allocation among tree organs: A review of basic processes

and representation infunctional-structural tree models," Ann. For. Sci., vol. 57, pp. 521-533, 2000, doi: 10.1051/forest:2000139.

[187] G. Deleo, L. Delfuria, and M. Gatto, "The interaction between soil acidity and forest dynamics: A simple-model exhibiting catastrophic behavior," Theor. Popul. Biol., vol. 43, no. 1, 1993, doi: 10.1006/tpbi.1993.1002.

[188] J. B. Shukla, A. Agarwal, P. Sinha and B. Dubey, "Modelling Effects of Primary and Secondary Toxicant on Renewable Resources.," Nat. Resour. Model., vol. 16, pp. 99–120, 2008.

[189] A. Overman, "A memoir on mathematical models of crop growth and yeild: Effect of geographic location," Univ. Florida.

[190] D. Sharsma, S. Sundar and R. Naresh, "Modelling the effect of toxicant on plant biomass with time delay," Int. J. non linear Sci., vol. 17, pp. 254–267, 2014.

[191] K. R. Schneider, "Hassard, B. D. / Kazarinoff, N. D. / Wan, Y.-H., Theory and Applications of Hopf Bifurcation. London Mathematical Society Lecture Note Series 41. Cambridge, Cambridge University Press 1981. 320 S., £ 15.00 A P/B. ISBN 0-521-23158-2," ZAMM - Zeitschrift für Angew. Math. und Mech., vol. 62, no. 12, 1982, doi: 10.1002/zamm.19820621221.

[192] C. Sun, M. Han, and Y. Lin, "Analysis of stability and Hopf bifurcation for a delayed logistic equation," Chaos, Solitons and Fractals, vol. 31, no. 3, 2007, doi: 10.1016/j.chaos.2005.10.019.

[193] G. A. Bocharov and F. A. Rihan, "Numerical modelling in biosciences using delay differential equations," J. Comput. Appl. Math., vol. 125, no. 1–2, 2000, doi: 10.1016/S0377-0427(00)00468-4.

[194] H. T. Banks, D. Robbins, and K. L. Sutton, "Generalized sensitivity analysis for delay differential equations," in International Series of Numerical Mathematics, vol. 164, 2013. doi: 10.1007/978-3-0348-0631-2_2.

[195] Dipesh and P. Kumar, "Effect of time delay on dynamic of plant competition under allelopathy," Math. Method Appl. Sci.,vol. 45, pp.9308-9321,2022.

[196] J. Chattopadhyay, "Effect of toxic substances on a two-species competitive system," Ecol. Modell., vol. 84, no. 1–3, 1996, doi: 10.1016/0304-3800(94)00134-0.

[197] O. P. Misra and P. Kalra, "Effect of toxic metal on the structural dry weight of a plant: A Model," Int. J. Biomath., vol. 6, no. 5, 2013, doi: 10.1142/S1793524513500289.

[198] S. Guala, F. A. Vega, and E. F. Covelo, "Modeling the plant-soil interaction in

presence of heavy metal pollution and acidity variations," Environ. Monit. Assess., vol. 185, no. 1, 2013, doi: 10.1007/s10661-012-2534-z.
[199] P. Kalra and P.Kumar, "Modelling on Plant Biomass With Time Lag Under the Effect of Toxic Metal," Ecol. Environ. Conserv., vol. 24, no. 1, 2018.
[200] S. Ruan and J. Wei, "IMA Journal of Mathematics Applications in Medical Biology," IMA J. Math. Appl. Med. Biol. 1841-52 (2001)., vol. 18, pp. 41–52, 2001
[201] H. T. Banks, D. Robbins, and K. L. Sutton, "Generalized sensitivity analysis for delay differential equations," in International Series of Numerical Mathematics, vol. 164, 2013. doi: 10.1007/978-3-0348-0631-2_2.
[202] D. Pankaj Kumar, "Effect of time delay on dynamic of plant competition under allelopathy," Math. Methods Appl.Sci., 2022.